



Danmarks  
Tekniske  
Universitet



Technische  
Universität  
München

# Chemically Enhanced Biodegradation of cis-1,2 Dichloroethylene in a Limestone Aquifer

Remediation using iron sulphide and microbes  
through batch tests

**Sithara Dhinethi Weeratunga**

School of Engineering and Design  
Department of Civil and Environmental Engineering  
Master of Sciences in Environmental Engineering

Kongens Lyngby , June 2025



Technical University  
of Denmark

Technical  
University  
of Munich



# Chemically Enhanced Biodegradation of cis-1,2 Dichloroethylene in a Limestone Aquifer

Remediation using iron sulphide and microbes  
through batch tests

**Sithara Dhinethi Weeratunga**

**Supervisor:** Mette Martina Broholm  
*Associate Professor, Technical University of Denmark*

**Supervisor:** Thomas Baumann  
*Professor, Technical University of Munich*

**Co-supervisors (DTU):** Annika Sidelmann Fjordbøge  
*Senior Researcher*

**Co-supervisors (DTU):** Cecilie Fisker Ottosen  
*Assistant Professor*

School of Engineering and Design  
Department of Civil and Environmental Engineering  
Master of Sciences in Environmental Engineering

*Master's Thesis*

Kongens Lyngby , June 2025





## DECLARATION OF AUTHORSHIP

Has undersigned, hereby it his declared that this work entitled "Chemically Enhanced Biodegradation of cis-1,2 Dichloroethylene in a Limestone Aquifer" is the original work and that it has not previously in its entirety or in part been submitted at any university or higher education institution for the award of any degree, diploma, or other qualifications. It is also hereby declared that to the best of the knowledge, this work contains no material previously published or written by another person, except where due reference, acknowledgement, and citation is made.

*Kongens Lyngby , June 2025*

---

Sithara Dhinethi Weeratunga



## ACKNOWLEDGEMENTS

First and foremost, I would like to express my deepest gratitude to my parents for their unwavering support throughout this journey. Their financial sacrifices and steadfast encouragement gave me the freedom to pursue my dreams. Their belief in me has been my anchor, and I owe this achievement to their love and resilience.

I am incredibly grateful to my thesis supervisors, Mette Martina Broholm, Annika Sidelmann Fjordbøge, Cecilie Fisker Ottosen, and Thomas Baumann for their invaluable guidance, patience, and expertise. Their mentorship shaped this project and my growth as a researcher. Thank you for trusting in my ideas, challenging me to think critically, and supporting me through every hurdle. This work would not have been possible without their dedication and wisdom.

Special thanks to the technicians: Jens Schaarup Sørensen, Jacob Friis-Grigoncza, Klaus Bræmer and Jørn Lykke Jensen, and Mikael Emil Olsson, who helped me through the experimental set-up of this project. I am especially grateful to Jens, who generously made time for me despite his busy schedule.

To Marie and Enrico - thank you for your collaboration and support, from bouncing ideas with me to assisting me with limestone collection, groundwater sampling, and batch experiments.

A heartfelt thank you to my friends Aastha, Bee, Giulia and Tomasz. Your reassurance pushed me to keep going. You defended my passion when others couldn't see its worth; I am forever thankful for that.

Finally, to the countless individuals working to innovate and advocate for sustainable solutions: your dedication inspires me daily. This thesis is a small contribution to a much larger fight; one I am proud to join.



## ABSTRACT

Groundwater contamination by chlorinated solvents, particularly cis-1,2-dichloroethylene (cDCE), poses a significant threat to drinking water resources, especially in fractured limestone aquifers. This thesis assess the potential of three remediation strategies: Biogeochemical Reductive Dechlorination (BiRD), Enhanced Reductive Dechlorination (ERD), and their combined application to treat a cDCE-dominated contaminant plume at the Naverland site in Denmark. Laboratory-scale batch experiments were conducted using bioactive groundwater and limestone to simulate site-specific conditions. Four scenarios were tested: natural attenuation, GeoForm® Soluble (a ferrous sulfate-based amendment), KB-1® (a containing microbial consortium *Dehalococcoides* ), and a combination of GeoForm® and KB-1®.

The results demonstrated that ERD using KB-1® was the most effective approach, achieving complete dechlorination of cDCE to ethene with high degradation rates. Despite its theoretical potential, BiRD produced no observable degradation of target compounds within the study's duration due to delayed formation of reactive iron sulphide (FeS) and insufficient reductive conditions. The combined treatment accelerated FeS formation through sulfate-reducing bacteria (SRB) in KB-1®. The high iron and sulphide concentrations from GeoForm® inhibited *Dehalococcoides* activity, significantly reducing degradation efficiency. Despite this inhibition, the detection of vinyl chloride and ethene at low levels confirmed persistent biotic degradation."

These findings highlight the importance of redox control, amendment compatibility, and microbial resilience in remediation design. Given the site's hydrogeology and buffering capacity, ERD using KB-1® is recommended for field-scale implementation.

**Keywords:** Chlorinated ethenes, Groundwater treatment, Bioaugmentation, Aquifer geochemistry, Laboratory microcosms



# CONTENTS

<b>Contents</b>	x
<b>List of Figures</b>	xiii
<b>List of Tables</b>	xvi
<b>Acronyms</b>	xvii
<b>1 Introduction</b>	1
<b>2 Objectives</b>	4
<b>3 DCE Degradation Mechanisms and Their Application to Naverland</b>	5
3.1 DCE properties, degradation and toxicity . . . . .	5
3.1.1 Properties . . . . .	5
3.1.2 Natural attenuation . . . . .	6
3.1.3 Toxicology and ecotoxicology . . . . .	8
3.2 Remediation methods based on reductive dechlorination . . . . .	9
3.2.1 Bioremediation . . . . .	9
3.2.2 Biogeochemical reductive dechlorination . . . . .	11
3.2.3 Combination of biotic and abiotic remediation . . . . .	15
<b>4 Site: Naverland</b>	17
4.1 Geology and Hydrogeology . . . . .	17
4.2 Contamination . . . . .	19
4.3 Remediation strategies . . . . .	20
<b>5 Methodology</b>	22
5.1 Field sampling and storage . . . . .	22
5.2 Preparation of materials . . . . .	26
5.3 Set up of microcosm . . . . .	27
5.3.1 Biotic control . . . . .	29
5.3.2 GeoForm® dilution . . . . .	29
5.3.3 KB-1® . . . . .	29

---

5.4 Monitoring . . . . .	30
5.4.1 Chlorinated ethenes . . . . .	31
5.4.2 Volatile fatty acids . . . . .	32
5.4.3 Redox parameters . . . . .	32
5.4.4 pH . . . . .	33
5.5 Data treatment . . . . .	34
<b>6 Results</b>	<b>35</b>
6.1 Physical observations . . . . .	35
6.2 Data analysis . . . . .	39
6.2.1 Chlorinated ethenes . . . . .	39
6.2.2 Volatile fatty acids . . . . .	44
6.2.3 Iron . . . . .	46
6.2.4 Sulphate . . . . .	48
6.2.5 Redox parameters . . . . .	51
6.2.6 pH . . . . .	51
<b>7 Discussion and Perspectives</b>	<b>52</b>
7.1 BiRD . . . . .	52
7.2 BiRD + ERD . . . . .	53
7.3 ERD . . . . .	53
7.4 Pilot-scale implementation . . . . .	54
7.5 Perspectives . . . . .	55
<b>8 Conclusion</b>	<b>56</b>
<b>Appendices</b>	
<b>A Appendix A</b>	<b>77</b>
A.1 Other remediation techniques . . . . .	77
A.1.1 Green rust (GR) . . . . .	77
A.1.2 Zero Valent Iron (ZVI) . . . . .	77
A.1.3 Combined ZVI-Biotic Systems . . . . .	78
A.2 Grain size . . . . .	79
A.3 Reagent calculations . . . . .	80
A.3.1 Hydrogen consumption . . . . .	80
A.4 Experimental setup . . . . .	82
A.4.1 GeoForm to water ratio . . . . .	82
A.4.2 KB-1 . . . . .	83
A.4.3 Oxygen . . . . .	84
A.5 Sampling frequency and instruments . . . . .	84
A.5.1 Chlorinated ethylenes and ethanes . . . . .	85
A.5.2 Gas analysis . . . . .	85

A.5.3 VFA . . . . .	85
A.5.4 Anions . . . . .	85
<b>A.6 Results . . . . .</b>	<b>87</b>
A.6.1 Molar fraction of CE . . . . .	91
A.6.2 Manganese . . . . .	97
A.6.3 Nitrate . . . . .	97
A.6.4 NVOC . . . . .	100
<b>B Appendix B</b>	<b>103</b>

## LIST OF FIGURES

2.1 Batch test design . . . . .	4
3.1 Conceptual illustration for back diffusion of reactive contaminant from a stratified low-permeability aquitard with internal contaminant sources [Ding et al., 2025]. . . . .	7
3.2 Biotic pathway under anaerobic conditions [C. B. Ottosen, 2020] . . . . .	9
3.3 Possible pathways for the reductive dechlorination of chlorinated ethenes by iron sulphides [Lee et al., 2002; Han et al., 2012] . . . . .	11
3.4 Recirculation system configuration for engineering ISBGT [Darlington and Rectanus, 2015] . . . . .	14
3.5 Degradation pattern for CE; biotic vs abiotic [Darlington and Rectanus, 2015]	14
4.1 Geology of the Naverland site [COWI, 2023] . . . . .	18
4.2 cDCE plume in Naverland (in m/DVR90) [Sø, 2023] . . . . .	20
5.1 Limestone blocks in Faxe Kalkbrud . . . . .	23
5.2 Results from the monitoring of the pollution spread in 2023 shown as sum concentrations of all chlorinated solvents (in µg/l). Screen 1 is the deepest screen and screen 4 is the uppermost screen. The yellow line shows the approximate course of the geological section presented in Figure 4.2 [Sø, 2023].	24
5.3 Set up for groundwater extraction . . . . .	25
5.4 Groundwater from the field a few days after extraction . . . . .	26
5.6 Procedure for experimental set up . . . . .	28
5.7 Addition of KB-1 to batch D1 . . . . .	30
6.1 Appearance of all the microcosms on at the start of the experiment . . . . .	36
6.2 On day 3 GeoForm (B) and GeoForm + KB1 (C) look similar . . . . .	37
6.3 Comparison of the microcosms on Day 23 . . . . .	38
6.4 GeoForm (B) and GeoForm + KB1 (C) on day 43, B1 darkened . . . . .	38
6.5 Average cDCE concentration of all the batches over time. On day -22, ELS was added and day -12, KB-1 was added only to batch D (KB-1) and then on day 0, GeoForm was added to batch B and GeoForm and KB-1 was added to batch C . . . . .	40

---

6.6 Average VC levels and ethene level in the control, GeoForm and GeoForm + KB-1 batches. The ethene level was only for day 51 . . . . .	40
6.7 Average chlorinated ethenes and ethene concentration in KB-1 batch. ELS was added on day -22, and KB-1 was added -12 and day 0 . . . . .	41
6.8 cDCE degradation rate in the KB-1 batch . . . . .	42
6.9 VC degradation rate in the KB-1 batch . . . . .	43
6.10 VFA levels in the controls over the 38 days . . . . .	45
6.11 acetate levels in the GeoForm batches over the 38 days . . . . .	45
6.12 acetate levels in the GeoForm + KB-1 batches over the 38 days . . . . .	45
6.13 acetate levels in the KB-1 batches over the 38 days . . . . .	46
6.14 Average dissolved iron in the biotic control and KB-1 batches over time . . . . .	47
6.15 Dissolved iron in the GeoForm containing batches over time (note the axis) . . . . .	47
6.16 Sulphate concentration over time in the biotic controls . . . . .	49
6.17 Sulphate concentration over time in the GeoForm batches (note the axis) . . . . .	49
6.18 Sulphate concentration over time in the GeoForm + KB-1 batches (note the axis) . . . . .	50
6.19 Sulphate concentration over time in the KB-1 batches . . . . .	50
6.20 average pH over time . . . . .	51
A.1 Batch test bottles after the limestone settles . . . . .	79
A.2 Vials of water extracted after the limestone settles . . . . .	79
A.3 Addition of groundwater to the batches . . . . .	82
A.4 Results of dissolving GeoForm powder in varying water quantities . . . . .	83
A.5 GeoForm and ELS Microemulsion prepared for batches B and C . . . . .	83
A.6 KB-1 comparison . . . . .	84
A.7 Sampling frequency and volume . . . . .	84
A.8 Batch B1 and B3 on day 57, showing darkening of B3 similar to B1 on day 43	87
A.9 ISTD Area is the internal standard . . . . .	88
A.10 cDCE levels in the control batches over time . . . . .	89
A.11 cDCE levels in GeoForm batches over time, on day 0, ELS Microemulsion and GeoForm was added . . . . .	89
A.12 cDCE levels in GeoForm + KB-1 batches over time, on day 0, ELS Microemulsion, KB-1 and GeoForm was added . . . . .	90
A.13 cDCE levels in KB-1 batches over time . . . . .	90
A.14 Molar fraction of control over time . . . . .	91
A.15 Molar fraction of GeoForm over time . . . . .	91
A.16 Molar fraction of GeoForm+KB-1 over time . . . . .	92
A.17 Molar fraction of KB-1 over time, without ethane or ethene except for day 73 (day 51 if. Ethene probably formed . . . . .	92
A.18 VC levels in the control batches . . . . .	93

A.19 VC levels in the GeoForm batches. The outliers seen in B1 and B3 were ignored and not considered because it was not seen on day 51 and there was no ethene formation for it to be degradation and in this microcosm would have to be abiotic, if any. The interferences in the VC measurements is also a reason the error bars are not in all points of the GeoForm-containing batches.	94
A.20 VC levels in the GeoForm+KB-1 batches . . . . .	95
A.21 VC levels in the KB-1 batches . . . . .	96
A.22 Average Mn concentration over time in the GeoForm containing batches (batch B and C) . . . . .	97
A.23 Nitrate levels over time in the control batches . . . . .	97
A.24 Nitrate levels over time in GeoForm batches . . . . .	98
A.25 Nitrate levels over time in the GeoForm + KB-1 batches . . . . .	99
A.26 Nitrate levels over time in the KB-1 batches . . . . .	99
A.27 NVOC levels in batch A, only points below the red line should be considered	100
A.28 NVOC levels in batch B, only points below the red line should be considered	101
A.29 NVOC levels in batch C, only points below the red line should be considered	101
A.30 NVOC levels in batch D, only points below the red line should be considered	102
B.1 Geology of the Naverland site COWI, 2023 . . . . .	104
B.2 The transect of the geology cross-section shown in Figure 4.1 from COWI, 2023	105
B.3 Smaller scale geology of the site COWI, n.d. . . . .	106

## LIST OF TABLES

3.1	Physical and chemical properties of TCE, cDCE, and VC . . . . .	5
3.2	Soil and groundwater quality criteria in Denmark . . . . .	8
3.3	Common amendments used in ISBGT engineered systems [Darlington and Rectanus, 2015] . . . . .	13
3.4	Time period for the mechanism of ISBGT [Darlington and Rectanus, 2015] . .	13
5.1	CE concentrations from borehole M1 (200.5730) in all screens in October 2024 GEUS, n.d. . . . .	23
5.2	Reagents used in each batch . . . . .	27
5.3	Sampling frequency for each parameter . . . . .	31
6.1	Sulphide concentration [mg/L] in all batches on day 57. "nd" indicates below detection limit . . . . .	48
A.1	The calculated maximum hydrogen consumption in moles for a batch con- sisting 1000 mL groundwater. . . . .	80
A.2	The calculated maximum hydrogen consumption in moles for a batch con- sisting 1000 mL groundwater. . . . .	81
A.3	NVOC levels [mg/L] in all 12 batches throughout the experiment . . . . .	100

## ACRONYMS

$K_d$	Soil-Water Distribution Coefficient. (p. 6, 34)
$K_{oc}$	Organic Carbon-Water Partition Coefficient. (p. 6)
$K_{ow}$	Octanol-Water Partition Coefficient. (p. 6)
<b>BiRD</b>	Biogeochemical Reductive Dechlorination. (p. 2–4, 12, 52, 53, 55, 56)
<b>cDCE</b>	cis-1,2-Dichloroethylene. (p. xiii, xiv, xvi, 1, 2, 4–6, 8, 10–12, 14, 20, 22, 23, 25, 31, 34, 39–42, 44, 52, 54, 56, 77, 79, 89, 90)
<b>CE</b>	Chlorinated Ethylenes. (p. xvi, 1, 2, 6, 8, 13–15, 20, 23, 27, 32, 34, 39, 52–55, 77)
<b>CSIA</b>	Compound-Specific Isotope Analysis. (p. 78)
<b>DCE</b>	Dichloroethylene/DiChloroethene. (p. 2, 6, 8, 9, 15, 77)
<b>DNAPLs</b>	Dense Non-Aqueous Phase Liquids. (p. 1, 2)
<b>DVR90</b>	Dansk Vertikal Reference 1990. (p. xiii, 17, 20)
<b>ERD</b>	Enhanced Reductive Dechlorination. (p. 2–4, 16, 21, 22, 52–56, 78)
<b>FLUTE</b>	Flexible Liner Underground Technologies. (p. 19)
<b>GR</b>	Green Rust. (p. 11, 15, 16, 77)
<b>ISBGT</b>	In-Situ BioGeochemical Transformation. (p. xiii, xvi, 2, 12–14, 21, 52)
<b>ISCR</b>	In-Situ Chemical Reduction. (p. 78)
<b>LNAPLs</b>	Light Non-Aqueous Phase Liquids. (p. 1)
<b>mbs</b>	metres below surface. (p. 19–21, 78)
<b>MNA</b>	Monitored Natural Attenuation. (p. 56, 78)
<b>NAPLs</b>	Non-Aqueous Phase Liquids. (p. 1)
<b>NVOC</b>	Non-Volatile Organic Compounds. (p. 31–33, 48, 54, 55, 100)

<b>OHRB</b>	Organohalide-respiring Bacteria. ( <i>p. 10, 15, 78, 79</i> )
<b>PCE</b>	Perchloroethene/tetrachloroethylene. ( <i>p. 2, 8–11, 15, 16, 19, 20, 25, 78</i> )
<b>PFAS</b>	Per- and polyfluoroalkyl substances. ( <i>p. 1</i> )
<b>SRB</b>	Sulfate-Reducing Bacterium. ( <i>p. 12, 15, 22, 35, 36, 48, 53, 55, 56, 78</i> )
<b>TCA</b>	Trichloroethane. ( <i>p. 19</i> )
<b>TCE</b>	Trichloroethylene. ( <i>p. xvi, 2, 5, 8–11, 15, 19, 20, 25, 77, 78</i> )
<b>VC</b>	Vinyl Chloride. ( <i>p. xiv, xvi, 2, 4, 5, 8–10, 12, 16, 20, 23, 25, 31, 39, 40, 52–54, 56, 77, 78</i> )
<b>VFAs</b>	volatile fatty acids. ( <i>p. 21, 31–33, 44, 54, 55</i> )
<b>VOCs</b>	Volatile Organic Compounds. ( <i>p. 1</i> )
<b>ZVI</b>	Zero Valent Iron. ( <i>p. 2, 16, 53, 77, 78</i> )



## INTRODUCTION

Groundwater is an essential resource, supplying daily water needs for over two billion people globally. Aquifers, the geological formations storing this water, account for 99% of Earth's available freshwater [Puri, 2003]. For example, Denmark relies entirely on clean groundwater for drinking water, industrial use, and irrigation [Jorgensen et al., 2024]. Consequently, groundwater contamination represents a significant concern, necessitating rigorous monitoring and simulation of its quantitative and chemical status, aligning with EU directives to balance legal usage with natural environmental requirements [Jorgensen et al., 2024]. This highlights the urgent need for effective remediation strategies to address contamination and safeguard this vital resource for future generations [Gejl et al., 2019].

In Denmark, excluding PFAS, the group of organic pollutants exceeding regulatory limits in groundwater well inspections is chlorinated solvents [Thorling et al., 2024]. For example, cis-1,2-Dichloroethylene (cDCE) was detected in 3.9% of the wells sampled. These compounds are often poorly miscible in water and are classified as Non-Aqueous Phase Liquids(NAPLs) [Lemke et al., 2004; Thiruvenkatachari et al., 2008]. NAPLs are further divided into Dense Non-Aqueous Phase Liquids (DNAPLs) and Light Non-Aqueous Phase Liquids (LNAPLs). DNAPLs can infiltrate below the water table and migrate into underlying aquifers, particularly when the aquitard is fractured. This creates persistent zones of contamination that act as long-term sources of dissolved-phase groundwater pollution [Stroo et al., 2003; Christ et al., 2005; Popek, 2018]. Additionally, Chlorinated Ethylenes (CE) are Volatile Organic Compounds (VOCs), characterised by their significant volatility and strong resistance to degradation (depending on redox conditions) [B. Huang et al., 2014].

One-third of the total drinking water supply in Denmark is drawn from chalk and limestone aquifers, which are vulnerable to potential deterioration due to intensive abstraction as well as land use activities [Gejl et al., 2019; Sonnenborg, 2006]. Copenhagen, for instance, is underlain by semi-confined, fractured, and locally karstic carbonate rocks. In karst aquifers, water is stored in the matrix (pore spaces of the low-permeability host rock), while groundwater travels rapidly along preferential flow paths through a network of conduits

and fractures [Nilsson et al., 2018]. The transport of contaminants in such systems is heavily influenced by this dual porosity [Nilsson et al., 2018]. The fast passage of groundwater through conduits and fractures limits chemical reactions that could otherwise reduce contaminant concentrations before discharge at karstic springs or streams, making carbonate aquifers particularly vulnerable to contamination [Nilsson et al., 2018].

This thesis uses controlled laboratory experiments to study one of the largest chlorinated ethylene contaminant plume in Denmark, located at Naverland in Glostrup/Albertslund, west of Copenhagen [Sø, 2023]. This site's hydrogeology consists of a limestone aquifer beneath a clayey till layer, with contamination originating from a DNAPLs leakage. While natural attenuation, which "encompasses processes that lead to a reduction of the mass, toxicity, mobility, or volume of contaminants without human intervention", can contribute to contaminant reduction, the Naverland plume exhibits a common limitation: [Siegel et al., 2003]. Perchloroethene/tetrachloroethylene (PCE) and Trichloroethylene (TCE) often stalls at cis-1,2-Dichloroethylene (cDCE) or Vinyl Chloride (VC). The plume at this site predominantly consists of cDCE, impacting the integrity of nearby drinking water abstraction wells. Microbial degradation of DCE and VC occurs via two main mechanisms: anaerobic biodegradation, and aerobic biodegradation [Popek, 2018]. Given that the aquifer is anoxic, remediation using anaerobic biodegradation is required.

Considering the limitations of natural attenuation and the need for complete dechlorination, this thesis explores Enhanced Reductive Dechlorination (ERD) and Biogeochemical Reductive Dechlorination (BiRD) through laboratory-scale experiments. While there have been numerous cleanup solutions created and used at different locations on a pilot and full-scale basis during the past 35 years [Kueper et al., 2014], ERD is particularly relevant as ERD, in general, addresses conditions such as insufficient bacterial activity, insufficient redox conditions, competition with different bacterial communities for molecular hydrogen, or a high concentration of inhibitory substances [Stroo et al., 2003]. At the Naverland site, there is insufficient bacterial activity, more specifically, *Dehalococcoides* was below the detection limit, attributed to the mildly reducing conditions[Sørensen, 2013; C. F. Ottosen et al., 2024].

The other potential remediation approach is In-Situ BioGeochemical Transformation (ISBGT) or, more specifically, BiRD, which uses highly reduced iron minerals formed by microbial activity to facilitate chemical reduction of CE, similar to Zero Valent Iron (ZVI) [Kennedy et al., 2006]. The typical minerals are iron sulfides; mackinawite ( $FeS$ ) and pyrite ( $FeS_2$ ) [Darlington and Rectanus, 2015]. The iron and sulfate are usually naturally present in the aquifer, but might also be supplemented [Kennedy et al., 2006]. BiRD relies on common sulfate-reducing soil bacteria to facilitate the conversion of ferrous iron into iron sulfides [Kennedy et al., 2006]. Though this thesis is limited to lab-scale experiments, the results could provide insights for future field applications. Unlike ZVI, finer-grained ZVI,

BiRD, and ERD do not require excavation and backfill or trenching to be put into the subsurface and can be injected, a significant advantage for remediating deep limestone aquifers such as the one at the Naverland site [Vidic, 2001; Thiruvenkatachari et al., 2008]. The distinction lies in their delivery mechanisms: while micro-scale ZVI (mZVI) and nano-scale ZVI (nZVI) are particle injections, BiRD and ERD are injected as dissolved compounds, which could affect the distribution .

## OBJECTIVES

The overall purpose of this thesis is to provide specific knowledge on the potential for biogeochemical remediation of chlorinated solvents in chalk aquifers using the plume originating from Naverland 26AB, Albertslund by:

- Assessing the feasibility of using iron-bearing minerals to remediate limestone aquifers contaminated with cis-1,2-dichloroethylene cDCE.
- Assessing the feasibility of using ERD to remediate limestone aquifers contaminated with cis-1,2-dichloroethylene cDCE.
- Developing and performing batch tests quantifying the cDCE and VCdegradation rates ([Figure 2.1](#)).

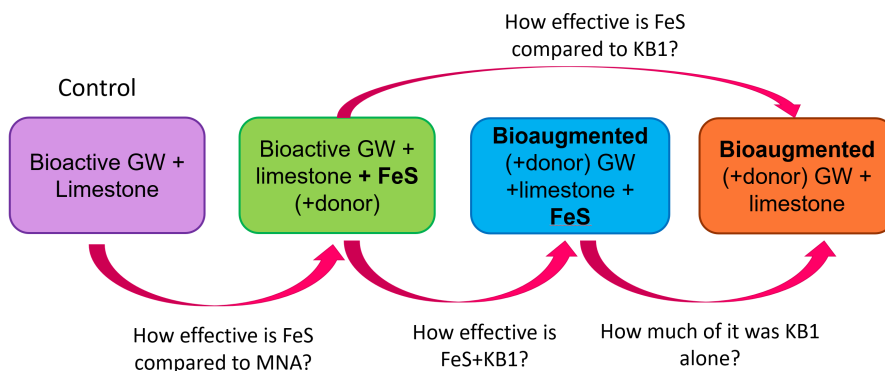


**Figure 2.1:** Batch test design

- Analyse the results of the batch experiments in relation to existing literature and site-specific conditions to identify key factors influencing DCE degradation.
- Evaluate the effectiveness of BiRD or a combination of BiRD and ERD based on the experimental results and reflect on a pilot field project for the implementation of the most promising approach.

# DCE DEGRADATION MECHANISMS AND THEIR APPLICATION TO NAVERLAND

This chapter establishes the environmental risks of cDCE by examining its properties, transport behaviour and toxicity [Section 3.1](#). This is followed by the possible remediation methods [Section 3.2](#) before focusing on the Naverland site's specific conditions to develop a site-specific strategy [Chapter 4](#).

## 3.1 DCE properties, degradation and toxicity

### 3.1.1 Properties

cDCE is a colourless, sweet-smelling light liquid that is not naturally occurring and yet can be found in both groundwater and the atmosphere [[Toxic Substances et al., 1996](#); [Dreher et al., 2014](#)]. Key properties relevant to the plume are summarised in [Table 3.1](#).

**Table 3.1:** Physical and chemical properties of TCE, cDCE, and VC.

Property	TCE	cDCE	VC
Boiling point [°C] <sup>1</sup>	86.7	60.0	-13.4
Density, 20 °C [g/cm <sup>3</sup> ] <sup>2</sup>	1.478	1.284	0.910
Vapour pressure, 20 °C [kPa] <sup>1</sup>	5.8	24.0	333.0
Water Solubility, 25 °C [mg/L] <sup>3,4</sup>	1280	3500	2700
Viscosity [Pa·s] <sup>1</sup>	$0.58 \cdot 10^{-3}$	$0.47 \cdot 10^{-3}$	$0.19 \cdot 10^{-3}$
$\log K_{OW}$ <sup>5,3</sup>	2.61	1.86	1.46
$\log K_{OC}$ <sup>4,6</sup>	1.69 - 2.66	1.61 - 1.69	2.38-2.95
Henry's Law Constant, 24.8 °C [atm·m <sup>3</sup> /mol] <sup>7</sup>	0.00958	0.00408	0.0278

<sup>1</sup> [[Dreher et al., 2014](#)] <sup>2</sup> [[Haynes, 2014](#)] <sup>3</sup> [[Horvath et al., 1999](#)] <sup>4</sup> [[U.S. Environmental Protection Agency, 2011](#)] <sup>5</sup> [[Hansch et al., 1995; Sakuratani et al., 2007](#)] <sup>6</sup> [[Brigmon et al., 1998; Chiou et al., 1998; Garbarini et al., 1986; Mouvet et al., 1993; Rathbun, 1998; Sahoo et al., 1997; Lu et al., 2011](#)] <sup>7</sup> [[Gossett, 1987](#)]

Henry's law constant quantifies the equilibrium partitioning of a compound between aqueous and gaseous phases, is fundamentally temperature-dependent. It may be defined either as the liquid-to-gas phase abundance ratio (reflecting solubility) or its inverse (reflecting volatility) [Sander et al., 2022]. For cDCE, Henry's law constant increases from 0.00178  $atm \cdot mm^3/mol^1$  at 8°C to 0.00396  $atm \cdot mm^3/mol^1$  at 24.0°C [F. Chen et al., 2012]. The associated aqueous solubility rises from 6,954 to 7,026 mg/L when temperature is increased from 8 to 21°C [F. Chen et al., 2012]. A Henry's Law constant of 0.00408  $atm \cdot m^3/mol$  (24.8 °C) indicates that cDCE might volatilize from moist soil surfaces and is expected to volatilize from dry soil due to its high vapour pressure [PubChem, 2025]. With an estimated  $K_{oc}$  of 36-49 mL/g, cDCE is highly mobile in soil and can leach into groundwater if the DCE did not directly enter the groundwater network [Chu et al., 2000; U.S. Environmental Protection Agency, 2011]. Its solubility of 3500 mg/L in water and low adsorption to soil particles ( $\log K_{ow}$  of 1.86) explain its high mobility in groundwater, contributing to the large plume at Naverland.

### 3.1.2 Natural attenuation

Natural attenuation in the groundwater aquifer is caused by naturally occurring physical, chemical and biological processes such as volatilisation, sorption, dispersion, and biodegradation [Popek, 2018]. Sorption is a process by which a substance (sorbate) is sorbed (adsorbed or absorbed) on or in another substance (sorbent)[Brusseau et al., 2019]. It involves adsorption, absorption and precipitation [Brusseau et al., 2019]. Sorption is quantified using the relationship between the concentration of contaminant in the sorbed state and the concentration in the aqueous phase, called the sorption isotherm [Brusseau et al., 2019]. The simplest is the linear coefficient  $K_d$ ; the larger this value, the more the contaminant is sorbed by the sorbent [Brusseau et al., 2019]. The  $K_d$  for chlorinated solvents in a limestone aquifer is low [Miljøstyrelsen, 1998]. According to the calculations performed by Salzer, 2013 in their master's thesis, it was 0.03  $LKg^{-1}$  for DCE [Salzer, 2013]. The degree of sorption is primarily governed by the intrinsic properties of the chlorinated solvent (e.g., solubility and polarity) and the characteristics of the aquifer material itself (e.g., organic carbon content and clay-fraction content) [Cwiertny et al., 2010]. To a lesser extent, the geochemical conditions of the aquifer, such as pH, temperature, ionic strength, and the presence of other dissolved chemicals, can also modulate sorption processes [Cwiertny et al., 2010]. As a consequence of these interactions, CE often migrate at velocities slower than that of the surrounding groundwater, a process termed retardation [Cwiertny et al., 2010]. The retardation in the matrix, expressed by the retardation factor  $R_m$ , is moderate for cDCE, 1.13 in limestone aquifers calculated where the matrix porosity ( $\phi_m$ ) is 0.4 and bulk density ( $\rho_b$ ) is 1.75 [Salzer, 2013; Broholm et al., 2016.]

As previously mentioned, long-term sources of dissolved-phase groundwater pollution are created in fractured aquifers [Stroo et al., 2003; Christ et al., 2005; Popek, 2018] because as chlorinated ethene concentrations decrease in the fractures, contaminants stored within the low-permeability matrix can diffuse back into the fractures due to the establishment of a concentration gradient, a phenomenon known as back diffusion (as illustrated in Figure 3.1) [Broholm et al., 2016; Ding et al., 2025]. Lateral advection and hydrodynamic dispersion dominate in the fissure system of chalk aquifers [Little et al., 1996]. The contaminant in the microporous matrix will be attenuated as a result of sorption and diffusion of dissolved chlorinated solvents from the fractures [Jacobsen, 1991; Witthüser et al., 2003]. When flow is high, sorption processes predominate at the fracture surfaces because matrix diffusion is a comparatively slow mechanism [Rosenbom, 2005]. On the other hand, sorption processes mainly occur within the matrix for considerable mean resident periods because the matrix's accessible exchange surfaces are far more significant than the fracture's [Rosenbom, 2005].

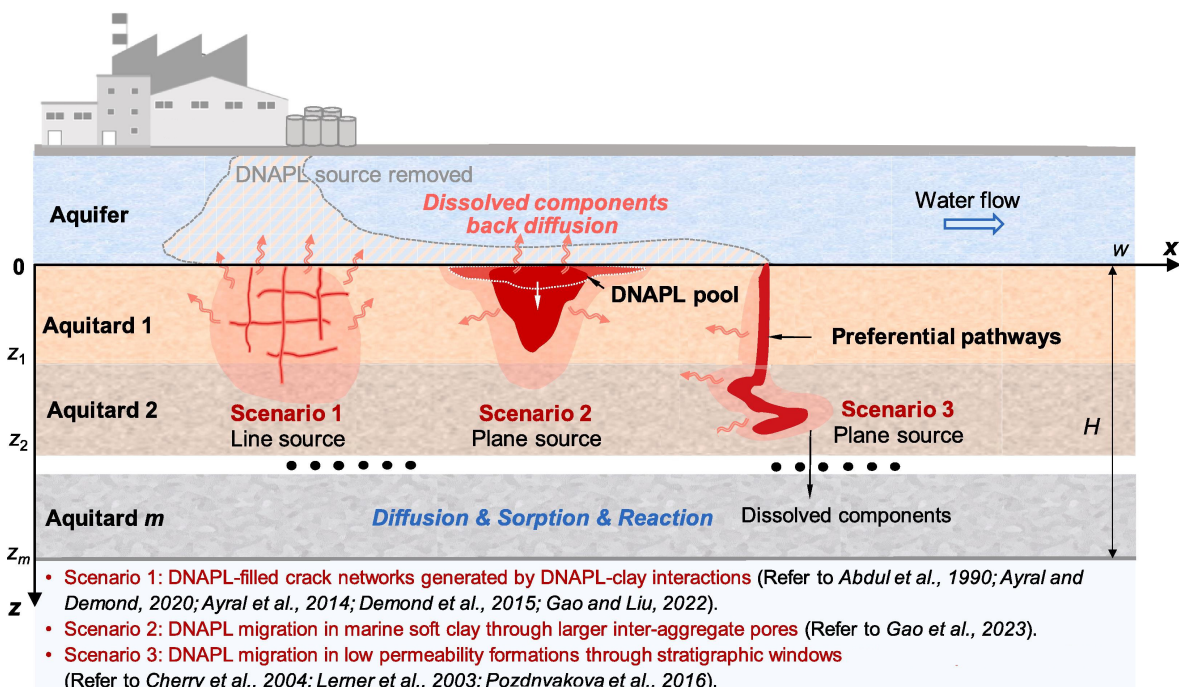


**Figure 3.1:** Conceptual illustration for back diffusion of reactive contaminant from a stratified low-permeability aquitard with internal contaminant sources [Ding et al., 2025].

Supplementary to the matrix, there may be areas of immobile fluid in "dead-end" fractures for a network and within individual fractures (assuming flow through the fracture is channelled) [Rosenbom, 2005]. Since the impact of dispersion that may occur along the fracture walls is negligible, dispersion in the fractures is frequently ignored in pollutant transport in chalk aquifers [Reilly et al., 1994]. However, Schulze-Makuch, 2005's assessment of dispersion in aquifers with varying geology revealed significant variances in the longitudinal dispersivity for carbonates and, hence, significant on an aquifer scale.

Similar to volatilisation, biodegradation rates are governed by temperature. Temperature fundamentally controls reaction kinetics, with biological and chemical degradation typically increasing at higher temperatures within the microbial tolerance ranges; hence, microcosm studies often accelerate biodegradation by incubating at elevated temperatures with agitation, though such artificial conditions may limit direct field applicability [Henry, 2010]. pH similarly constrains biodegradation, as it must remain within species-specific thresholds for microbial activity, *Dehalococcoides* dechlorinate CE within a fairly narrow pH range of 6.5–8 [Löffler et al., 2013; Y. Yang et al., 2017]. Additionally, aquifer minerals such as oxides exhibit pH-dependent surface charges, which influence whether the surface is favourable for bacterial sorption [Scholl et al., 1992]. In contaminated groundwater, bacterial sorption was lower at low pH and higher at high pH compared to uncontaminated systems [Scholl et al., 1992].

### 3.1.3 Toxicology and ecotoxicology

Due to its volatility (Table 3.1), human exposure to chlorinated ethylenes is assumed to be inhalation from ambient and urban air or groundwater [Cichocki et al., 2016; B. Huang et al., 2014]. Chlorinated ethylenes have been studied in environmental toxicology since the mid- to late 1970s and mid-1980s and, therefore, are not classified as emerging contaminants [Lash, 2019]. Inhaled DCE has the acute effects of eye irritation, nausea, narcosis and death and unknown long-term effects in humans [Galizia et al., 2010]. VC and TCE are classified as a human carcinogen with the target tissue being the kidney for TCE while PCE is a probable human carcinogen [Cichocki et al., 2016]. P. T. McCauley et al., 1995's study showed toxicity at subacute and subchronic oral exposure levels as low as 31,988.88 µg/kg/day. Liver abnormalities were observed at 96,936 µg/kg/day, and kidney abnormalities at 31,988.88 µg/kg/day [P. T. McCauley et al., 1995]. Tests on cDCE for genetic activity in yeast (*Saccharomyces cerevisiae*) showed that it was toxic but not genetically active, even with metabolic activation [Bronzetti et al., 1984].

Fortunately, as the bioconcentration factor of DCE is estimated to be 15 to 22 and therefore does not tend to bioconcentrate in aquatic organisms based on the linear regression equations involving low  $K_{OW}$  and water solubility [U.S. Environmental Protection Agency, 2011]. Hence, the potential of DCE biomagnifying in aquatic food chains is low [U.S. Environmental Protection Agency, 2011].

**Table 3.2:** Soil and groundwater quality criteria in Denmark

CE	Soil quality criterion [mg/kg]	Groundwater quality criteria [µg/L]
TCE	5	1
DCE	85	1
VC	0.4	0.2

## 3.2 Remediation methods based on reductive dechlorination

### 3.2.1 Bioremediation

As noted in [Section 3.1.2](#), natural attenuation encompasses biodegradation, including reductive dechlorination. However, because natural attenuation is inherently inconsistent and frequently results in contaminants being only partially degraded, it is crucial to better understand the underlying degradation pathways and explore strategies for targeted improvement. Among these processes, reductive dechlorination is of particular importance for chlorinated ethenes. As a distinct anaerobic pathway, reductive dechlorination involves the stepwise removal of chlorine (Cl) atoms from the contaminant, replacing them with hydrogen (H) as shown in [Figure 3.2](#). In this process, chlorinated ethylenes act as respiration aids and electron acceptors rather than as a food source [Popek, 2018]. Consequently, an external carbon source is often required to generate electron donors (H) (through fermentation) to facilitate reductive dechlorination [Popek, 2018]. There must be a suitable ratio of electron acceptors to donors for reductive dechlorination to occur. Furthermore, the reductive dehalogenation of PCE and TCE typically occurs more readily than that of DCE and VC [Han et al., 2012; Schmidt et al., 2008]. This means that the rate of reduction is higher for PCE and TCE, and it can occur under mildly reducing conditions such as nitrate or iron-reducing conditions [Spormann, 2006]. In contrast, the degradation of DCE and VC requires stronger reducing conditions, such as sulfate-reducing or methanogenic conditions [Bradley et al., 2010; Spormann, 2006; Maymó-Gatell et al., 1999; Ballapragada et al., 1997; T. M. Vogel et al., 1985].

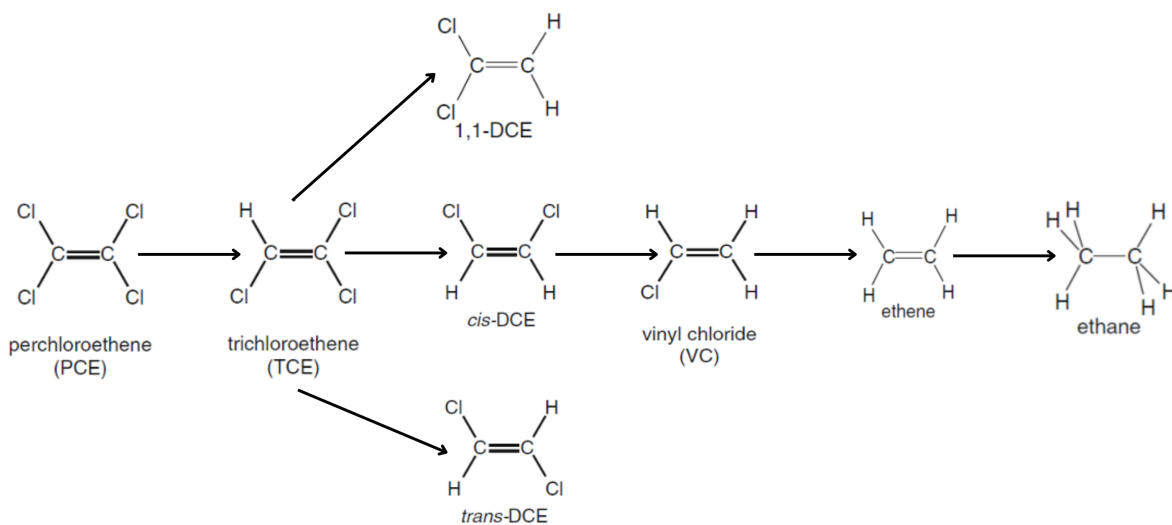


**Figure 3.2:** Biotic pathway under anaerobic conditions [C. B. Ottosen, 2020]

Bioremediation typically can be categorised into:

1. Biostimulation: enrichment of indigenous microorganisms. This is done by supplementing micronutrients and electron acceptors [Mohamed et al., 2023].
2. Bioaugmentation: enrichment with non-indigenous microorganisms [H. Huang et al., 2020].

There are several Organohalide-respiring Bacteria (OHRB), known to be able to degrade PCE and TCE [Hug et al., 2013]. Until fairly recently, *Dehalococcoides* was the only known genus that could break down cDCE and VC but then Y. Yang et al., 2017 discovered the VC reductase gene, cerA, in a *Dehalogenimonas* species. Additionally, the vcrA and bvcA genes in *Dehalococcoides* (different strains) are crucial for the complete reductive dechlorination of VC to ethene [Müller et al., 2004; Krajmalnik-Brown et al., 2004]. The presence of vrcA gene is vital for cDCE and/or VC dechlorination while bvcA gene encodes a vinyl chloride reductase that is highly effective in converting VC to ethene [Müller et al., 2004; Krajmalnik-Brown et al., 2004]. The fact that most known OHRB genomes have numerous putative reductive dehalogenase genes, but only a small number have been described, supports this discovery and suggests that there are likely further unidentified and potentially significant biomarkers [Molenda et al., 2016].

The micro-nutrients *Dehalococcoides* require is vitamin B12 (cobalamins), which are produced by other species hence, in commercially produced cultures, they consist of a community rather than a pure culture; the *Dehalococcoides* use it as an enzymatic cofactor [J. He et al., 2007]. Interestingly, using titanium citrate as a reductant and vitamin B12 (a natural cobalt-containing porphyrin) catalyses the dechlorination of CE. This is an abiotic vitamin-mediated degradation, as the heat killed the microorganisms, but it is 4 to 5 times lower than the corresponding microbiological degradation [Guerrero-Barajas et al., 2005].

Major et al., 2002 conducted a pilot-scale field test in south central Texas, United States, consisting of gravel, sand, silt, and clay, which demonstrated the dechlorination of cDCE to ethene through bioaugmentation with KB-1, a microbial consortium containing the phylogenetic relatives of *Dehalococcoides ethenogenes*. Within 200 days, PCE, TCE and cDCE concentrations in the test zone dropped below 5 µg/L, with ethene production accounting for the mass loss. A more recent study found similar results in the urban area of Suzhou, Jiangsu, China, in a site primarily consisting of silty sand, R. Wu et al., 2023 reported 99.7% of VC dechlorination to ethene within 3 months. It should be noted that this study employed thermal pretreatment, maintaining groundwater temperatures at ~30°C - a condition known to accelerate microbial dechlorination rates, as discussed in Section 3.1.2.

### 3.2.2 Biogeochemical reductive dechlorination

A handful of iron-bearing minerals have been used in kinetic batch tests studied for their abiotic dechlorination include iron sulphides (mackinawite and pyrite) [Lee et al., 2002; Weerasooriya et al., 2001], iron oxides (magnetite) [Lee et al., 2002], Green Rust (GR) (fougerite)[Lee et al., 2002; Jeong et al., 2011], and phyllosilicate clays (vermiculite and biotite) [Lee et al., 2004]. Among these, mackinawite (FeS) under anoxic conditions can effectively reduce PCE and TCE to acetylene as the main product [Butler et al., 1999], while pyrite degrades more slowly [Tobiszewski et al., 2012]. Figure 3.3 shows the possible pathways for reductive dechlorination. According to Liang et al., 2009, chloride GR and pyrite are more effective at PCE and TCE degradation than sulphate GR, magnetite and goethite. Therefore, this work focuses on iron sulphides, as they demonstrate superior degradation efficiency compared to other iron-bearing minerals. However, the field study conducted by Darlington, Lehmicke, et al., 2013 in southern California, United States, reported that pyrite is not likely the mineral involved in transforming cDCE, although it was abiotically under anaerobic conditions in a sandstone aquifer. Furthermore, magnetite was identified to remove cDCE in a sandy aquifer in Minnesota; the first-order rate of attenuation over 13 years of monitoring was  $0.52 \pm 0.195$  per year for cDCE [Ferrey et al., 2004].

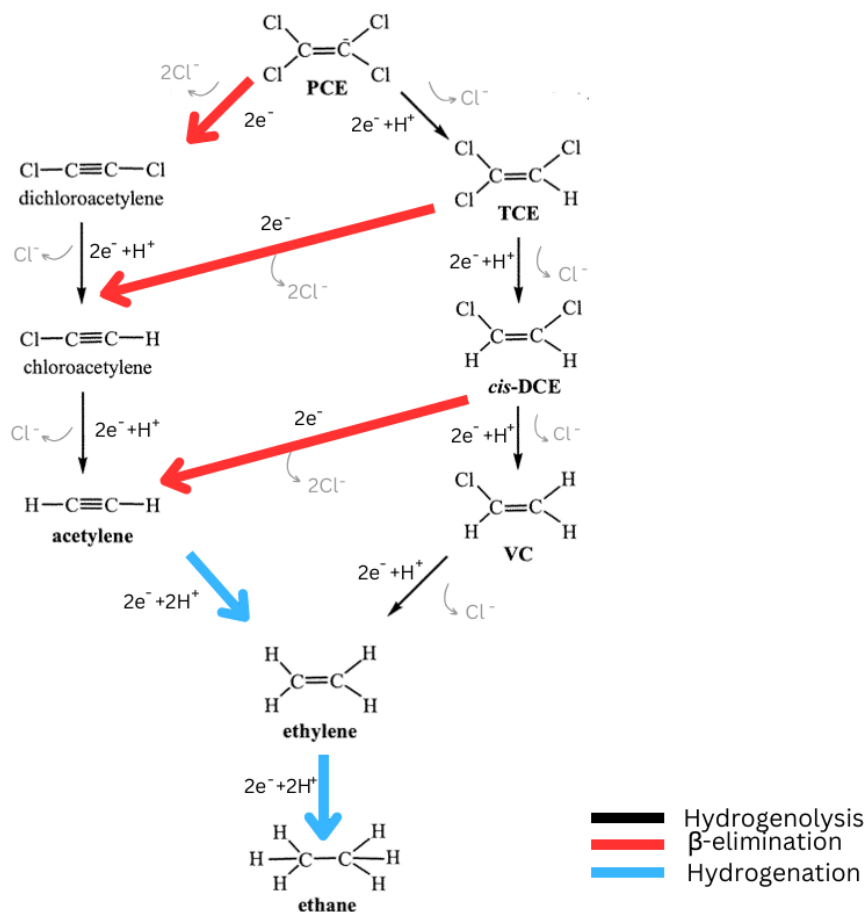


Figure 3.3: Possible pathways for the reductive dechlorination of chlorinated ethenes by iron sulphides [Lee et al., 2002; Han et al., 2012]

The pathway cDCE → acetylene (by  $\beta$ -dichloroelimination) → ethylene (by hydrogenation) → ethane (hydrogenation) is the preferred pathway as it avoids the formation of VC and only possible abiotically [Hyun et al., 2015; Han et al., 2012]. Furthermore, acetylene is energetically favourable and therefore quickly used to support microbial growth after its formation [Darlington and Rectanus, 2015].

## Iron sulphide

FeS plays a crucial role in biogeochemical processes are brought about from microbial interactions [Pósfai et al., 2006] serving as an energy source in the absence of solar irradiation and acting as a "naturally occurring electrical wire, bridging spatially discrete environments and mediates long distance extracellular electron transfer" [Kondo et al., 2015]. Furthermore, FeS is able to enter the periplasm of Sulfate-Reducing Bacterium (SRB) to accelerate electron transport [Y. Zhang et al., 2025]. FeS also act as an electrocatalyst because of its semi-conductive and/or metallic qualities, enabling electron-transfer processes and microbial metabolism [Nakamura et al., 2010; Yamamoto et al., 2013; Yamaguchi et al., 2014].

Effective ISBGT requires a balance of high sulfate loading, presence of iron oxides and sufficient organic carbon [Darlington and Rectanus, 2015; Y. T. He et al., 2015]. High loading of sulfates is reduced into hydrogen sulphide ( $\text{HS}^-$ ) by SRB [Darlington and Rectanus, 2015], who uses organic carbon as an electron donor for sulphide production. Ideally, the site is under sulphate-reducing conditions and avoids supporting competitive methanogenic bacteria [Darlington and Rectanus, 2015]. The aforementioned iron oxides present in the sediments then react with  $\text{HS}^-$  to form iron sulphides, which then dechlorinate chlorinated ethenes [Kennedy et al., 2006]. A column experiment conducted by C. Sun et al., 2025 was able to effectively suppress the competition with methanogenic bacteria through the high flux of  $\text{SO}_4^{2-}$  while also forming  $\text{FeS}$ ,  $\text{FeS}_2$ , and  $\text{Fe}_3\text{S}_4$ , which were capable of  $\beta$ -eliminating contaminants (ISBGT)

Enhanced ISBGT is the injection of amendments into the contaminated zone to promote optimal conditions for the preferred abiotic mechanism [Y. T. He et al., 2015]. BiRD is stimulated by the addition of sulphate and organic carbon [Kennedy et al., 2006]. Iron, a mineral typically present in the aquifer, might also be supplemented [Kennedy et al., 2006]. The possible amendments for ISBGT are shown in Table 3.3. Additionally, without iron oxides, the high levels of sulphides are toxic to microorganisms. For example, according to Mao et al., 2017, environments with sulphate concentration of 5 mM, had no effect on the cell yield of *Dehalococcoides* (strain 195) but decreased by about 65% in sulphide environments.

**Table 3.3:** Common amendments used in ISBGT engineered systems [Darlington and Rectanus, 2015]

Component	Bioreactors and Trench biowalls	Liquid injections
Iron	Sand with natural high iron content, Iron oxide	Iron sulfate, Iron chloride, Ferrous lactate
Sulfate	Calcium sulfate	Iron sulfate, Magnesium sulfate, Sodium sulfate, Calcium sulfate
Electron donor	Tree mulch, Cotton gin compost, Mulch coated with vegetable oil	Sodium lactate, Emulsified vegetable oil, Lecithin, Soybean oil
Additional amendments	Sand and/gravel for permeability, Buffer	Buffer

The recommended hydraulic retention time is 15 to 30 days to provide sufficient time for the FeS formation as well as the dechlorination [Darlington and Rectanus, 2015]. The engineered hydraulic residence time of the target treatment zone is controlled by the hydrogeology [Darlington and Rectanus, 2015]. The specific time period is shown in **Table 3.4** [Darlington and Rectanus, 2015].

**Table 3.4:** Time period for the mechanism of ISBGT [Darlington and Rectanus, 2015]

Biotic sulfide formation	FeS formation (precipitation)	Abiotic dechlorination
$SO_4^{2-} + 9H^+ + 8e^- = 8HS^- + 4H_2O$ $SO_4^{2-} + 2CH_2O \rightarrow H_2S + 2HCO_3^-$	$HS^- + Fe^{2+} = FeS + H^+$ $2FeOOH + 3HS^- = 2FeS + S + H_2O + 3OH^-$	$C_2Cl_4 * + FeS + 4H_2O = C_2H_2$ $+ Fe^{3+} + SO_4^{2-} + 4Cl^- + 6H^+$
Days	Instantaneous	$t_{1/2} = 30 \pm 15$ days

\*For other CE, please refer to **Figure 3.3**

ISBGT seems to work best when a recirculating injection method is used (shown in **Figure 3.4**) [Darlington and Rectanus, 2015]. Installing injection wells to add amendments and using extraction wells or points to gather groundwater, combined with the amendments, and then reinjecting them into the injection wells are both recirculation parts [Darlington and Rectanus, 2015]. Doing this continuously creates a mixing zone in the treatment area where the contaminant can come into contact with the reactive amendments [Darlington and Rectanus, 2015]. Most effective in unconsolidated geology and in groundwater plumes with high hydraulic conductivity, as excessive flow rates would prevent the reaction and restrict hydraulic retention time [Darlington and Rectanus, 2015].

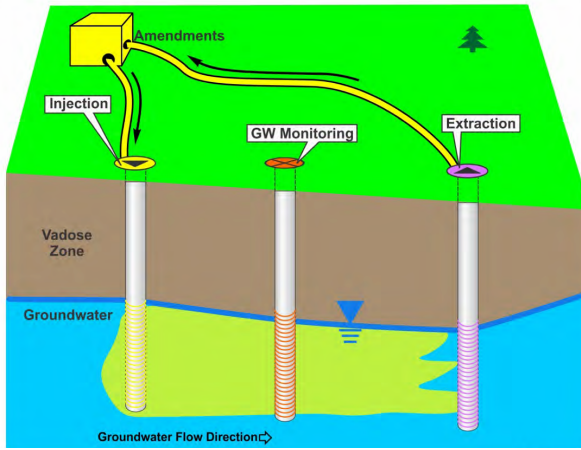


**Figure 3.4:** Recirculation system configuration for engineering ISBGT [Darlington and Rectanus, 2015]

To differentiate between abiotic and biotic degradation, Figure 3.5 shows that biological degradation is sequential dechlorination of parent followed by daughter products compared to abiotic degradation, where it is simultaneous degradation of all the CE present [Darlington and Rectanus, 2015].

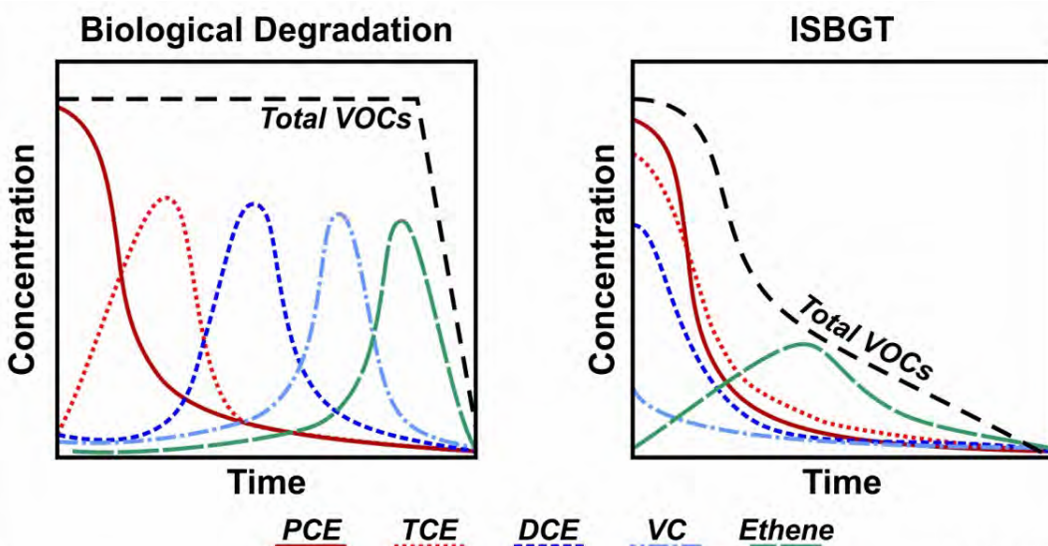


**Figure 3.5:** Degradation pattern for CE; biotic vs abiotic [Darlington and Rectanus, 2015]

There have been various laboratory tests simulating environmental conditions to figure out the optimal conditions for mackinawite synthesis and dechlorination. In Hyun et al., 2015's study, including sediments and mixing had no impact, while the higher the pH, the faster the degradation rate and the presence of citrate accelerated the dechlorination of cDCE. As frambooidal FeS has a higher surface area, hence, higher reactivity compared to crystalline FeS, citrate probably acts as an inhibitor for crystal growth [Darlington and Rectanus, 2015; Hyun et al., 2015]. Therefore, nucleation being dominant is more desired than crystal growth [Whiting et al., 2014]. Additionally, freeze-dried mackinawite is unreactive and therefore, fresh mackinawite or pyrite should be formed in the site [Hyun et al., 2015]. The cause could be aggregation development or the loss of reactiv-

ity in nano-sized mackinawite suspensions during the rinse and freeze-drying processes [Y. Chen et al., 2019]. While non-stabilized FeS could only degrade 25% of lindane ( $\gamma$ -hexachlorocyclohexane) in the same amount of time, it has been discovered that FeS nanoparticles stabilised by fungal polymer, which is produced from a basidiomycetous fungus called *Itajahia* sp., could catalyse a rapid reductive dehalogenation reaction of lindane (5 mg/L) with an efficiency of 94% in 8 hours [K.M. Paknikar et al., 2005]. When compared to bare nanoparticles, stabilised FeS nanoparticles have been shown to degrade chlorinated hydrocarbons far more effectively [Y. Chen et al., 2019].

Whiting et al., 2014 conducted a geochemical model to forecast which mineral phases go into solution (undersaturated), be in equilibrium (saturated) and precipitate out of solution (supersaturated) and found that FeS e.g. mackinawite were near equilibrium while  $FeS_2$  e.g. pyrite precipitated out of solution in all sites. Furthermore, the previously mentioned nucleation is supported in this environmental condition [Whiting et al., 2014]. The study used electron microprobe analyses to determine the composition and grain size of Fe-bearing species (iron monosulfides, iron disulfides, GR, etc) as well as its dechlorinating potential.

### 3.2.3 Combination of biotic and abiotic remediation

The effect of FeS on OHRB-mediated (i.e., *D. mccartyi* CG1, *G. lovleyi* LYY) dechlorination through batch experiments was studied by Liu et al., 2023 in soil (brown, laterite, black, and paddy soil, river sediment and SiO<sub>2</sub>). Acetate was used as a carbon source and the pH was 7.2. The results were interesting; Pure cultures of *Dehalococcoides mccartyi* CG1 and *Geobacter lovleyi* LYY showed a substantial inhibition of the PCE-to-DCE dechlorination process when 25 g/L FeS was added, but both tolerated 2.5 g/L of FeS. Nevertheless, these cultures showed the greatest resistance to FeS's inhibitory effects when they were mixed together in a microcosm. The development of flocs or biofilms, which may protect *Geobacter* and *Dehalococcoides* from direct exposure to FeS, may be the cause of this enhanced tolerance. FeS may hinder OHRB-mediated dechlorination, but OHRB can also affect FeS-mediated abiotic dechlorination by changing the products of dechlorination. To elaborate, biotic PCE-to-DCE dechlorination had greater percentages of acetylene than abiotic controls, suggesting that OHRB-mediated dechlorination may help FeS-mediated acetylene synthesis by supplying intermediates such as DCEs and/or TCE. Furthermore, by regenerating FeS, the enrichment of *Desulfovibrio*, a SRB that can reduce  $SO_4^{2-}$  and  $Fe^{3+}$  may enhance abiotic PCE-to-acetylene dechlorination. By blocking direct interaction between FeS and OHRB cells, organic matter (e.g. humic substance) and the formation of biofilms or flocs may also lessen the inhibition of OHRB caused by FeS. Therefore, these biotic and abiotic mechanisms most likely work together to dechlorinate CE in soil overall. Likewise, a study by Yaru Li et al., 2021 demonstrated that *in-situ* formed FeS nanoparticles (0.2 mM  $Fe^{2+} + S^{2-}$ ) enhanced TCE dechlorination by *Dehalococcoides mccartyi* strain 195, increasing rates from  $25.46 \pm 1.15$  to  $37.84 \mu mol \cdot L^{-1} \cdot day^{-1}$  as well as the abundance of key genes. These results suggest low FeS concentrations may stimulate Dhc 195's electron transport.

Similar to Liu et al., 2023's observation, dechlorination rate of TCE was inhibited slightly at 0.6 mM (higher concentrations). This study also showed that the ratios of  $\text{Fe}^{2+}/\text{S}^{2-}$  (i.e., 0.5, 1, and 2) had negligible effects on TCE dechlorination rates, possibly due to the similar electrical conductivity of each iron–sulfur compounds. Yoshikawa et al., 2021 studied reductive dechlorination of PCE with a groundwater sample *Dehalococcoides* and 2 mg/L of iron. When 28 mg/L of ferrous iron was supplied, the time required for complete dechlorination of 1 mg/L of PCE decreased 84 to 49 days.

In summary, whilst biotic degradation carries the inherent risk of VC accumulation, abiotic or abiotic + biotic degradation doesn't. Though GR shows higher surface-normalised rate constants in some cases, it is unstable, pH-dependent and cannot be used in freeze-dried form; therefore, it is not available as a commercial product, limiting its practical application at this site [Han et al., 2012; Moreno et al., 2007; Lee et al., 2002]. Granular ZVI is constrained by reactivity primarily at the particle surface interface. In contrast, the reductive mineral zone established through FeS formation can extend a significant distance down-gradient, facilitating broader contaminant interaction [EVONIK, n.d.(a)]. Furthermore, FeS enhances ZVI performance when combined through sulfidation, improving electron-mediated dechlorination without the limitations of pure ZVI systems; however, as this site does not have a high concentration of sulfate, sulfate would need to be added [N. Wu, Yi Li, et al., 2025; Guo et al., 2023; Islam et al., 2021]. ZVI can also be combined with lactic acid to accelerate the initiation of biotic dehalogenation using the intrinsic reductive capabilities of ZVI [N. Wu, Yi Li, et al., 2025; Herrero et al., 2019]. Both ZVI combinations would be useful for this site if it can be injected. Another combination is composite material Carbo-Iron, which combines colloidal activated carbon and nano-ZVI (nZVI) to accumulate PCE for ERD, but the site being studied here is slightly deeper than Katrin et al., 2016's, and they had a higher pH. A more detailed discussion of these alternative methodologies can be found in Section A.1

## SITE: NAVERLAND

### 4.1 Geology and Hydrogeology

Naverland 26AB is situated in Vestegnen, Herstedøster's industrial district. With an elevation of roughly +21.5 m/DVR90, Vestegnen is a topographically flat region [Hovedstaden, 2007]. The regional geological settings are shown in Figure 4.1. The moraine clay at Naverland 26AB can be divided into two units: a coarse-elastic lower unit and a fine-grained upper unit [COWI, 2023]. Followed by a broad layer of sand and gravel with the limestone beneath [COWI, 2023]. The upper metre of the Bryozoan limestone is thought to have been crushed [COWI, 2023]. The transect of this profile is in Appendix B. Bryozoan limestone consists of skeletal fragments of bryozoans, the size of sand to silt, mixed with subordinate amounts of lime mud and clay [Andersen et al., 2018]. Additionally, chalk can be found beyond -30m/DVR90 [GEUS, n.d.] (map in Appendix B). To distinguish, chalk is a soft, nearly white, fine-grained formation that is poorly or unlithified and pure calcilutite, while limestone is a more general term [Bromley, 1979]. To be more specific, on this site, there is Cretaceous (Maastrichtian) chalk, which is a carbonate mudstone composed primarily of calcareous nannofossils (especially coccoliths) [Jakobsen et al., 2017].

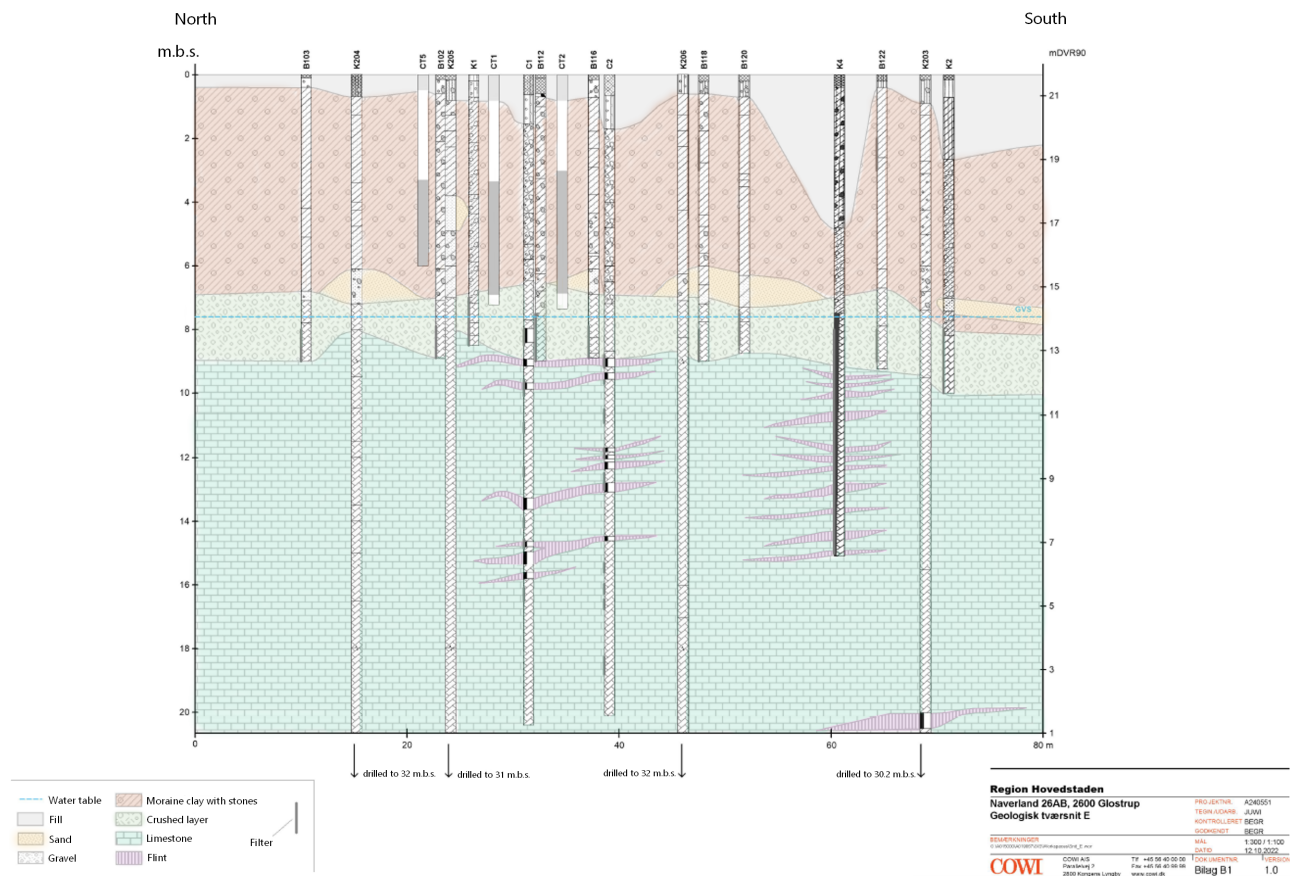


Figure 4.1: Geology of the Naverland site [COWI, 2023]

The limestone's bulk density ranges from 1.42 to 2.36 g/cm<sup>3</sup>. It has a high porosity, which ranges from 13% to 48% (average 33% in boreholes at the source, C1-C3). Larger flint layers are typically located in the upper 2-4 m but have also been discovered down to 19 metres below surface (mbs) in C3 [Broholm et al., 2016]. According to Broholm et al., 2016, the hardness of the limestone increases with depth, and cracks are more widespread in the soft portions of the limestone, near flint layers, or inside thick hard limestone zones. While the crushed layer is mostly saturated (largely porous groundwater flow) and in hydraulic contact with the underlying primary reservoir in the limestone (primarily fracture transport), the moraine clay is primarily unsaturated.

Naverland is situated on a regional groundwater divide and in a location with a small water table gradient (1-2% in a northeasterly direction and 2-3% in a southeasterly direction). North of the source area the flow direction is northeast towards Glostrup Forsyning's abstraction in Vestskoven and near Ejby, and south of the source area the flow direction is south and southeast [Sø, 2023]. While the flow in the limestone is horizontal, the main dispersion path of infiltrating groundwater is downward towards its primary reservoir. The primary reservoir's predominant flow direction is northeast when local groundwater subsidence is omitted. According to slug and pump tests, the hydraulic conditions in the crushed layer at the source site vary significantly, with hydraulic conductivities ranging from  $5 \cdot 10^{-4} \text{ m/s}$  to  $3 \cdot 10^{-6} \text{ m/s}$  [COWI, 2023; Damgaard et al., 2012]. The hydraulic conductivity for the top 10 meters of limestone ranges from  $1 \cdot 10^{-4} \text{ m/s}$  to  $2.3 \cdot 10^{-4} \text{ m/s}$  [COWI, 2023; Damgaard et al., 2012]. When pumped from K11, the flow rate is roughly 150 m/yr [Damgaard et al., 2012; COWI, 2023]. According to earlier estimates, the flow rate in the upper portion of the limestone is between 1 and 16 m/yr [Hedeselskabet, 2002]. The natural seasonal variation in the water table is approximately 1.2 m [Sø, 2023]. FLUTe® transmissivity profiles were conducted in C1–C3 to further understand the vertical variation in hydraulic conductivity, revealing potential fracture sites and preferred flow routes [Damgaard et al., 2012; Broholm et al., 2016]. The geological layers in the source site are expected to be the same for the plume [C. F. Ottosen et al., 2024].

## 4.2 Contamination

From 1965 to 1982, the company Ingolf Jacobsen resold chlorinated solvents, handling an estimated 500 ton PCE, 1500 ton TCE and 200 ton Trichloroethane(TCA) [Sø, 2023]. PCE was stored in underground tanks, while TCE and TCA was traded in unbroken drums [C. F. Ottosen et al., 2024]. In 1977, the original tank was replaced with a new, larger one, which was used till 1982, when it was emptied and filled with sand. According to Hedeselskabet, 2002, the site has contaminated soil and groundwater around the tank for storing PCE at levels indicating the presence of a free phase. Hence, it is reasonable to assume there was improper handling or disposal of PCE, e.g. spills, leaks or incomplete emptying, especially since the storage and handling practices were probably not as strict as modern standards

[Sørensen, 2013]. CE are most frequently used as degreasing solvent in the metal industries as well as cleaners and adhesives [Goodman et al., 2022]. Nearby, there were dry cleaning and industrial painting operations where chlorinated solvents were also used [Sø, 2023]. PCE and TCE have degraded to DCE under anaerobic conditions, resulting in a maximum cDCE concentration of 7100 µg/l in the groundwater [Goodman et al., 2022; Sø, 2023]. The contamination has spread over 1.8 km from the source to the primary limestone aquifer [Sø, 2023]. Additionally, hydraulic contamination control is maintained by remedial pumping in the source area, which forms a local subsidence funnel that draws water from the crushed layer and the top 10 meters or so of the limestone [Sø, 2023]. Additionally, there has been continued extraction since 2017 from Glostrup Forsyning's borehole 200.4416 for Ejby, this has led to the cDCE concentration in borehole 200.3705 (Ejby 1), which is 2.5 km away from the source area, to rapidly increase, currently at 2.2 µg/L, which is above the threshold for drinking water [Sø, 2023]. However, boreholes 200.5308 (K21), 200.5728 (M2) and 200.5730 (M1) are unaffected by the 2 extractions. M2 is located south of the source area, while boreholes M1 and K21 are located northeast of the source area (K21 furthest from the source area).

The well M1 is to be sampled because, as shown in Figure 4.2 (in m/DVR90), this well has the highest concentration of cDCE in the plume between +4.69 and +2.69 m/DVR90 (18 and 20mbs) [GEUS, n.d.]. At this depth, the cDCE concentration was 200 µg/L in October 2021 but has decreased to 150 µg/L in October 2024 (PCE: <0.02 µg/l, TCE 0.054 µg/l, VC 2,1 µg/l and TCA <0,02 µg/l) [GEUS, n.d.].

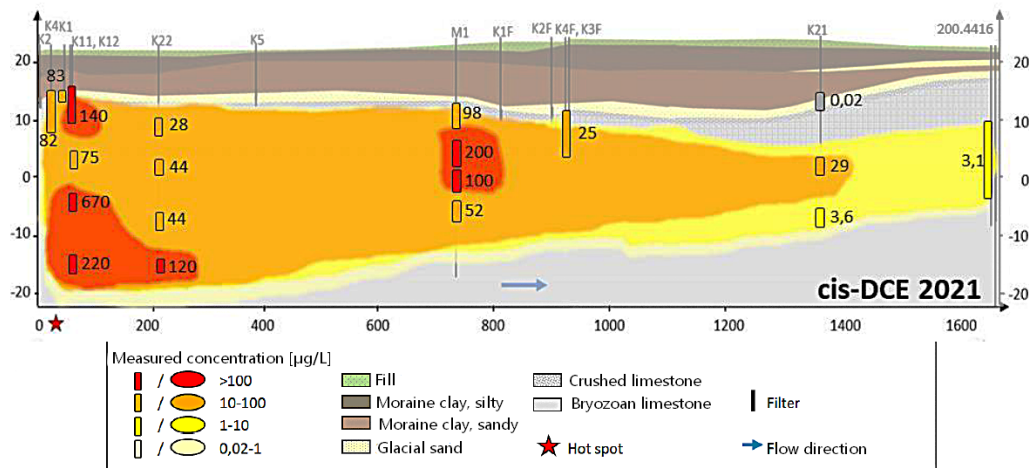


Figure 4.2: cDCE plume in Naverland (in m/DVR90) [Sø, 2023]

### 4.3 Remediation strategies

A student project consisting of biostimulation was done by Sørensen, 2013 using lactate, groundwater and sediment samples from the Naverland site, but no degradation of cDCE was observed. This is because *Dehalococcoides* were below the detection limit due to the mildly reduced redox conditions [Sørensen, 2013]. When Sørensen, 2013 carried out bioaug-

mentation using the bacteria in KB-1® (SiREM) (containing *Dehalococcoides*) at 15 mbs and was successful at reaching complete dechlorination at day 85, showing that there is a potential for using ERD at the site. The study also highlighted the importance of limestone for the degradation to occur. Fortunately, in Sørensen, 2013's experiment, no methane was produced. This was the case because KB-1® (SiREM) cannot use acetate as a donor, and therefore, methanogenesis (the fermentation of acetate to  $CO_2$  and  $CH_4$ ) does not occur [Duhamel et al., 2004]. Additionally, methanogens may compete with *Dehalococcoides* for the H from the donor. Lack of methane production is desired because the methane will escape out of the groundwater if it comes into contact with the air [Chilingar et al., 2005]. There is a risk of fire or explosion if this takes place indoors or in a small area and the amount of methane in the air reaches 5% [Chilingar et al., 2005].

As previously mentioned, injection systems are the only feasible option for the Naverland site; liquid amendments (listed in Table 3.3) would be injected into permanent wells [Darlington and Rectanus, 2015]. This thesis uses the commercial product available, GeoForm® Soluble, which is a soluble sulfate and ferrous iron mix added to an emulsified organic carbon substrate (ELS® Microemulsion was made using ELS® Concentrate, a 25% organic carbon substrate) [EVONIK, n.d.(b)]. This amendment, therefore, provides iron, sulfate, electron donors, pH buffer, and nutrients for ISBGT [EVONIK, n.d.(b)]. ELS® products contain approximately 90 % lecithin (common formula for lecithin is:  $C_{42}H_{80}NO_8P$ ) and approximately 10% surfactant and release volatile fatty acids (VFAs) such as lactic, propionic and butyric when bacteria ferment it [EVONIK, n.d.(b)]. The scope of this thesis does not include considerations of the contamination in the hot spot, the plume extending south-east and west of the site, or the low concentration of contamination by 1,1,1-trichloroethane.

## METHODOLOGY

This study evaluates GeoForm® and ERD (KB-1®) for enhanced biodegradation of cDCE through batch tests with bioactive groundwater and limestone. The bioactive groundwater is essential because the system relies on SRB to generate *in situ* iron sulphide (FeS), which is critical for abiotic dechlorination. Limestone was included in all the batch tests because the study by Sørensen, 2013 indicated that limestone is essential for initiating dechlorination and possibly influences contaminant availability through matrix diffusion and surface interactions. While Hyun et al., 2015 found no impact of sediment with pre-synthesised FeS, this system is SRB-driven and relies on *in situ* FeS precipitation, where limestone's dual-porosity (fracture/matrix) and carbonate buffering may assist microbial FeS formation and degradation kinetics. Four experimental conditions were established (refer to Figure 2.1): Scenario A serves as the biotic control with only bioactive groundwater to simulate natural attenuation; Scenario B combines bioactive groundwater with GeoForm® (primarily ferrous sulfate monohydrate, which reduces to FeS) and ELS® liquid concentrate as electron donors for SRB; Scenario C tests potential interactions between GeoForm® and KB-1® to identify synergistic or inhibitory effects; while Scenario D contains only KB-1® with bioactive groundwater as a reference for comparing stand-alone bioaugmentation performance against the GeoForm®-amended systems. This design enables the evaluation of abiotic (FeS-mediated) and biotic (Dehalococcoides-driven) degradation pathways under controlled batch conditions, with limestone present in all scenarios to maintain consistency with prior findings. The comparison clarifies GeoForm®'s individual contribution and its combined effects with biological treatment approaches.

### 5.1 Field sampling and storage

Limestone blocks were collected from Faxe Kalkbrud, an active limestone excavation site where rock samples are openly accessible for collection from exposed quarry walls and debris piles, eliminating the need for digging. In contrast, obtaining limestone from the Naverland site would require invasive drilling due to its unexcavated subsurface deposits. Although Naverland's native sediments would be ideal for bioremediation, given their inherent anaerobic conditions, organic carbon content, and diverse microbial communities

[Himmelheber et al., 2007], the logistical constraints made Faxe Quarry a practical alternative. Geologically, both sites share comparable bryozoan-dominated cool-water carbonate deposits, with Danian limestone overlying Maastrichtian chalk and containing flint nodules/layers [Hvid et al., 2021; C. F. Ottosen et al., 2024]. The Faxe limestone thus provides an adequate surrogate, offering microbial attachment surfaces and carbonate buffering to maintain neutral pH, preventing metabolic inhibition during fermentation.



**Figure 5.1:** Limestone blocks in Faxe Kalkbrud

Groundwater was collected from screen 3 of the borehole M1 (200.5730) because it has the highest concentration of  $150 \mu\text{g/L}$  cDCE in late 2024 while still being in the plume, the location of this well and the concentration in each screen in 2023 is shown [Figure 5.2](#) and the concentration of cDCE and VC in late 2024 for each screen is shown in [Table 5.1](#).

**Table 5.1:** CE concentrations from borehole M1 (200.5730) in all screens in October 2024 GEUS, n.d.

Screen	cDCE	VC
1	$35 \mu\text{g/l}$	$0.46 \mu\text{g/l}$
2	$96 \mu\text{g/l}$	$2.9 \mu\text{g/l}$
3	$150 \mu\text{g/l}$	$2.1 \mu\text{g/l}$
4	$63 \mu\text{g/l}$	$0.3 \mu\text{g/l}$

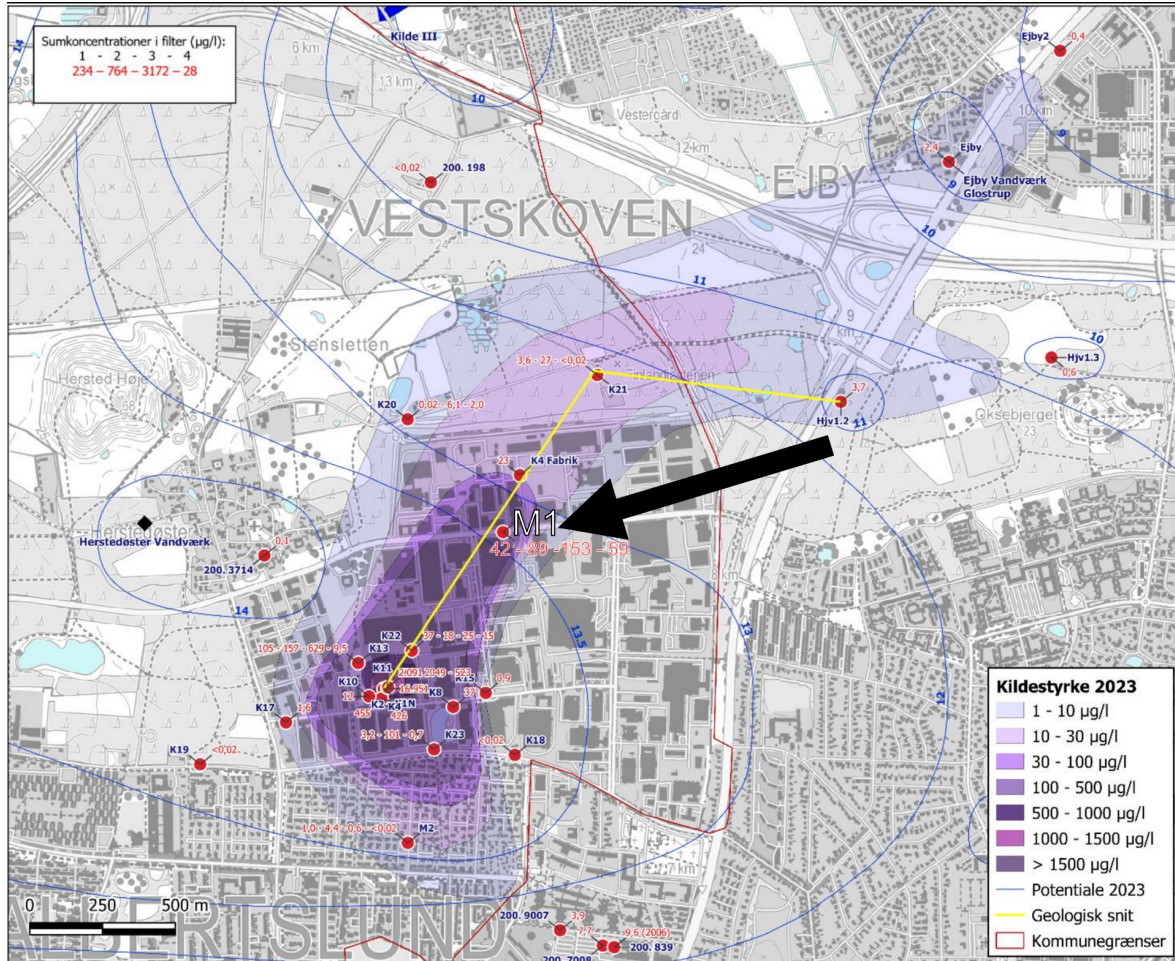


**Figure 5.2:** Results from the monitoring of the pollution spread in 2023 shown as sum concentrations of all chlorinated solvents (in µg/l). Screen 1 is the deepest screen and screen 4 is the uppermost screen. The yellow line shows the approximate course of the geological section presented in Figure 4.2 [Sø, 2023].

The water table was 8.66 mbs. The water extracted using a submersible MP1 pump and the first 210 L of it was discarded, and then 14 L of groundwater was collected into 1 L glass flasks with no headspace and stored in coolers. The oxygen level was 0.01 mg/L, and the temperature was 13.9 - 14.0°C; however, the temperature of the aquifer might be lower as the flow cell with electrodes was exposed to the sun. The pH of the water was 6.900, and its conductivity was  $1380\mu S/cm$  (at 14.5 °C). The conditions here are generally anaerobic, [Hemendorff, 2013](#) reported locally close to the source, the conditions are least reduced, while the majority of the plume area is primarily iron-reducing. There was 2.48 mg/L of nitrate, 101.09, 1.67 - 2.56 mg/L of total iron analysed by the lab. And 179.80 – 192.14 $\mu gL$  cDCE, 0.38 – 0.41 $\mu g/L$  VC and no detectable PCE or TCE levels at this well. Until the chemical amendments required for this experiment arrived, the groundwater was stored in a 10°C room.



**Figure 5.3:** Set up for groundwater extraction

Unfortunately, while sampling, some oxygen exposure occurred, leading to oxidised iron precipitation shown below (Figure 5.4).



**Figure 5.4:** Groundwater from the field a few days after extraction

## 5.2 Preparation of materials

The limestone was crushed using a Laboratory Jaw Crusher Pulverisette and passed through 5 mm and 1 mm sieves. As <1 mm would not settle and would be difficult during the sampling of water, it was not considered. >5 mm was not considered because larger grains have less surface area per unit mass than smaller grains, which limits the chemical reactivity (buffering capacity) and improves access to the matrix micropores where diffusion-controlled processes dominate. More information is found in Section A.2.



**(a)** Limestone after passing through lab jaw crusher



**(b)** Sieving crushed limestone

### 5.3 Set up of microcosm

All flasks (approximately 1138 mL in volume) were heated in an oven at 220°C overnight, with stoppers and metal screw caps autoclaved beforehand to ensure sterile conditions. The following set-up took place at room temperature on a sterile flush bench. 300 g of limestone is transferred to each of the glass flasks, followed by flushing with  $N_2$  for 10 minutes each as the limestone was stored in aerobic conditions. The addition of groundwater using a dispenser and then capped with Teflon-coated rubber stoppers to ensure the conservation of the anaerobic conditions within the system and the CE does not leak out of the closed system. Each scenario contained a variable volume of contaminated groundwater and different amendments. The microcosms are presented in [Table 5.2](#). All the microcosms are prepared in triplicate. Oxygen levels and pH were measured to verify that initial conditions were suitable for microbial activity prior to inoculation.

After adding all the relevant materials for each scenario, the microcosms were stored upside down at 10° C and frequently gently shaken by hand to allow the system to reach equilibrium.

**Table 5.2:** Reagents used in each batch

Scenario	Comment	Sediment 300g	Groundwater	ELS® Micro- emulsion	GeoForm®	KB-1®
A	Biotic control	X	X			
B	GeoForm	X	X	X	X	
C	GeoForm + KB1	X	X	X	X	X
D	KB1	X	X	X		X

Figure 5.6 shows the steps taken for each scenario.

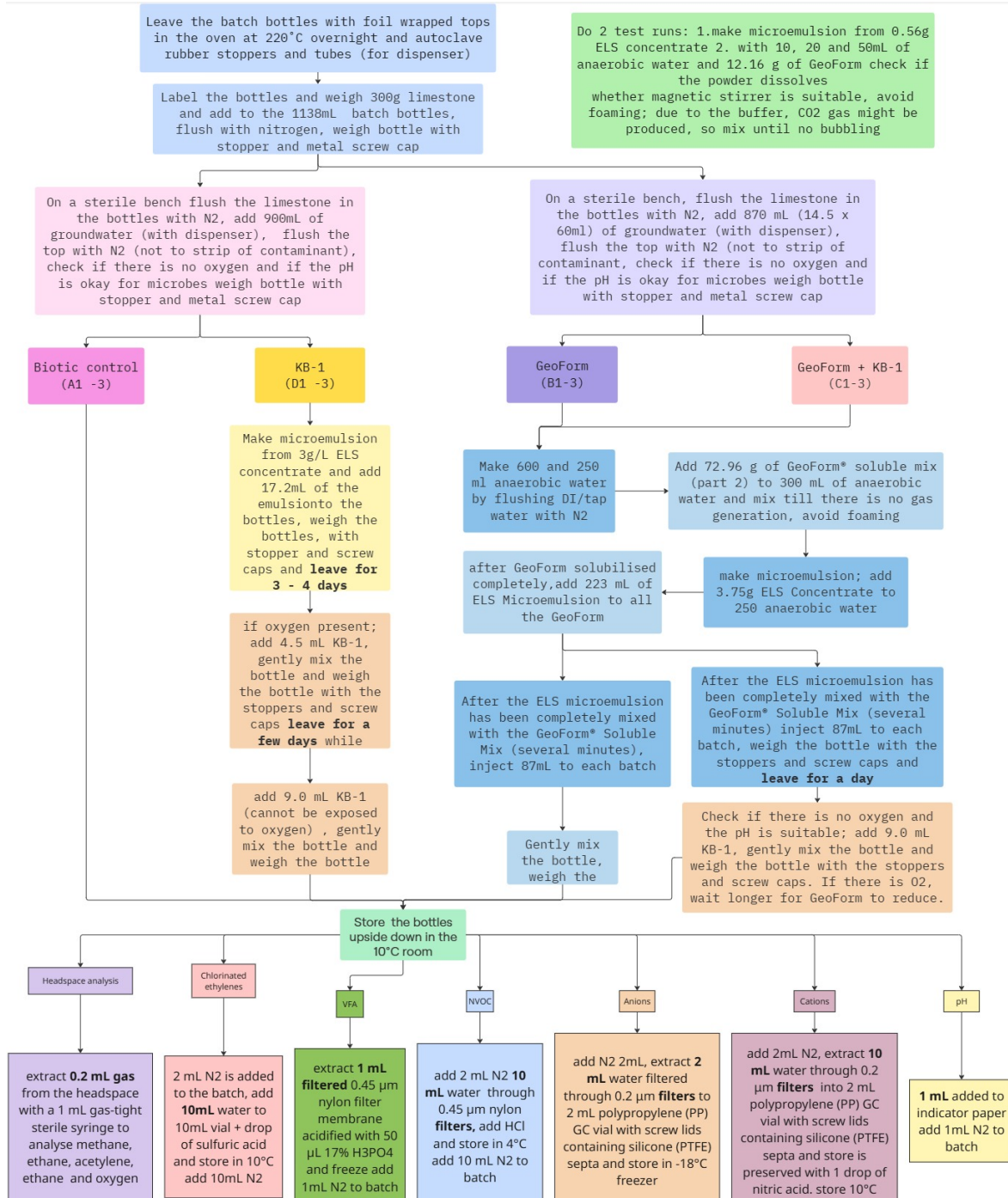


Figure 5.6: Procedure for experimental set up

This study did not use buffers like other experiments (e.g. [Hyun et al., 2015](#)) as limestone already buffers, and the GeoForm® mixture already includes of a buffer. Furthermore, citrate was not be added like [Hyun et al., 2015](#) suggests in order to simulate field conditions.

### 5.3.1 Biotic control

#### Scenario A

900 mL of contaminated groundwater and no amendments.

### 5.3.2 GeoForm® dilution

#### Scenario B

According to [EVONIK, n.d.\(b\)](#), the target sulfate concentration ranges from 1000 to 3000 mg/L, with Geoform soluble mix containing approximately 22.2% sulfate. Both EVONIK and [Hyun et al., 2015](#) recommend an optimal molar Fe:S ratio of 1:1. Based on this stoichiometry, the target iron (Fe) concentration can be estimated at 1000 mg/L.

For preparation, deionised water was made anaerobic by nitrogen purging in a separate flask. To 50 ml of anaerobic water, 12.16 g of GeoForm® and to 37 ml of anaerobic water, 0.556 g of ELS® liquid concentrate were added to achieve the target concentrations. The GeoForm® and ELS ® Microemulsion (concentration 15g/L) were mixed using a stirrer. This prepared solution was then injected into each of the batch bottles containing 810 ml of contaminated groundwater.

#### Scenario C

This scenario maintained identical GeoForm® (12.16 g) and ELS® concentrate (0.556 g) dosages as Scenario B, as both scenarios address a similar amount of contaminant mass and thus require equivalent electron donor quantities to support either sulfate-reducing bacteria (Scenario B) or KB-1® dechlorinating cultures (Scenario C). The preparation method mirrored Scenario B, with GeoForm® and ELS® liquid concentrate added to nitrogen-purged deionised water before injection into each batch reactor containing 800 ml of contaminated groundwater. This parallel treatment enables direct comparison of GeoForm®'s performance with *Dehalococcoides* under otherwise identical chemical conditions.

### 5.3.3 KB-1®

KB-1® culture has a Dhc cell count equal to approximately  $1 \cdot 10^{11}$  cell/mL. Assuming all is present in the aqueous phase, the resulting Dhc count in the bioaugmented flasks equals approximately  $10^8$  -  $10^9$  cells/mL. This concentration corresponds to a cell density 1 – 10 times higher than the minimum density strived for in the site barrier ( $10^8$  cells/L). To scenario C, 9.0 ml of KB-1® culture was added.

### Scenario D

0.050g of ELS® liquid concentrate was required for each batch. After consulting EVONIK, the ELS Microemulsion, with a concentration of 3000mg/L was made, and 17 ml was added to stimulate KB-1®. These batches contain approximately 895 ml of groundwater. When the oxygen levels were measured a few days after the addition of the donor, the concentration was 1.08mg/L which higher than 0.2mg/L; the concentration KB-1® would be able to tolerate [Aziz et al., 2013](#) and therefore, the KB-1 culture was added in two steps: (1) First, 4.5mL of KB-1 was added to let the fermentative bacteria and sulfate reducers already present in KB-1 consume the remaining oxygen and reduce the oxidized iron. (2) The second round of KB-1 (9mL) was added 2 weeks later, once conditions were fully anaerobic (oxygen level was  $\leq 0.06\text{mg/L}$ ), to provide enough Dehalococcoides for dechlorination.



**Figure 5.7: Addition of KB-1 to batch D1**

### 5.4 Monitoring

Sampling the water phase was done by laying the bottles horizontally and then extracting using sterile 0.6 x 30 mm needles and syringes. Gas phase samples was taken by extracting from the headspace.

Aqueous sampling was taken about every 3 days for the chlorinated ethenes and later on for their degradation products (gas samples, intended for measuring methane, ethene, acetylene and ethane concentrations), which were extracted directly from the headspace within the flasks and manually injected into the GC-FID. The water samples for redox parameters were taken for all scenarios and were used to support the interpretations attained from the degradation products. The infusion flasks were weighed before and after each extraction for mass balance. Nitrogen was added into the infusion flasks before extractions over 1 mL to avoid making a vacuum that sucks air so the system remains anaerobic.

The sampling frequency is presented in [Table 5.3](#) and is the same for all scenarios. A detailed description of the sampling frequency and the procedure for each sampling round is given in [Section A.5](#). The protocol for each parameter is available in

**Table 5.3:** Sampling frequency for each parameter

Exact day	CE	Gases	VFAs	NVOC	Anions	Cations	pH
0	X	X	X	X	X	X	X
1	X	X	X	X	X	X	
3	X	X	X	X			
7	X	X	X	X	X	X	
10	X						
13	X	X			X	X	X
17	X	X	X	X			X
21	X	X	X	X	X	X	X
24	X	X					
29	X	X	X	X	X	X	X
34	X	X	X	X			
38	X	X	X	X	X	X	X
51	X	X					

#### 5.4.1 Chlorinated ethenes

The initial concentration of cDCE in the water phase is  $150\mu\text{g}/\text{L}$ , and the desired concentration in water phase would be  $1\mu\text{g}/\text{L}$  because then the concentration reaches below the limit of detection which is less than 1% of the original concentration and it is the drinking water threshold. 10 mL water sample was extracted and preserved with a drop sulphuric acid and storing at  $10^\circ \text{C}$ . Then when possible, chlorinated aliphatic hydrocarbons were analysed from water samples by headspace- Gas Chromatograph (GC) -Mass Spectrometry (MS) ; the standard/calibration curve needs to be done every time. The detection limit for VC and cDCE is  $0.200\mu\text{g}/\text{L}$ .

The internal standard area (ISTD Area) double the rest of the data for the first 16 samples, this is shown in [Figure A.9](#) (appendix) and therefore the cDCE concentration of the first 16 samples should be doubled from approximately  $60$  to  $120\mu\text{g}/\text{L}$ . This would also need to be done for the VC concentration but they were below the detection limit.

The dip seen on day 1 for A2 and the data points on day 34 and 38 for all microcosms were measured on the same batch however when checked with the lab, no calibration or internal standard issues were mentioned ([Figure A.10](#) in the appendix).

Most samples from the GeoForm-containing batches had an interference for the VC measurement (could be the precipitation/limestone/white powder in the vials).

### Ethene, Ethane and Acetylene - Headspace analysis

For later samples, ethene, ethane, and acetylene are valuable as they are degradation products, allowing for conclusions regarding the remediation. 1.2mL is taken using a gas-tight sterile syringe from the headspace of the microcosms into 5.9mL gas vials that were flushed with nitrogen. Unfortunately, these samples could not be analysed due to a lack of standards and therefore 10mL water samples taken on the 51st day and sent to an external lab for analysis in order to reduce costs. Because the ethene concentration was not known throughout the experiment as planned, the molar concentration of CE over time is in the appendix (Figure A.14, Figure A.15, Figure A.16 and Figure A.17)

### 5.4.2 Volatile fatty acids

VFAs (acetic acid, propionic acid , iso-butyric acid , butyric acid, iso-valeric acid, valeric acid, hexanoic acid) were measured to monitor the fermentation of ELS® microemulsion as well as give information regarding the consumption of electron donors. 1 mL of the water sample is filtered through 0.45  $\mu\text{m}$  nylon filters and added into 2 mL brown glass vials. A high-performance liquid chromatography (HPLC) from the brand Agilent 1100, combined with a Viable Wavelength Detector, is used. With a detection limit of 5 $\mu\text{g}/\text{L}$ . 1mL of water sample was passed through 0.45 $\mu\text{m}$  filters and acidified.

### 5.4.3 Redox parameters

#### Oxygen - headspace analysis

Oxygen is measured because the limestone was aerobic, hence important at the start, 0.2 mL gas samples were taken directly from the headspace of the batch bottles with a 1 mL gas-tight sterile syringe as direct on-column injections into the gas chromatograph (Thermo Scientific TRACE 1310 gas Chromatograph) with a flame ionisation detector (GC-FID) connected to a CBM-102 Communication Bus Module. The extracted amount is substituted by nitrogen. Lowest concentration in the calibration curve is 1%.

#### Methane- headspace analysis

Unfortunately methane and carbon dioxide could not be measured as there was too long time between the sample being extracted into the vials and measured so the samples came out as below the detection limit

#### Non-volatile organic compounds

NVOC is measured to help assess the natural capacity of the system to support dechlorination and is done using a TOC 5000A Shimadzu analyzer equipped with an ASI-5000 autosampler. The samples were be filtered through 0.45  $\mu\text{m}$  nylon filters, and then preserved by refrigeration at 4°C. The NVOC quantification limit was 0.1 mg/L based on C<sub>8</sub>H<sub>5</sub>KO<sub>4</sub>

standard solutions [Broholm et al., 2016].

Most of the samples' concentrations were too high (>100 mg/L) for the method used by the analytical lab for NVOC for all microcosms. The data is available in [Table A.3](#) and [Figure A.6.4](#) (appendix). Additionally, the data exhibited no discernible pattern. The fact that the NVOC levels are high indicates there is organic matter that the microbes can consume and therefore explains why VFAs was not consumed.

## Anions

Sulfate gives information about the GeoForm, using mass balance, the amount of sulfate converted to sulphide can be estimated. At the same time, sulfate and nitrate provide information regarding the redox potential. A 1 mL water sample is filtered through a 0.2  $\mu\text{m}$  filter into 2mL plastic vial and then analysed by ion-chromatography (IC) – suppressed conductivity detection using and anion-exchange column under isocratic conditions with a carbonate/bicarbonate eluents system. The quantification limit is 7.5 mg/L. As mentioned in [Section 5.3.2](#), the target concentration for sulphate is 1000 mg/L but the results first showed the sulphate in the GeoForm-containing batches are  $\approx$ 140 mg/L at its maximum and therefore the sulphide concentration was measured using test kits for the field and the levels measured on day 57. However then there was a confirmed calibration issue so sulphate concentration in the GeoForm-containing batches were measured again.

## Cations

Iron gives information about the GeoForm, at the same time iron and manganese provide information regarding the redox potential. Fe and Mn were measured using an inductively coupled plasma device equipped with an optical emission spectrophotometer. For this, 10 mL of the water sample is passed through 0.2  $\mu\text{m}$  filters and added to a plastic vial and stored at 10°C. The detection limit is 0.5mg/L.

### 5.4.4 pH

The pH was measured by adding 0.5 mL of the water sample to pH strips (MERCK pH indicator strips 6.5-10 and later Cytiva Whatman indicator paper pH 4.5 - 10). The pH measured using the pH strips seems to fluctuate when it shouldn't, especially at the start, where the pH was 6 for the control, lower than the pH measured at the M1, F3 well (pH 7) and then rose to 7.5 on day 17, therefore the pH was simply measured on day 57 using a pH electrode instead.

## 5.5 Data treatment

To account for the decrease in CE concentration due to sampling and therefore removal from the microcosms, a balance of the CE should be applied. This theoretical curve confirmed that the control's trend aligned with sampling losses, providing a critical baseline to distinguish between passive mass removal and active degradation. Without this correction, the concentration drop could misleadingly imply natural attenuation, complicating the interpretation of treatment efficacy. The theoretical curve also acts as a quality control check, revealing any deviations that might indicate measurement errors such as volatilisation losses of CE (refer to [Table 3.1](#)) or calibration issues.

The theoretical CE concentration curves was calculated using the following formula:  
 $C_w[mg/L] = Mt[mg]/(V_w[L] + k_d[1/g] \cdot M_s[g] + K_h \cdot V_a)[L]$  where:

$C_w$  is the aqueous concentration of the chlorinated ethene

$V_{tot}$  is the total volume of glass flasks, 1.138L

$V_w$  is the water volume in the system

$K_d$  is assumed to be 0.00003 1/g [[Hemendorff, 2013](#)]

$M_s$  is sediment mass in the system, 300g

$K_h$  is assumed as 0.0741 for cDCE and 0.631 for VC [[Friis, 2006; Gossett, 1987](#)]

$V_a$  is the volume of headspace in the system (determined by subtracting the volume of sediment and water from the total volume)

The initial total mass in the system,  $Mt$  [mg] is taken as  $0.150[mg/L] \cdot V_{tot}[L]$  instead of  $0.184[mg/L] \cdot V_{tot}[L]$  to account for the fact that the groundwater was added to the control two weeks later. Given limestone's negligible sorption, the CE concentration before and after limestone was not measured.  $K_h$  is critical for accurate mass accounting because cDCE continuously re-equilibrates between phases after sampling. Each removal of water or headspace gas disturbs the system's equilibrium, causing dissolved cDCE to partition anew into the headspace. Without  $K_h$ , repeated sampling would artificially depress aqueous concentrations - not from degradation, but from this dynamic redistribution.

For the degradation rate, the initial concentration of cDCE was assumed to be 421.19  $\mu mol/L$  (averaged for day -12) and 38.94  $\mu mol/L$  (averaged for day -0) for VC. The first-order kinetic rate is calculated by taken by plotting the  $\ln(C/C_0)$  vs time and calculating the gradient of this graph.

$r = K_{1,i} \cdot C_i$  where:

$r$  is the rate of dechlorination [ $\mu mol L^{-1} day^{-1}$ ]

$K_{1,i}$  is the first-order kinetic rate constant [ $day^{-1}$ ]

$C_i$  is the initial CE concentration in  $\mu mol L^{-1}$

For cDCE day -12 to day 29 was considered and for VC day 10 to 51 was considered which excludes the production of VC.

## RESULTS

### 6.1 Physical observations

Upon mixing, all microcosms initially appeared milky or pastel-colored due to suspended limestone particles (all figures shown immediately after mixing).

[Figure 6.2](#) shows the GeoForm-containing batches (B and C) on the 3rd day of the experiment. As predicted, GeoForm-containing batches (B and C) appear yellowish-green in colour (shown in [Figure 6.2](#)), likely from dissolved ferrous sulfate monohydrate (greenish characteristic of  $Fe^{2+}$ ) and the lecithin's yellowish-brown hue. These batches maintained greenish tones under iron-reducing conditions; any orange/red-brown precipitates would indicate oxidation of ferrous iron or other redox disturbances, similar to what was seen in [Figure 5.4](#).

[Figure 6.3a](#) shows that by the 13th day, the GeoForm (B) and GEOF + KB-1 (C) batches look different to each other. Compared to GeoForm batch (B), GeoForm + KB-1 (C) became much darker as the microcosm amended with both GeoForm and KB-1 (C) should undergo more rapid darkening since the KB-1 culture contains SRB at optimal concentrations for iron sulphide formation compared to the GeoForm-only batch (B) which would have a lower SRB abundance. [Figure 6.4](#) shows the darkening of B1 by Day 38. B3 also followed this pattern of darkening on day 57 (shown in [Figure A.8](#), appendix). [Figure 6.4](#) also shows further darkening of batch C3 (compared to day 23, [Figure 6.3](#)) this is confirmation for the formation of iron sulphide. It was expected that the precipitation of iron sulphide would occur and, this black colour of the water would then start clearing up, but this not observed within the timeframe of the thesis.

Both the control and KB-1 only batches had colourless water ([Figure 6.1b](#)). [Figure 6.1b](#) and [Figure 6.3b](#) illustrates that due to the characteristic black pigmentation of KB-1 (shown in [Figure 5.7](#)), the KB-1 containing batches have darker-looking limestone, more greyish, as that limestone provides an attachment surface for microbial colonisation. Furthermore, both batches B and C were difficult to filter compared to control and KB-1-only batches (A and D), but on the 13th day onwards, batch C became much easier to filter.

The control and KB-1-only batches (A and D) exhibited a more pronounced stagnant water odour compared to GeoForm-containing batches (B and C). While GeoForm's high

iron content generated a metallic odor, the expected "rotten egg" smell from HS formation (via SRB activity) was not observed in the first few days ([Table 3.4](#)), suggesting rapid iron sulphide precipitation.



(a) GeoForm (B) compared to Control(A) (A3 is darker than A1 and A2)



(b) KB-1 (D) compared to Control(A)

**Figure 6.1:** Appearance of all the microcosms on at the start of the experiment

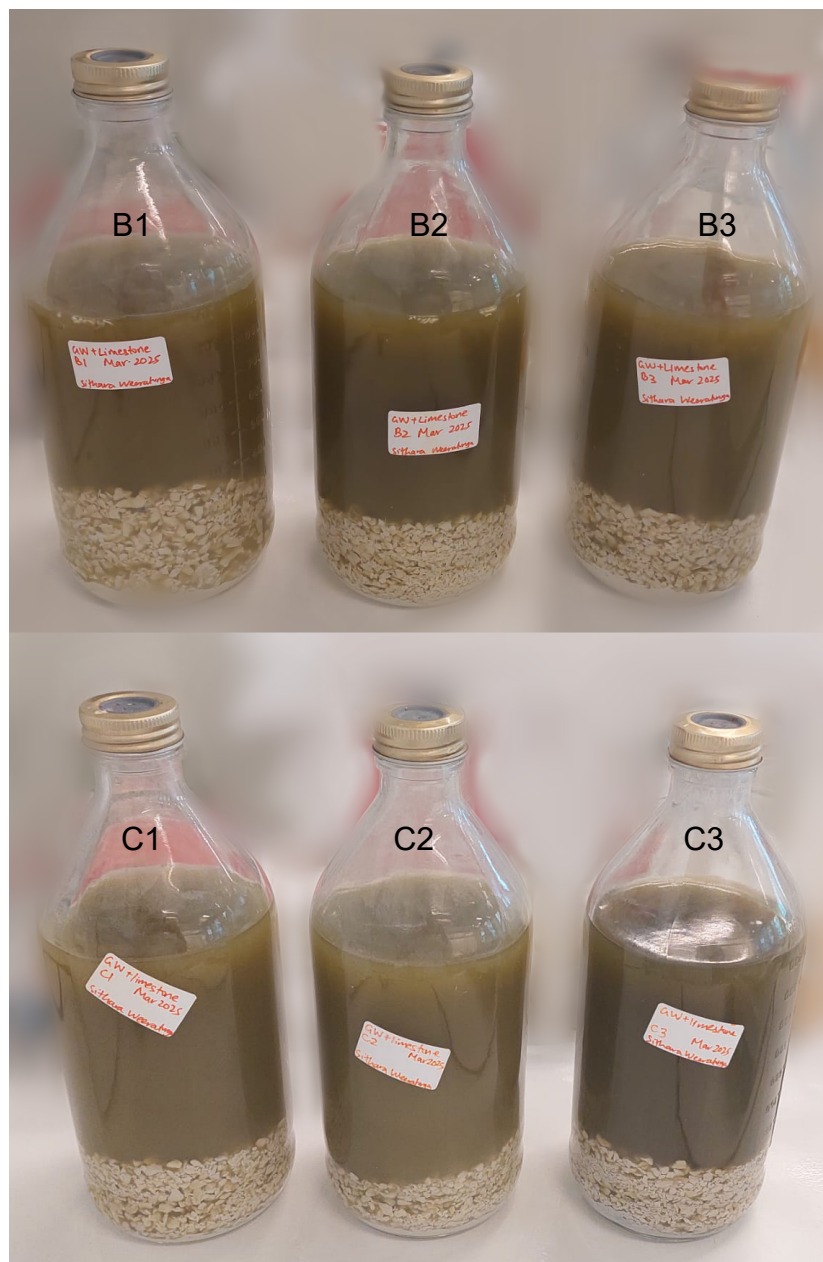
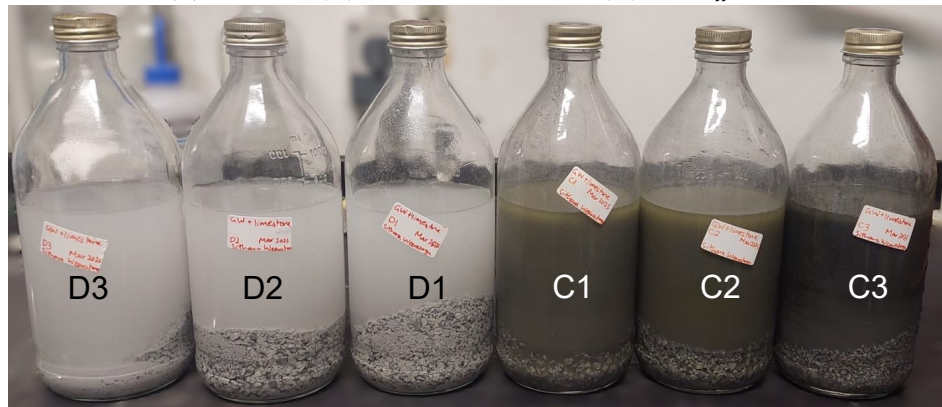


**Figure 6.2:** On day 3 GeoForm (B) and GeoForm + KB1 (C) look similar



(a) GeoForm (B) and GeoForm + KB1 (C) look different



(b) KB-1 (D) compared to Geoform + KB-1 (C)

**Figure 6.3:** Comparison of the microcosms on Day 23



**Figure 6.4:** GeoForm (B) and GeoForm + KB1 (C) on day 43, B1 darkened

## 6.2 Data analysis

### 6.2.1 Chlorinated ethenes

The expected outcome was once the black precipitate forms, FeS should react with CE, resulting in concurrent decreases in both cDCE and the small amount of VC seen in the groundwater from the well. These microcosms would also exhibit greater VC formation compared to GeoForm-only batches. As depicted in [Figure 3.5](#), KB-1-amended microcosms should demonstrate sequential degradation of CE, with cDCE degradation preceding VC degradation. However, in microcosms containing both GeoForm and KB-1, the CE degradation pattern would depend on the dominant processes. If *Dehalococcoides* remain uninhibited, the pattern would resemble KB-1-only systems. Conversely, if *Dehalococcoides* activity is suppressed by elevated iron, sulphate, or sulphide concentrations, the degradation profile would mirror GeoForm-only microcosms, exhibiting simultaneous decreases in cDCE and VC.

The observed concentration profiles revealed distinct degradation behaviours across experimental batches. In GeoForm-amended microcosms (B and C), the initial and final cDCE concentrations showed minimal difference, with fluctuations exceeding those observed in the control (about  $40\mu\text{g/L}$ ) [Figure 6.5](#). While GeoForm+KB-1 batch (C) demonstrated some degradation capacity, their efficacy remained substantially lower than KB-1-only systems (Batch D) ([Figure 6.5](#)). Notably, the GeoForm+KB-1 batch (C) exhibited VC formation followed by partial degradation and ethene production, though at significantly reduced levels compared to KB-1-only systems (D) ([Figure 6.6](#), [Figure A.21](#)). This suggests inhibitory effects from elevated iron, sulphate, and/or sulphide concentrations on *Dehalococcoides* activity in combined-treatment microcosms. As anticipated, GeoForm-only batches (B) had very little VC (around  $0.2\mu\text{g/L}$ ), while control systems (A) maintained stable cDCE concentrations throughout the experiment, confirming the lack of *Dehalococcoides* in Naverland. The peak seen in the cDCE concentration at Day 0 for KB-1 batches (D) is likely because of the second addition of KB-1 ([Figure 6.5](#)). [Figure 6.7](#) demonstrates the expected stepwise degradation sequence: first the decrease in cDCE concentration and then an accumulation of VC and finally degradation of VC to ethene in the KB-1 only batches (D). The formation of VC on Day 7 ([Figure 6.6](#)) and its degradation after day 38 observed in GeoForm +KB-1 microcosms (C) confirms biotic degradation as the dominant pathway albeit operating under partial inhibition from GeoForm as shown by previous studies ([Section 3.2.3](#)). The VC concentrations in the GeoForm +KB-1 microcosm (C) remained below  $1\mu\text{g/L}$  throughout the experiment ([Figure 6.6](#)). However, this limited VC accumulation occurred without an obvious corresponding decrease in cDCE concentrations.

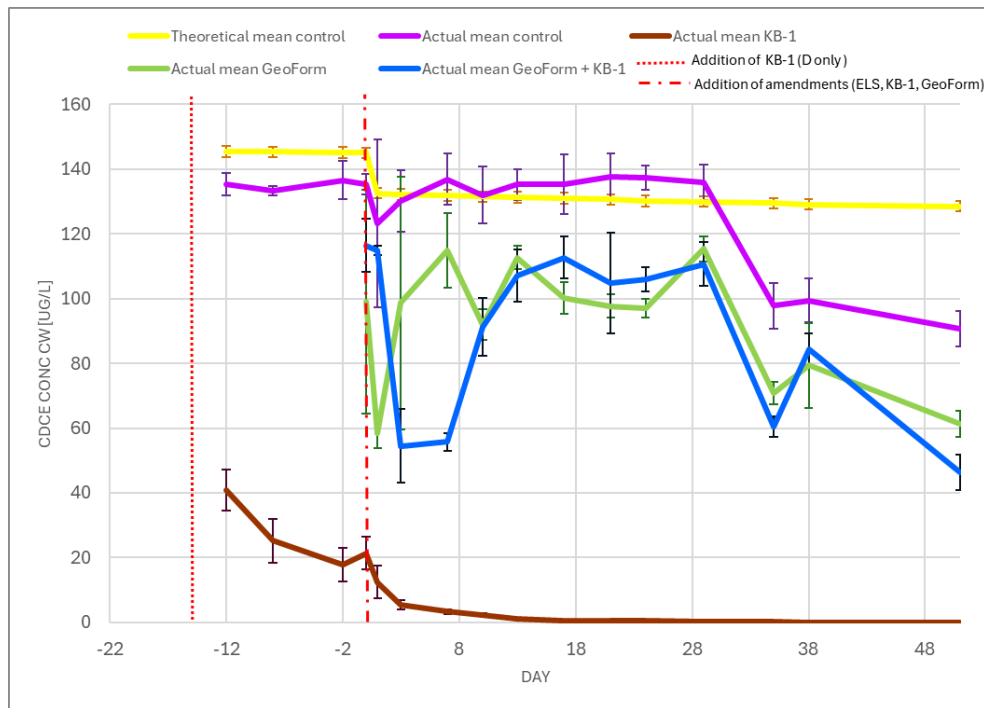


**Figure 6.5:** Average cDCE concentration of all the batches over time. On day -22, ELS was added and day -12, KB-1 was added only to batch D (KB-1) and then on day 0, GeoForm was added to batch B and GeoForm and KB-1 was added to batch C

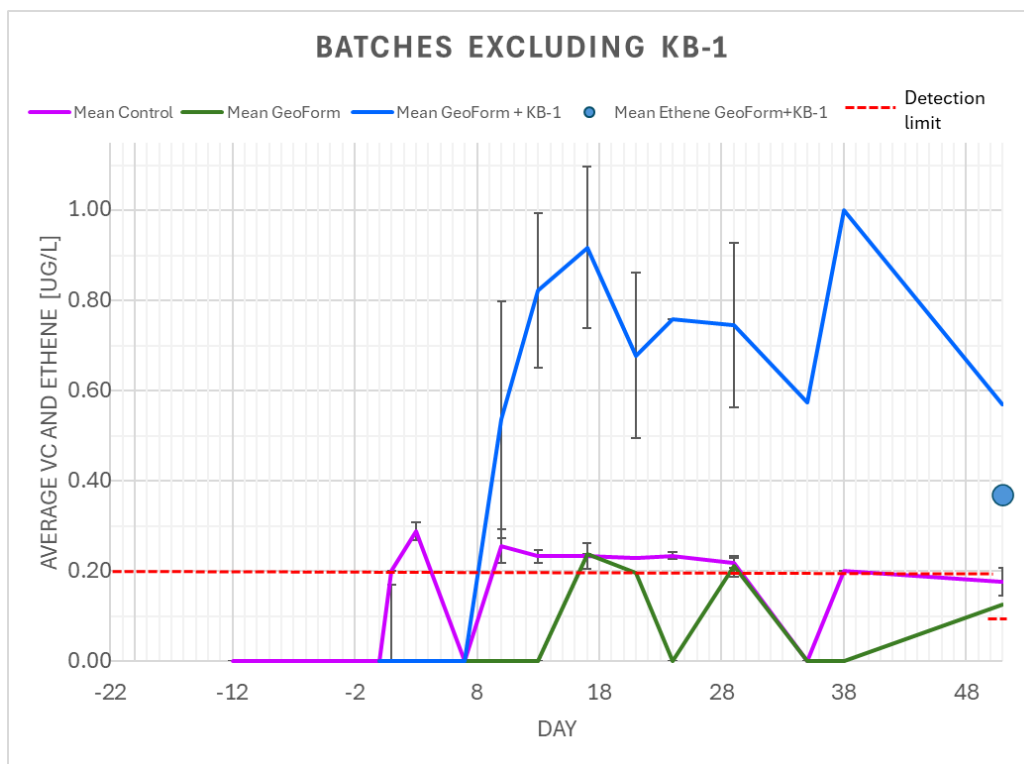


**Figure 6.6:** Average VC levels and ethene level in the control, GeoForm and GeoForm+KB-1 batches. The ethene level was only for day 51

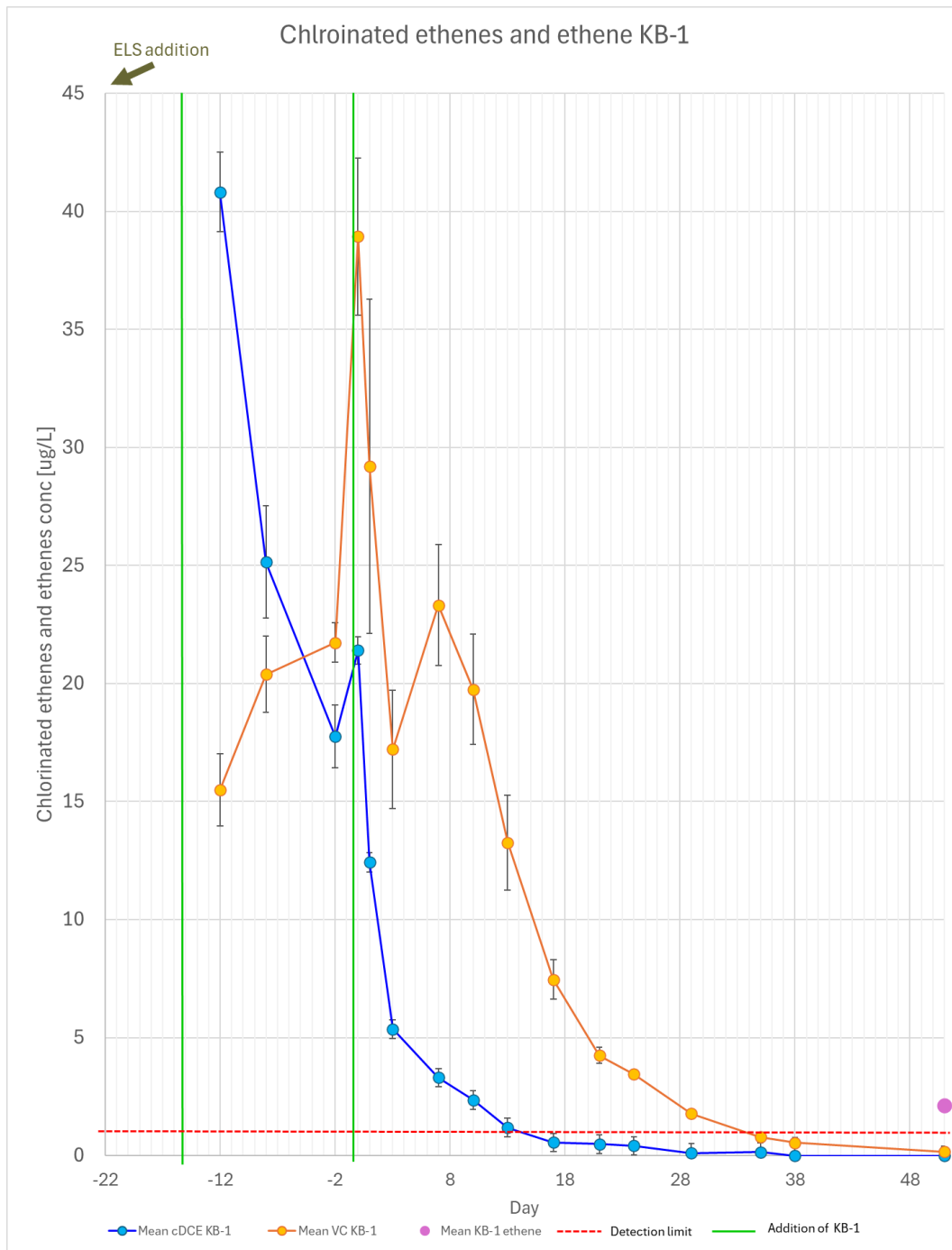


**Figure 6.7:** Average chlorinated ethenes and ethene concentration in KB-1 batch. ELS was added on day -22, and KB-1 was added -12 and day 0

The only batch that showed degradation is KB-1, and its average first-order rate constant is  $0.1252 \text{ day}^{-1}$  for cDCE (Figure 6.8) and  $0.1085 \text{ day}^{-1}$  for VC (Figure 6.9). The rate of dechlorination is  $52.73 \mu\text{mol L}^{-1} \text{ day}^{-1}$  which is faster than the enhanced dechlorination seen by [Yaru Li et al., 2021](#) who reported that the addition of  $0.2 \text{ mM } Fe^{2+}$  and  $S^2$  enhanced the dechlorination rate of TCE from  $25.46 \pm 1.15$  to  $37.84 \pm 1.89 \mu\text{mol L}^{-1} \cdot \text{day}^{-1}$  in a batch experiment. While the VC dechlorination observed is slower, the dechlorination rate is  $4.22 \mu\text{mol L}^{-1} \text{ day}^{-1}$ .

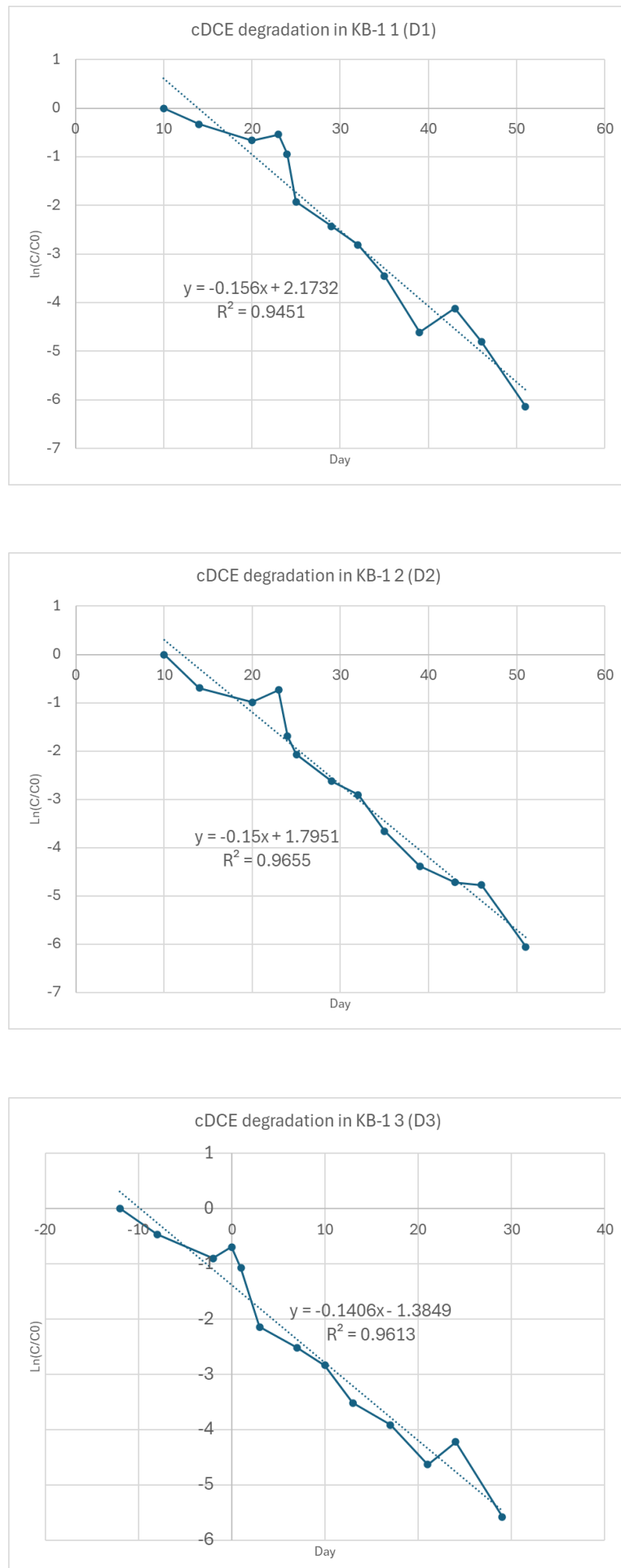


**Figure 6.8:** cDCE degradation rate in the KB-1 batch

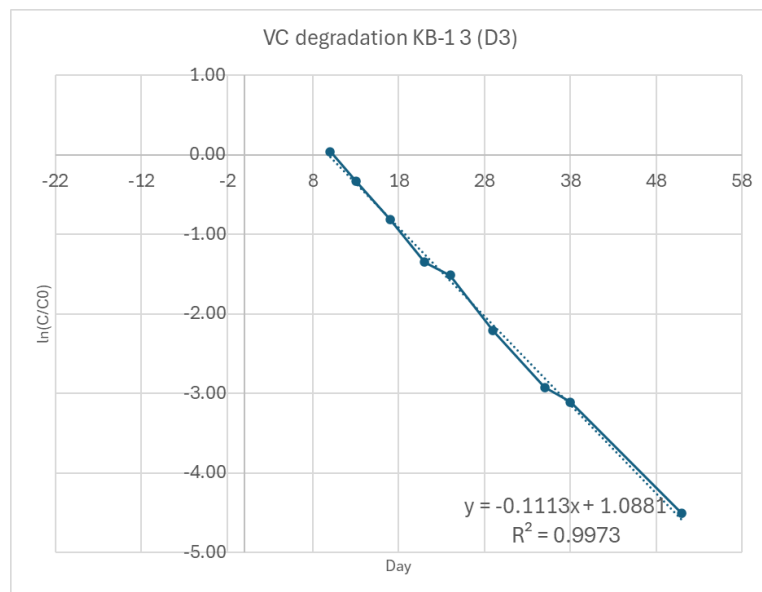
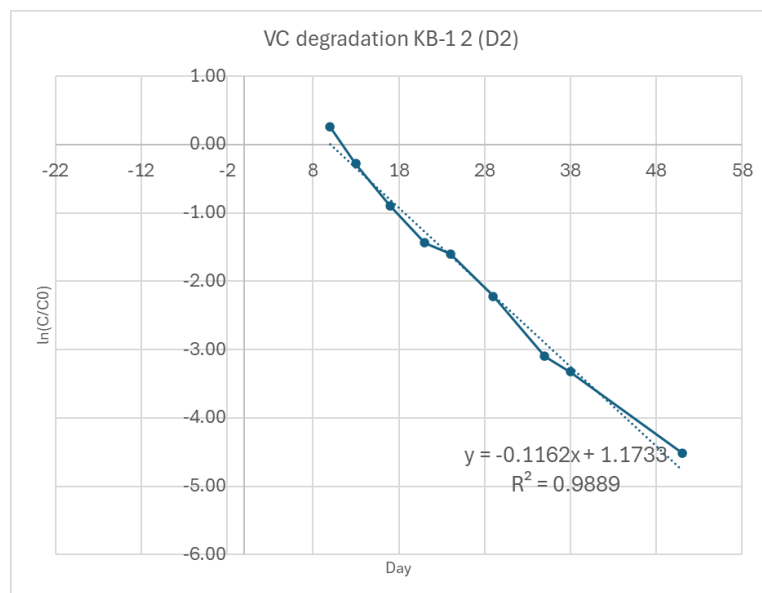
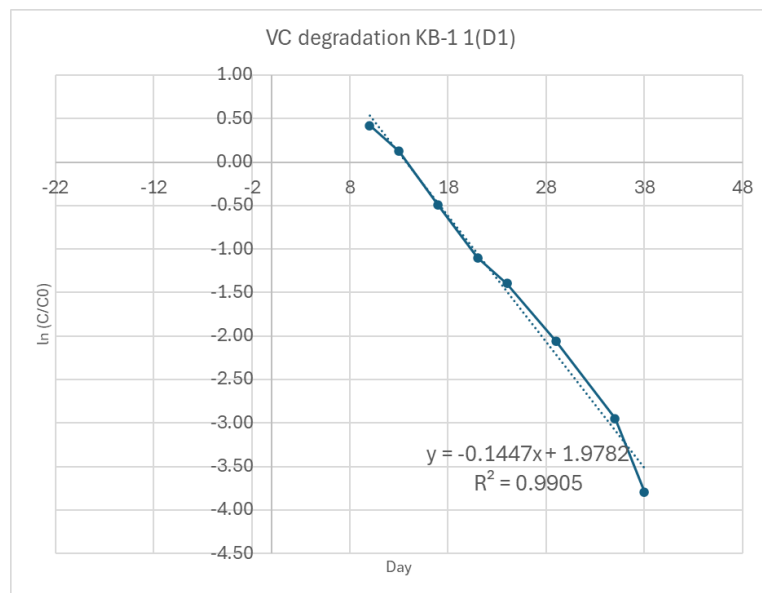


Figure 6.9: VC degradation rate in the KB-1 batch

### 6.2.2 Volatile fatty acids

Figure 6.10 shows a large difference in acetate concentration in A3 compared to A1 and A2 (control), which explains its much darker colour (shown in Figure 6.1a), suggesting the presence of organic matter in batch A3 however as there is no *Dehalococcoides*, the VFAs served as electron donor for indigenous bacteria and its the decreasing acetate concentration from Day 29 to 38 indicate it is being consumed.

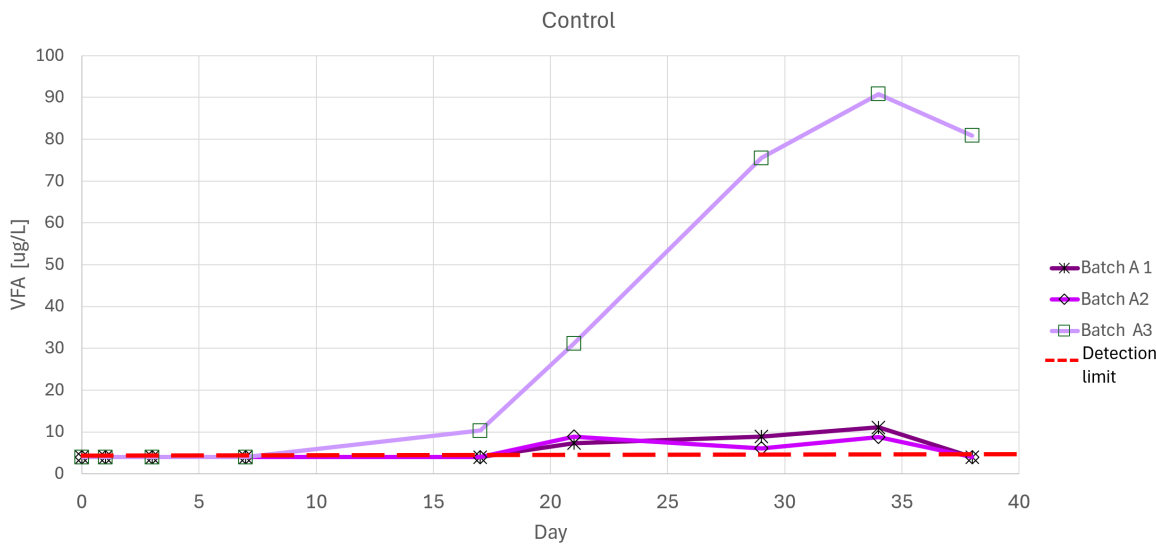
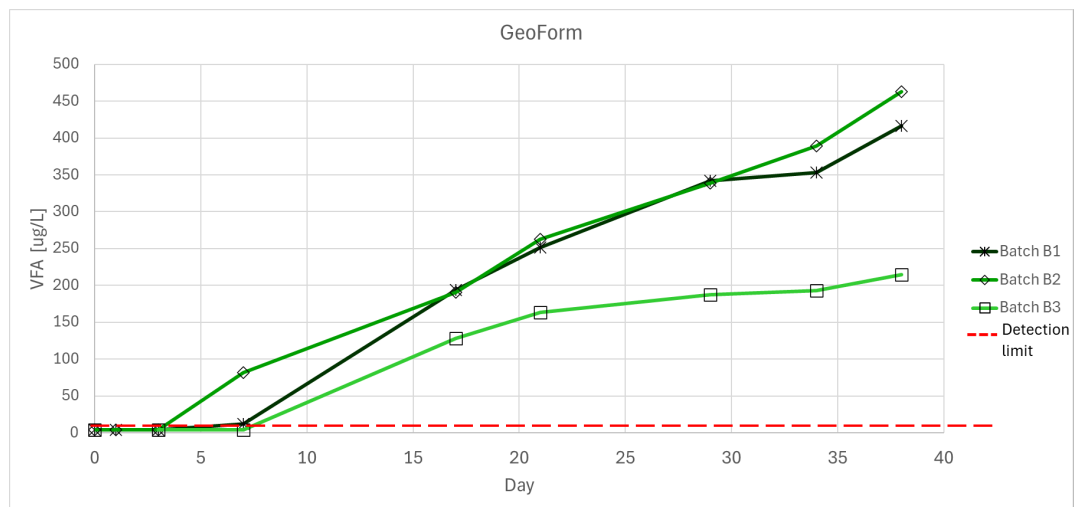
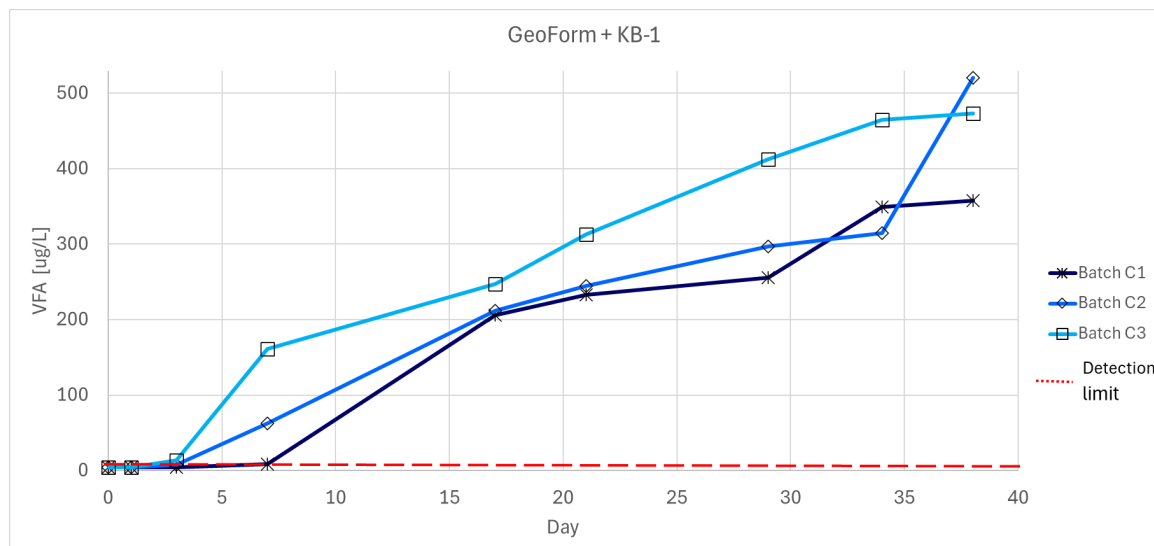
Although all the batches excluding the controls contained equal masses of ELS, the GeoForm-containing batches (B and C) exhibited acetate levels nearly ten times higher than the KB-1-only batches (D), indicating that GeoForm may contribute to this increase (Figure 6.11, Figure 6.12, and Figure 6.13).

Furthermore, amongst the Geoform-containing batch, the batch with KB-1 produced slightly more acetate at a higher rate than batch B, likely due to the presence of KB-1 culture, which could enhance ELS fermentation. C3 has the fastest VFA production and had the fastest VC production (Figure A.20) However, as there is continuous production of VFA, it is hard to say if it is being consumed or accumulated. If there is accumulation of VFA in the GeoForm-containing batches, it would indicate ELS Microemulsion is being broken down to acetate but not being consumed by bacteria (Figure 6.11, Figure 6.12, and Figure 6.13).

if the experiment could have been run for longer the VFA level of C3 (GeoForm + KB-1) could be observed to figure out whether VFA production stopped, if it is just a fluctuation or whether it is being consumed (Figure 6.12). This batch (C3) also has the Batch B3 (GeoForm) showed lower VFAs levels than B1 and B2 (Figure 6.11).

And as stated in Section 5.4.3, all the microcosms have organic matter. Amongst the KB-1 only batches, D1 produced acetate faster than D2 and D3 and these batches exhibited acetate consumption after day 20 (Figure 6.13). The consumption of acetate indicates acetate served as an electron donor for the *Dehalococcoides* and stimulated reductive dechlorination of cDCE and VC and cooperative interaction between the microbes fermenting ELS (and the natural organic matter), and the *Dehalococcoides*.

Finally, when lactic acid (a non-volatile fatty acid) was measured in all batches starting from day 38 (unintentionally), none exceeded the detection limit of 0.050 g/L. As the pH of the system is >5.5, the VFA is acetate instead of acetic acid. It is to be noted that other than acetate, no VFAs were detected despite being measured.

**Figure 6.10:** VFA levels in the controls over the 38 days**Figure 6.11:** acetate levels in the GeoForm batches over the 38 days**Figure 6.12:** acetate levels in the GeoForm + KB-1 batches over the 38 days

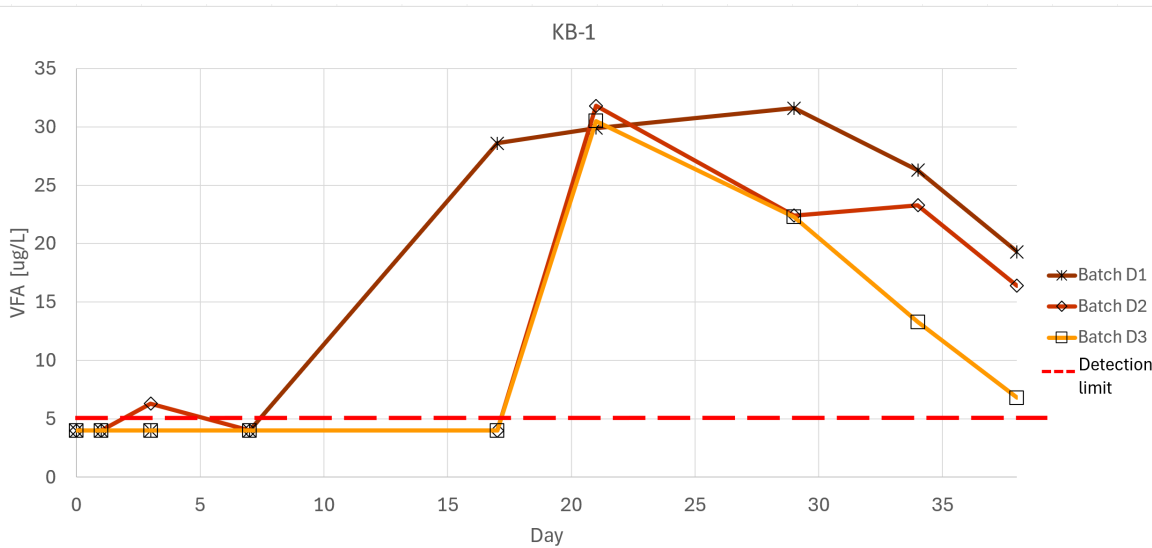


Figure 6.13: acetate levels in the KB-1 batches over the 38 days

### 6.2.3 Iron

The dissolved iron concentration in the control and KB-1 (A and D) batches was close to the detection limit and therefore, there is no pattern seen. Batches containing GeoForm only (B) started at 900 – 940 mg/L and then decreased over time, except for B2, which spiked after two weeks. This indicates that the GeoForm-containing microcosms are at least iron-reducing conditions and once again, suitable for the microbes. Like batch B, batches with both GeoForm and KB-1 (batch C) started with an Fe concentration of 820 – 900 mg/L and then decreased over time, which could be the formation of iron sulphide since, as previously mentioned, the colour darkens after day 13 (Figure 6.3a). As there is 2.68 g of Ferrous sulfate monohydrate, there should be 1.36 g of iron but only 810 mg and 738 mg (B and C respectively) was found the remaining 553 mg and 623 mg is because Ferrous sulfate monohydrate which is not as immediately soluble as the ferrous sulfate heptahydrate. Therefore, the ferrous iron and sulfate are more slowly released and tend to provide a continuous source of both sulfate and iron for maybe a couple of months depending on the water movement and rate of diffusion (which is somewhat controlled by the rate of sulfate reduction). The spike since on day 1 for C1 is not because the conditions were not reduced enough but the dissolving of Fe (Figure 6.15).

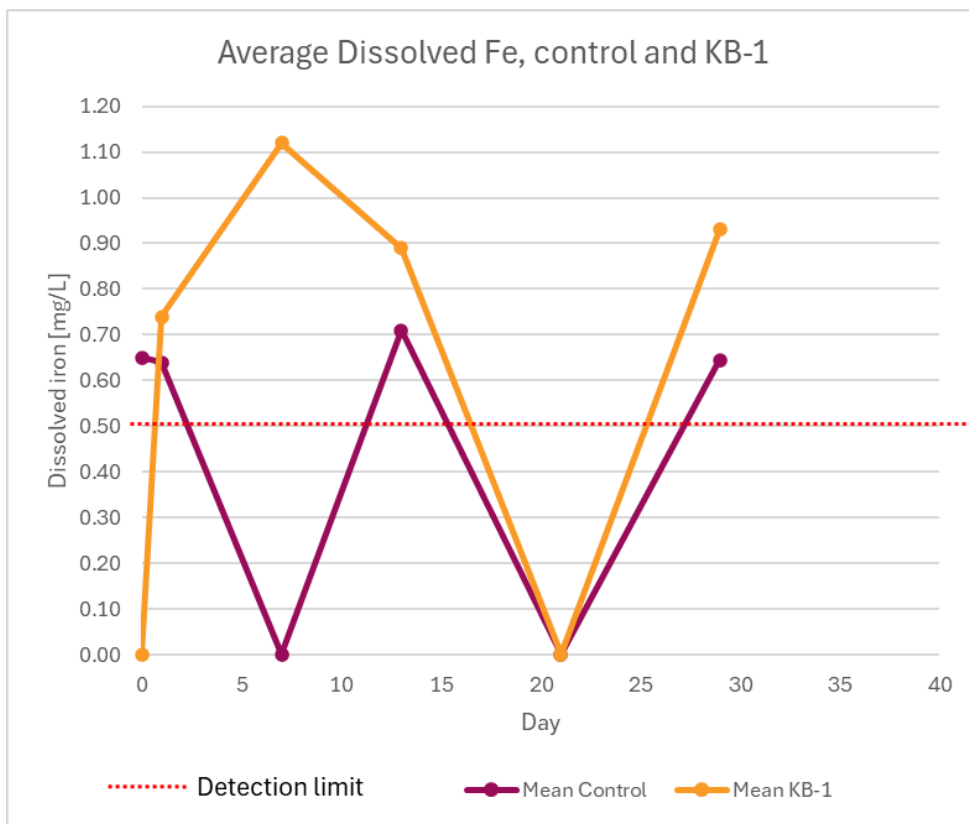


Figure 6.14: Average dissolved iron in the biotic control and KB-1 batches over time

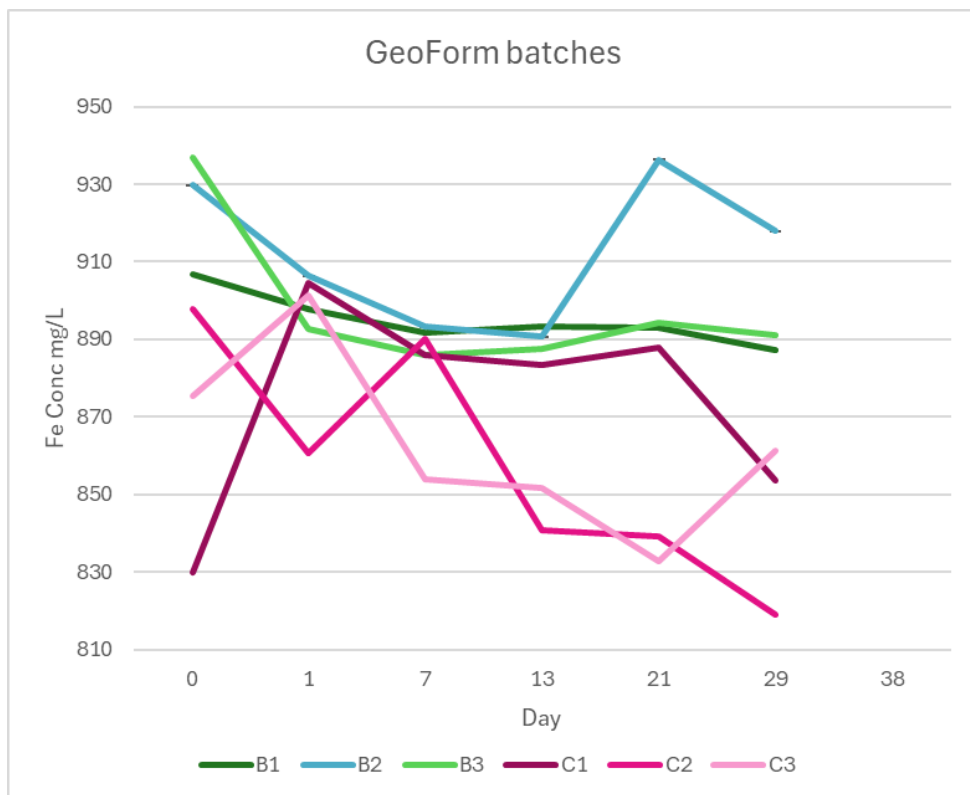


Figure 6.15: Dissolved iron in the GeoForm containing batches over time (note the axis)

### 6.2.4 Sulphate

The increasing concentration of sulphate in B2 (GeoForm) (shown in [Figure 6.17](#)) as well as the spike of dissolved iron concentration after two weeks ([Figure 6.15](#)), illustrates that this microcosm is not in sulphate reducing conditions and that the Ferrous Sulphate monohydrate is dissolving over time. The clear decreasing sulphate concentration of A3 (control), C3 (GeoForm +KB-1) and D (KB-1) batches shows that these microcosms are in sulphate reducing conditions ([Figure 6.16](#), [Figure 6.18](#), [Figure 6.19](#)). As mentioned in [Figure 6.4](#), batch B1 darkened and at the same time as when the sulfate concentration started to dip, proving the microcosm has sulphate-reducing conditions. As expected, the GeoForm+KB-1 batches reached sulphate-reducing conditions faster than the batches with only GeoForm ([Figure 6.18](#)). C1 (GeoForm +KB-1) also shows a steep decrease in sulfate concentration from the 29th to 38th day but once again, it is difficult to assess whether it is a fluctuation or not ([Figure 6.18](#)).

The results also from KB-1 batches confirm that KB-1 has SRB and sulphate reducing conditions ([Figure 6.19](#)). The sulphide concentration on day 57 is shown in [Table 6.1](#). Despite evidence of sulphate reduction across multiple batches, sulphide concentrations remained low in most, except for C3. This disparity cannot be attributed to sulphide volatilisation or measurement limitations, as sulphide is detectable in at least one batch. The more plausible explanation is that redox conditions in the other microcosms were not sufficiently reducing to allow for consistent sulphide generation. Competing electron acceptors (Fe) may have delayed or limited the onset of sulphate-reducing conditions. The decreasing sulphate concentration for A3, high sulphide concentration and consumption of acetate indicates there are SRB and the presence of natural organic matter (as shown by the high NVOC), could be from the limestone collected. Additionally, the dark colour of C3 confirms the formation of iron sulphide and therefore indicates potential abiotic cDCE degradation however this was not observed but the redox conditions are ideal for the *Dehalococcoides* present in the bottle. As there is approximately 783 mg of Fe and 2187 mg of sulphate, the ratio is 1:1.6 Fe:SO<sub>4</sub> so it is more likely that mackinawite forms rather than pyrite. The measured sulfate concentration ( $\approx$ 2500 mg/L) substantially exceeded the expected 890 mg/L ([Table A.1](#)). Nevertheless, the system did not deplete its electron donor capacity during the experimental period.

As shown in [Figure 6.19](#), the triplicates for the KB-1 are similar to each other and therefore the results are reliable.

**Table 6.1:** Sulphide concentration [mg/L] in all batches on day 57. "nd" indicates below detection limit

Replicate	A (Biotic control)	B (GeoForm)	C (GeoForm + KB-1)	D (KB-1)
1	nd	0.066	0.381	3.39
2	nd	0.080	0.169	>3.5
3	3.93	0.041	1.43	>3.5
Average	1.31	0.062	0.66	>3.46

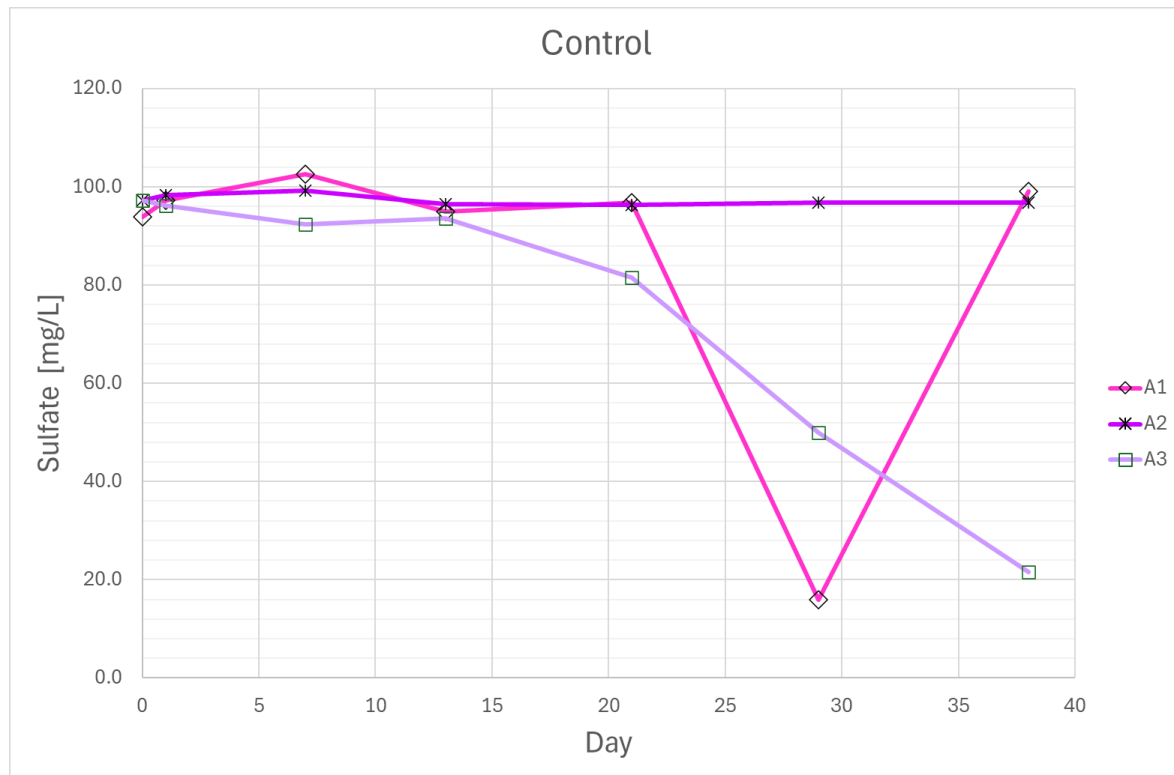


Figure 6.16: Sulphate concentration over time in the biotic controls

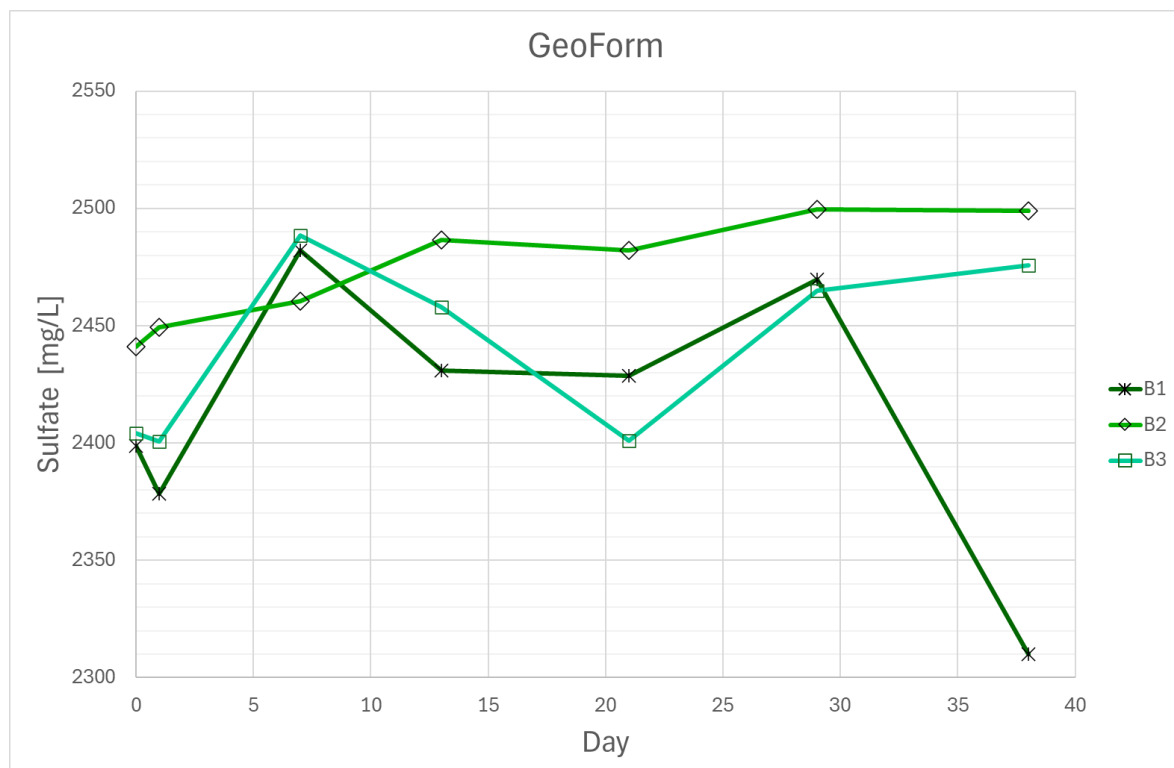
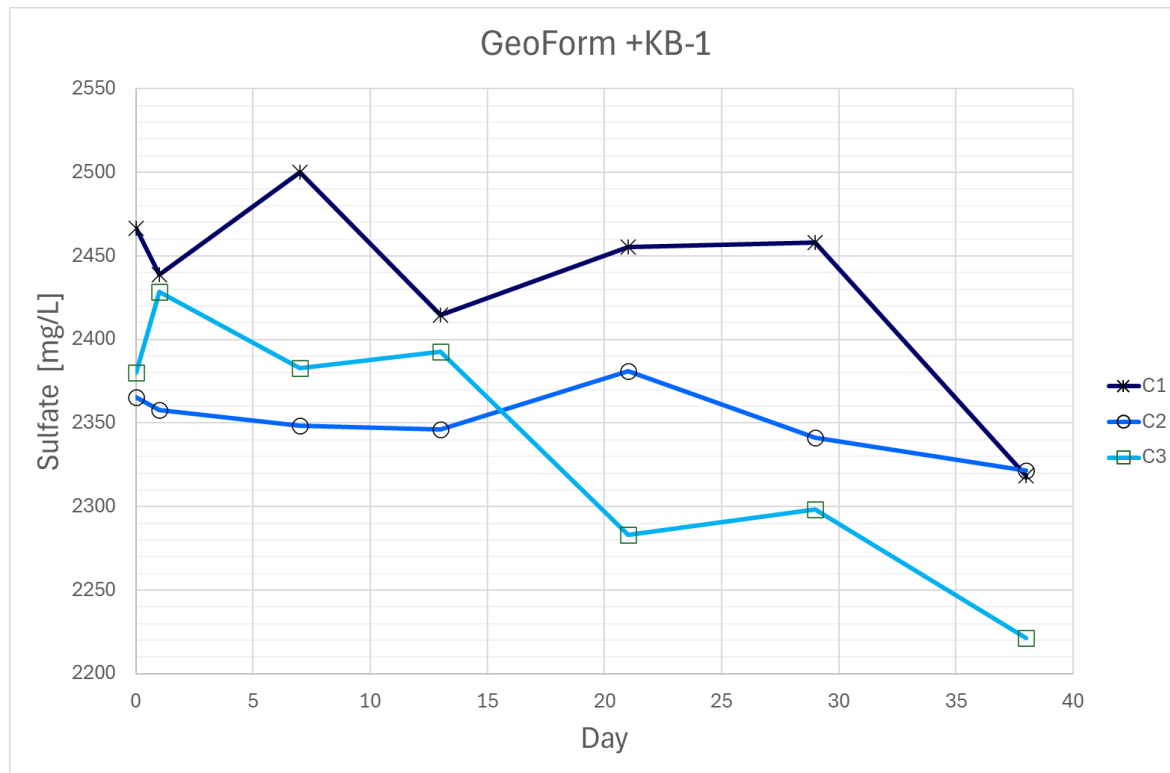
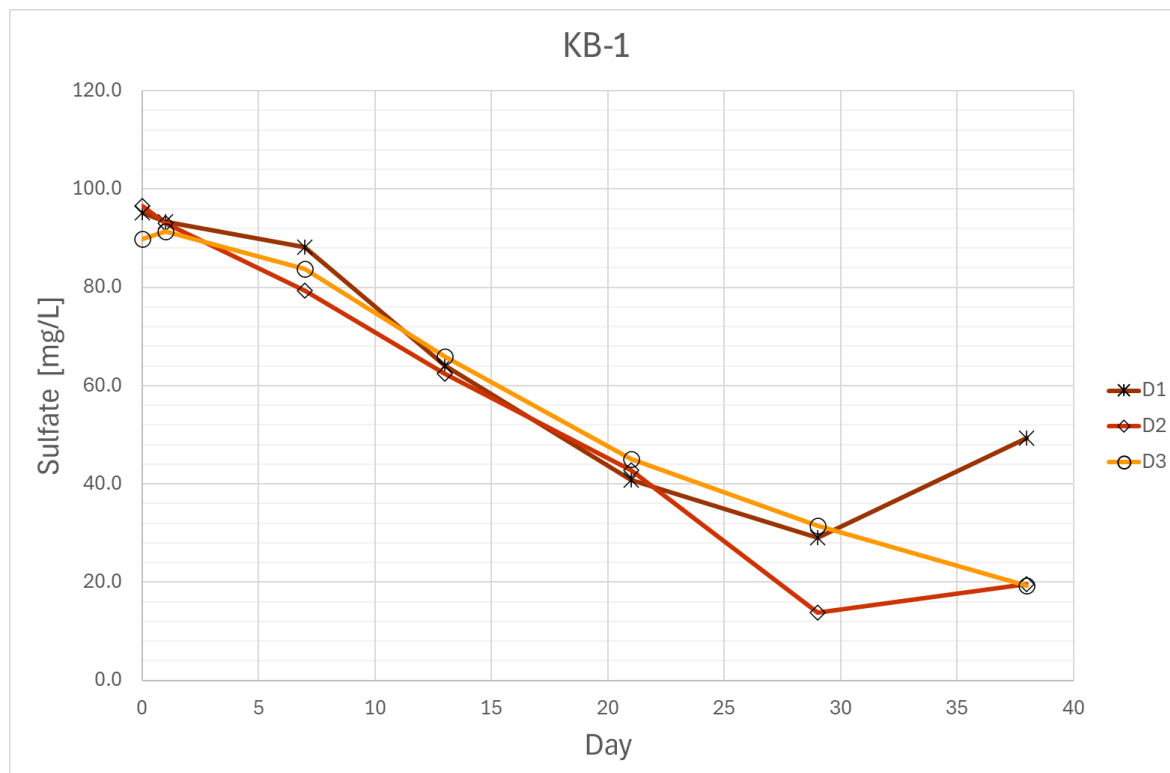


Figure 6.17: Sulphate concentration over time in the GeoForm batches (note the axis)



**Figure 6.18:** Sulphate concentration over time in the GeoForm + KB-1 batches (note the axis)



**Figure 6.19:** Sulphate concentration over time in the KB-1 batches

### 6.2.5 Redox parameters

#### Nitrate

The lowest standard for nitrate was 15 mg/L and therefore there might not be nitrate as the levels are between 0 and 3 mg/L especially since the microcosms are more reduced than nitrate-reducing conditions. ([Figure A.23](#),[Figure A.24](#), [Figure A.25](#) and [Figure A.26](#) in the appendix) .

#### Manganese

None of the controls or the batches with only KB-1 had Mn >0.5 mg/L (the detection limit); therefore, the only detections are for the batches with GeoForm which had Mn that was decreasing over time as the redox conditions are more than manganese-reducing. (The mean dissolved Mn concentration is in the appendix, [Figure A.22](#).)

### 6.2.6 pH

[Figure 6.20](#) shows the mean pH over time for each scenario, showing that though the pH fluctuates, it does not go below 6, or above 8 and therefore remained in a favourable range for microbes.

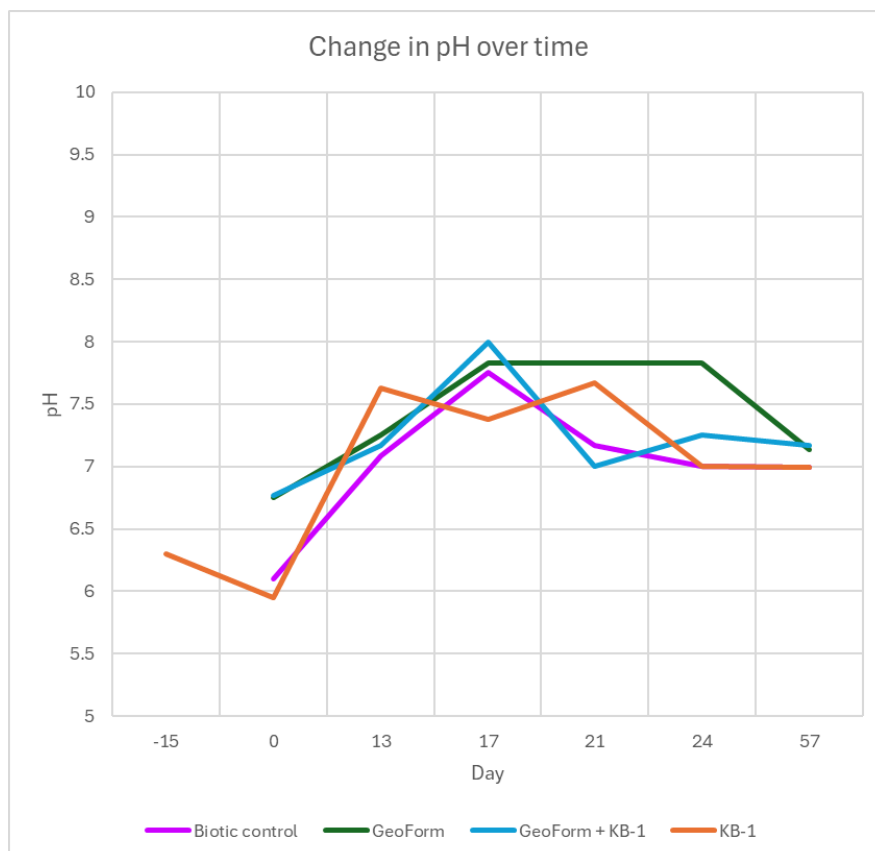


**Figure 6.20:** average pH over time

## DISCUSSION AND PERSPECTIVES

The main objective of this research is to advance the understanding of chlorinated solvent remediation in chalk aquifers, with particular focus on the cDCE contamination plume at Naverland 26AB in Albertslund. This investigation pursues four primary goals: first, to evaluate the feasibility of using iron-bearing minerals (BiRD) and ERD for cDCE remediation in limestone aquifers; to develop and conduct batch experiments quantifying degradation rates of both cDCE and VC; to analyse these experimental results in the context of existing literature and site-specific conditions to identify key factors influencing degradation; and to assess the effectiveness of BiRD and ERD approaches, culminating in recommendations for pilot-scale implementation.

### 7.1 BiRD

BiRD was considered a potentially viable remediation strategy for the Naverland site based on several site-specific and conceptual factors. cDCE as the primary contaminant in the plume aligns with the known reactivity of iron minerals, which have been shown to abiotically degrade CE without the formation of VC under reducing conditions. As noted by [Darlington and Rectanus, 2015](#); [Y. T. He et al., 2015](#), effective ISBGT requires a balance of high sulfate loading, the presence of iron oxides, and sufficient organic carbon, while the Naverland site contains relatively low natural iron concentrations (1.67 to 2.56 mg/L), its has sulfate (100 mg/L) and organic matter (fermented to provide electron donors), combined with the potential for iron supplementation (like GeoForm® Soluble), would create favourable conditions for implementing remediation strategies. Moreover [Pósfa et al., 2006](#) reported that FeS plays a crucial role in biogeochemical processes by mediating long distance extracellular electron transfer.

In contrast, based on the experimental results, BiRD would show limited effectiveness of cDCE remediation in the Naverland site. BiRD would be not supported under the available time-frame and test conditions. Clearly demonstrating that the recommended hydraulic retention time of 15 to 30 days for FeS formation and dechlorination by [Darlington and](#)

[Rectanus, 2015](#) is too short even with SRB supplementation. The critical constraint emerged from delayed FeS formation, which only occurred on the day 38 (for GeoForm) which led to insufficient time to measurably contribute to cDCE degradation. This delay likely reflects inadequate reducing conditions in the GeoForm-only microcosms. While these findings do not invalidate BiRD's theoretical basis, they underscore its dependence on sustained redox control, necessitating more aggressive engineering of reducing conditions for it's application. While it would have been methodologically advantageous to bypass the iron sulphide formation step (a key rate-limiting process in this system), the approach of using powdered FeS nor freeze-dried mackinawite according to [Jeong et al., 2011](#) wouldn't have exhibited reactivity with CE, necessitating the in situ formation of reactive iron sulphides . As previous studies that demonstrate iron sulphide minerals can dechlorinate CE (e.g. [Butler et al., 1999](#)) involved well-established FeS from the start which makes comparing this experiment with literature difficult .

## 7.2 BiRD + ERD

In the batches with KB-1 and GeoForm, there was VC formation, confirming that biotic dechlorination by *Dehalococcoides* was possible rather than abiotic degradation, where it is simultaneous degradation of all the CE present [[Darlington and Rectanus, 2015](#)] . Though as KB-1 contains SRB and there was faster formation of FeS, no significant decrease in cDCE was observed within the time-frame, especially when compared to the KB-1-only batch. regenerating FeS, the enrichment of *Desulfovibrio*, a SRB that can reduce  $SO_4^{2-}$  and  $Fe^{3+}$  may enhance abiotic PCE-to-acetylene dechlorination [[Liu et al., 2023](#)]. This suggests potential inhibition from competing processes, such as high iron or sulphate levels which is supported by prior studies [[Yaru Li et al., 2021](#) and [Liu et al., 2023](#)] which indicated that high FeS concentrations can inhibit *Dehalococcoides*. However, direct comparison for *Dehalococcoides* inhibition before the FeS formation is difficult because this system contained much higher iron levels (800 mg/L) than those tested by [Yoshikawa et al., 2021](#) (28 mg/L) which observed that ferrous iron shortened the time required for complete dechlorination. So this experiment did not show synergistic effects of the combination of BiRD and ERD. Additionally, in the batches where FeS should have mediated degradation, the expected sequence involves: (1) initial blackening of the water due to FeS formation, followed by (2) precipitation and settling of FeS, resulting in clarified water. In this experiment, the batches with GeoForm + KB-1, only showed the first step, blackening of the water.

## 7.3 ERD

ERD was also considered a promising approach, particularly due to the potential for complete dechlorination of cDCE and VC in the presence of *Dehalococcoides*. Unlike ZVI, which is particulate and dependent on surface area for reactivity (often leading to distribution challenges and potential aquifer clogging), ERD relies on dissolved-phase amendments

(dissolved electron donors and microbial culture), allowing for more effective delivery in fractured limestone systems.

The ERD trials using KB-1 alone demonstrated the best results, achieving complete cDCE reduction to VC within 46 days, followed by near-total VC degradation to trace levels (0.1–0.2 µg/L) and ethene formation within 73 days. The observed dechlorination indicate the presence of the *vcrA* and *bvcA* genes in *Dehalococcoides* [Müller et al., 2004; Krajmalnik-Brown et al., 2004]. This effective dechlorination likely benefited from the limestone aquifer's natural buffering capacity, which maintained a stable pH of 6.99—optimal for sustaining both SRB and *Dehalococcoides* activity in the KB-1 consortium. The site's existing sulphate and organic carbon levels suggest that only minimal supplementation (*Dehalococcoides*) would be required to stimulate microbial activity. According to Mao et al., 2017, environments with high sulphate had no effect on *Dehalococcoides* (strain 195) but inhibited its yield by about 65% in sulphide environments, indicating the addition of iron to form FeS could help regulate sulphide levels and create redox conditions more favourable for *Dehalococcoides*. In low concentrations, FeS has even been shown to enhance ERD by facilitating electron transfer and supporting microbial metabolism.

One of the aims of this thesis is to calculate the degradation rate for all the microcosms. However degradation was seen only in the batch with KB-1, which was  $0.1251\text{ day}^{-1}$  for cDCE and  $0.1302\text{ day}^{-1}$  for VC. Even if the experiment with GeoForm and GeoForm + KB-1 was extended, the potential abiotic degradation rates would not compete with the rapid biotic dechlorination demonstrated by KB-1 culture. The superior performance of ERD was evident in these experiments. This suggests ERD implementation would be more reliably effective for field applications.

## 7.4 Pilot-scale implementation

For pilot-scale implementation in limestone aquifers, ERD using KB-1 or similar cultures represents the most promising approach. Field deployment should incorporate measures such as supplying enough KB-1 and electron donors (e.g., lactate or ELS Microemulsion) should be injected directly into the aquifer, with recirculation to enhance contact between amendments and contaminants. This is particularly critical in limestone aquifers, where fracture-dominated flow may limit mixing. Monitoring protocols would need to be established to assess both short-term performance and long-term sustainability of the remediation effort. Parameters would include redox-sensitive species such as sulfate and ferrous iron, concentrations of CE, and VFAs to ensure enough electron donors are supplied if the NVOC levels in the Naverland site are different to the microcosm test done. The specific conditions at Naverland, including the chalk aquifer's depth and carbonate buffering capacity, appear generally favorable for ERD implementation. Previous failures of BiRD in

field applications [Darlington, Lehmicke, et al., 2013], further support the recommendation to prioritize ERD for this specific site.

## 7.5 Perspectives

Future iterations of this study should incorporate sediment material from the Naverland site into microcosms prepared under strictly anaerobic conditions (e.g., within an anaerobic glovebox) to better replicate the iron-reducing to sulfate-reducing conditions relevant for both ERD and BiRD processes. Although methanogenic conditions are theoretically ideal for ERD, Sørensen, 2013 did not observe methane production, suggesting SRB outcompeting methanogenic archaea for hydrogen and acetate [Stams, 1994; Muyzer et al., 2008]. The inclusion of site-specific sediments would enhance the representativeness of redox dynamics by preserving *in situ* microbial communities and geochemical profiles. Particular care must also be taken to prevent oxygen introduction during groundwater collection to maintain optimal redox conditions from the start of the experiment.

A more comprehensive characterisation of solid phases would significantly improve process understanding. This could involve: (1) quantitative analysis of sediment samples for total iron and sulfide content to verify precipitation dynamics; (2) selective sampling of precipitates through centrifugation or filtration of the aqueous phase; and (3) detailed characterization of collected solids using stoichiometric analysis to differentiate between iron sulphide phases (e.g., mackinawite ( $\text{FeS}$ ) versus pyrite ( $\text{FeS}_2$ )) or the use of X-ray diffraction to confirm the formation of these minerals.

The experimental duration should be extended beyond the current 38-day time-frame, with a minimum 60-day period recommended to allow for complete establishment of reducing conditions and subsequent degradation processes. This modification is particularly warranted given the delayed onset of iron sulphide precipitation observed in the current study. Additional analytical improvements would include: (1) measuring the CE before adding to the microcosm bottles to establish more accurate baseline conditions and enable better kinetic modelling; and (2) measure the NVOC concentration at the start of the experiment to see if it follows the VFAs levels and if not conclude that there is enough organic matter instead of measuring NVOC throughout the experiment. Conducting the experiment at room temperature (approximately 20 to 25 °C) rather than 10 °C would likely have accelerated key processes. In the GeoForm + KB-1 batch, the established iron sulphide ( $\text{FeS}$ ) would have promoted faster dechlorination through both biotic (Dehalococcoides) and abiotic ( $\text{FeS}$ -mediated) pathways due to enhanced reaction kinetics at elevated temperatures. Similarly, the lag phase observed in GeoForm-only batches, which was attributable to slow microbial acclimation at 10 °C, would probably have been shorter given the known temperature dependence of microbial metabolic rates.

## CONCLUSION

This thesis investigated the potential for Biogeochemical Reductive Dechlorination (BiRD) and Enhanced Reductive Dechlorination (ERD) to decontaminate the primarily cis-1,2-Dichloroethylene (cDCE) plume in a fractured limestone aquifer, using the Naverland site in Denmark as a case study. Through a comprehensive evaluation of available literature and laboratory-scale batch experiments, this study compared the effectiveness of Monitored Natural Attenuation (MNA), GeoForm® Soluble, a ferrous sulphate-based amendment, KB-1®, a consortium containing *Dehalococcoides*, and a combination of KB-1® and Geoform®, to degrade cDCE and Vinyl Chloride (VC) under site-relevant conditions. The results indicate that ERD using KB-1® was the most effective remediation strategy, achieving complete dechlorination of cDCE to ethene with high degradation rates of  $52.73 \mu\text{mol L}^{-1}\text{day}^{-1}$  on average while BiRD despite the theoretical promise, showed limited effectiveness within the given time-frame, mainly due to the delayed formation of reactive iron sulphide (FeS) minerals as the microcosms were not sufficiently reduced. When KB-1® and Geoform® was combined, the Sulfate-Reducing Bacterium (SRB) in KB-1® accelerated the production of FeS, but insufficient precipitation occurred to enable abiotic degradation. Consistent with previous studies, the resulting high iron sulphide concentration inhibited *Dehalococcoides* activity, slowing reductive dechlorination rather than showing synergistic effects. Nevertheless, the formation of VC and ethene confirmed that biotic degradation persisted, albeit at reduced rates. Therefore given the redox conditions, buffering capacity of limestone, and other site-specific factors, ERD using KB-1 and recirculation to enhance amendment delivery in the fracture for field-scale applications. Future work could focus on incorporating native sediments, avoiding oxygen introduction during groundwater collection to maintain optimal redox conditions from the start of the experiment and extending monitoring periods from 38 days to 60 days to capture long-term degradation dynamics. Ultimately, this study contributes valuable insights into the practical challenges and opportunities of treating chlorinated solvent plumes in limestone aquifers and supports the broader application of ERD as a robust remediation approach.



## BIBLIOGRAPHY

- Andersen, Thomas Breum and Mads Robenhagen Mølgaard (2018). *Copenhagen Area Overview of the geological conditions in the Copenhagen area and surrounding areas*. Tech. rep. GeoAtlas Live. URL: [https://wgn.geo.dk/geodata/modeldokumentation/Copenhagen%20\\_25m\\_2018-07-12.pdf](https://wgn.geo.dk/geodata/modeldokumentation/Copenhagen%20_25m_2018-07-12.pdf).
- Aziz, Carol E., Ryan A. Wymore, and Robert J. Steffan (2013). "Bioaugmentation Considerations". In: *Bioaugmentation for Groundwater Remediation*. Ed. by Hans F. Stroo, Andrea Leeson, and C. Herb Ward. New York, NY: Springer New York, pp. 141–169. ISBN: 978-1-4614-4115-1. doi: 10.1007/978-1-4614-4115-1\_5.
- Ballapragada, Bhaskar S., H. David Stensel, J. A. Puhakka, and John F. Ferguson (1997). "Effect of Hydrogen on Reductive Dechlorination of Chlorinated Ethenes". In: *Environmental Science & Technology* 31.6, pp. 1728–1734. doi: 10.1021/es9606539.
- Bradley, Paul and Francis Chapelle (May 2010). "Biodegradation of Chlorinated Ethenes". In: doi: 10.1007/978-1-4419-1401-9\_3.
- Brigmon, Robin, Nathan Bell, David Freedman, and Christopher Berry (July 1998). "Natural Attenuation of Trichloroethylene in Rhizosphere Soils at the Savannah River Site". In: *Journal of Soil Contamination - J SOIL CONTAM* 7, pp. 433–453. doi: 10.1080/10588339891334429.
- Broholm, Mette M., Gry S. Janniche, Klaus Mosthaf, Annika S. Fjordbøge, Anders G. Binning Philip J. and Christensen, Bernt Grosen, Torben H. Jørgensen, Carl Keller, Gary Wealthall, and . Henriette Kerrn-Jespersen (2016). "Characterization of chlorinated solvent contamination in limestone using innovative FLUTE® technologies in combination with other methods in a line of evidence approach". In: *Journal of Contaminant Hydrology* 189, pp. 68–85. ISSN: 0169-7722. doi: <https://doi.org/10.1016/j.jconhyd.2016.03.007>. URL: <https://www.sciencedirect.com/science/article/pii/S0169772216300444>.
- Bromley, Richard G. (1979). "Chalk and Bryozoan limestone: facies, sediments and depositional environments". In: *Institute of Historical Geology and Palaeontology, Øster Voldgade 10 , DK-13 50 Copenhagen K*. URL: <https://paleoarchive.com/literature/Birkelund&Bromley1979-03-Bromley-ChalkBryozoanLimestone.pdf>.
- Bronzetti, Giorgio, Carlo Bauer, Claudio Corsi, Renata Del Carratore, Alvaro Galli, Riccardo Nieri, Moreno Paolini, Enrico Cundari, Giorgio Cantelli Forti, and John Crenshaw (1984). "Comparative genetic activity of cis- and trans-1,2-dichloroethylene in yeast". In: *Teratogenesis, Carcinogenesis, and Mutagenesis* 4.4, pp. 365–375. doi: <https://doi.org/10.1002/tcm.1770040406>.
- Brusseau, M.L. and J. Chorover (2019). "Chapter 8 - Chemical Processes Affecting Contaminant Transport and Fate". In: *Environmental and Pollution Science (Third Edition)*. Ed. by Mark L. Brusseau,

- Ian L. Pepper, and Charles P. Gerba. Third Edition. Academic Press, pp. 113–130. ISBN: 978-0-12-814719-1. doi: <https://doi.org/10.1016/B978-0-12-814719-1.00008-2>.
- Butler, Elizabeth C. and Kim F. Hayes (1999). "Kinetics of the Transformation of Trichloroethylene and Tetrachloroethylene by Iron Sulfide". In: *Environmental Science & Technology* 33.12, pp. 2021–2027. doi: 10.1021/es9809455.
- Chen, Fei, David L. Freedman, Ronald W. Falta, and Lawrence C. Murdoch (2012). "Henry's law constants of chlorinated solvents at elevated temperatures". In: *Chemosphere* 86.2, pp. 156–165. ISSN: 0045-6535. doi: <https://doi.org/10.1016/j.chemosphere.2011.10.004>. URL: <https://www.sciencedirect.com/science/article/pii/S0045653511011453>.
- Chen, Yaoning, Weiyu Liang, Yuanping Li, Yanxin Wu, Yanrong Chen, Wei Xiao, Li Zhao, Jiachao Zhang, and Hui Li (2019). "Modification, application and reaction mechanisms of nano-sized iron sulfide particles for pollutant removal from soil and water: A review". In: *Chemical Engineering Journal* 362, pp. 144–159. ISSN: 1385-8947. doi: <https://doi.org/10.1016/j.cej.2018.12.175>. URL: <https://www.sciencedirect.com/science/article/pii/S1385894718326615>.
- Chilingar, G. V. and B. Endres (Jan. 1, 2005). "Environmental hazards posed by the Los Angeles Basin urban oilfields: an historical perspective of lessons learned". In: *Environmental Geology* 47.2, pp. 302–317. ISSN: 1432-0495. URL: <https://doi.org/10.1007/s00254-004-1159-0>.
- Chiou, Cary T. and Daniel E. Kile (1998). "Deviations from Sorption Linearity on Soils of Polar and Nonpolar Organic Compounds at Low Relative Concentrations". In: *Environmental Science & Technology* 32.3, pp. 338–343. doi: 10.1021/es970608g.
- Christ, John A., C. Andrew Ramsburg, Linda M. Abriola, Kurt D. Pennell, and Frank E. Löffler (2005). "Coupling Aggressive Mass Removal with Microbial Reductive Dechlorination for Remediation of DNAPL Source Zones: A Review and Assessment". In: *Environmental Health Perspectives* 113.4, pp. 465–477. doi: 10.1289/ehp.6932.
- Chu, Wei and Kwai-Hing Chan (2000). "The prediction of partitioning coefficients for chemicals causing environmental concern". In: *Science of The Total Environment* 248.1, pp. 1–10. ISSN: 0048-9697. doi: [https://doi.org/10.1016/S0048-9697\(99\)00472-6](https://doi.org/10.1016/S0048-9697(99)00472-6).
- Cichocki, Joseph A., Kathryn Z. Guyton, Neela Guha, Weihsueh A. Chiu, Ivan Rusyn, and Lawrence H. Lash (Oct. 1, 2016). "Target Organ Metabolism, Toxicity, and Mechanisms of Trichloroethylene and Perchloroethylene: Key Similarities, Differences, and Data Gaps". In: *The Journal of Pharmacology and Experimental Therapeutics* 359.1. Publisher: Elsevier, pp. 110–123. ISSN: 0022-3565. doi: 10.1124/jpet.116.232629. URL: <https://doi.org/10.1124/jpet.116.232629> (visited on 01/21/2025).
- COWI (2023). *Videregående forureningsundersøgelse - Naverland 26AB. Rapport, 118 sider.* Tech. rep. COWI.
- COWI (n.d.). "Forslag til undersøgelser i Naverland fanen – oplæg til møde den 1 oktober. Udkast (25. september 2024)". 2024.
- Cwiertny, David M. and Michelle M. Scherer (2010). "Abiotic Processes Affecting the Remediation of Chlorinated Solvents". In: *In Situ Remediation of Chlorinated Solvent Plumes*. Ed. by H.F. Stroo and C.H. Ward. New York, NY: Springer New York, pp. 69–108. ISBN: 978-1-4419-1401-9. doi: 10.1007/978-1-4419-1401-9\_4.

Damgaard, Jesper, Bernt Grossen, Kerim Martinez, Nielsen Ole Frits, Torben H. Jørgensen, Gry Sander Janniche, Mette Broholm, Henriette Kerrn-Jespersen, and Gary P. Wealthall (2012). *Geologisk, Geofysisk og Hydrologisk Karakterisering på Naverland 26; Opstilling af Hydrogeologisk Konceptuel Model*. Tech. rep. COWI.

Darlington, Ramona, Leo G. Lehmicke, Richard G. Andrachek, and David L. Freedman (2013). "Anaerobic abiotic transformations of cis-1,2-dichloroethene in fractured sandstone". In: *Chemosphere* 90.8, pp. 2226–2232. ISSN: 0045-6535. doi: <https://doi.org/10.1016/j.chemosphere.2012.09.084>. URL: <https://www.sciencedirect.com/science/article/pii/S0045653512012258>.

Darlington, Ramona and Heather Rectanus (2015). *Biogeochemical transformation handbook*. Tech. rep. Naval facilities Engineering command NAVFAC. URL: [https://www.enviro.wiki/images/7/78/Darlington-2015-Biogeochem\\_Transformation\\_Handbook.pdf](https://www.enviro.wiki/images/7/78/Darlington-2015-Biogeochem_Transformation_Handbook.pdf).

Ding, Xiang-Hong, Shi-Jin Feng, and Zhang-Wen Zhu (2025). "Analytical model for reactive contaminant back-diffusion from low-permeability aquitards with internal source zones". In: *Journal of Hydrology* 646, p. 132306. ISSN: 0022-1694. doi: <https://doi.org/10.1016/j.jhydrol.2024.132306>. URL: <https://www.sciencedirect.com/science/article/pii/S0022169424017025>.

Dong, Haoran, Long Li, Yue Lu, Yujun Cheng, Yaoyao Wang, Qin Ning, Bin Wang, Lihua Zhang, and Guangming Zeng (2019). "Integration of nanoscale zero-valent iron and functional anaerobic bacteria for groundwater remediation: A review". In: *Environment International* 124, pp. 265–277. doi: [10.1016/j.envint.2019.01.030](https://doi.org/10.1016/j.envint.2019.01.030). URL: <https://www.scopus.com/inward/record.uri?eid=2-s2.0-85060051787&doi=10.1016%2fj.envint.2019.01.030&partnerID=40&md5=6f60411cf8b793ef5bcf0aa112580478>.

Dreher, Eberhard-Ludwig, Klaus K. Beutel, John D. Myers, Thomas Lübbe, Shannon Krieger, and Lynn H. Pottenger (2014). "Chloroethanes and Chloroethylenes". In: *Ullmann's Encyclopedia of Industrial Chemistry*. John Wiley & Sons, Ltd, pp. 1–81. ISBN: 9783527306732. doi: [https://doi.org/10.1002/14356007.006\\_001.pub2](https://doi.org/10.1002/14356007.006_001.pub2).

Duhamel, Melanie, Kaiguo Mo, and Elizabeth A. Edwards (2004). "Characterization of a Highly Enriched Dehalococcoides Containing Culture That Grows on Vinyl Chloride and Trichloroethylene". In: *Applied and Environmental Microbiology* 70.9, pp. 5538–5545. doi: [10.1128/AEM.70.9.5538-5545.2004](https://doi.org/10.1128/AEM.70.9.5538-5545.2004).

EVONIK, Active Oxygens (n.d.[a]). *GeoForm®: Biogeochemical Reagent for Soil and Groundwater Remediation*. url<https://regenesis.com/en/geoform/>.

EVONIK, Active Oxygens (n.d.[b]). accessed 12.03.2025. URL: <https://active-oxygens.evonik.com/en/products-and-services/soil-and-groundwater-remediation/geoform-reagents>.

Ferrey, Mark L., Richard T. Wilkin, Robert G. Ford, and John T. Wilson (2004). "Nonbiological Removal of cis-Dichloroethylene and 1,1-Dichloroethylene in Aquifer Sediment Containing Magnetite". In: *Environmental Science & Technology* 38.6. PMID: 15074684, pp. 1746–1752. doi: [10.1021/es0305609](https://doi.org/10.1021/es0305609).

Friis, Anne Kirketerp (2006). "The potential for reductive dechlorination after thermal treatment of TCE-contaminated aquifers". PhD thesis. Technical University of Denmark.

Galizia, D. Audrey and Charles Thompson (2010). *Toxicological review of cis-1,2-dichloroethylene and trans-1,2-dichloroethylene*. Tech. rep. Integrated Risk Information System (IRIS) U.S. Environmental Protection Agency. eprint: <https://iris.epa.gov/static/pdfs/0418tr.pdf>.

Garbarini, Doug R. and Leonard W. Lion (1986). "Influence of the nature of soil organics on the sorption of toluene and trichloroethylene". In: *Environmental Science & Technology* 20.12. PMID: 22229435, pp. 1263–1269. doi: 10.1021/es00154a013.

Gejl, R.N., M. Rygaard, H.J. Henriksen, J. Rasmussen, and P.L. Bjerg (2019). "Understanding the impacts of groundwater abstraction through long-term trends in water quality". In: *Water Research* 156, pp. 241–251. issn: 0043-1354. doi: <https://doi.org/10.1016/j.watres.2019.02.026>. URL: <https://www.sciencedirect.com/science/article/pii/S0043135419301514>.

GEUS (n.d.). The Geological Survey of Denmark and Greenland, The GEUS Jupiter database, url = geus.dk.

Goodman, Julie E., Rebecca C. Ticknor, and Jean Zhou (2022). "Systematic review of perchloroethylene and non-Hodgkin's lymphoma". In: *Global Epidemiology* 4, p. 100077. issn: 2590-1133. doi: <https://doi.org/10.1016/j.gloepi.2022.100077>. URL: <https://www.sciencedirect.com/science/article/pii/S2590113322000074>.

Gossett, James M. (1987). "Measurement of Henry's law constants for C1 and C2 chlorinated hydrocarbons". In: *Environmental Science & Technology* 21.2. PMID: 22242591, pp. 202–208. doi: 10.1021/es00156a012.

Guan, Xiaohong, Yuankui Sun, Hejie Qin, Jinxiang Li, Irene M.C. Lo, Di He, and Haoran Dong (2015). "The limitations of applying zero-valent iron technology in contaminants sequestration and the corresponding countermeasures: The development in zero-valent iron technology in the last two decades (1994–2014)". In: *Water Research* 75, pp. 224–248. issn: 0043-1354. doi: <https://doi.org/10.1016/j.watres.2015.02.034>. URL: <https://www.sciencedirect.com/science/article/pii/S0043135415001074>.

Guerrero-Barajas, Claudia and Jim A. Field (June 1, 2005). "Enhancement of anaerobic carbon tetrachloride biotransformation in methanogenic sludge with redox active vitamins". In: *Biodegradation* 16.3, pp. 215–228. issn: 1572-9729. doi: 10.1007/s10532-004-0638-z.

Guo, Jiaming, Feilong Gao, Chengfang Zhang, Shakeel Ahmad, and Jingchun Tang (2023). "Sulfidation of zero-valent iron for enhanced reduction of chlorinated contaminants: A review on the reactivity, selectivity, and interference resistance". In: *Chemical Engineering Journal* 477, p. 147049. issn: 1385-8947. doi: <https://doi.org/10.1016/j.cej.2023.147049>. URL: <https://www.sciencedirect.com/science/article/pii/S1385894723057807>.

Han, Young-Soo, Sung Pil Hyun, Hoon Y. Jeong, and Kim F. Hayes (2012). "Kinetic study of cis-dichloroethylene (cis-DCE) and vinyl chloride (VC) dechlorination using green rusts formed under varying conditions". In: *Water Research* 46.19, pp. 6339–6350. issn: 0043-1354. doi: <https://doi.org/10.1016/j.watres.2012.08.041>. URL: <https://www.sciencedirect.com/science/article/pii/S0043135412006410>.

Hansch, C, A Leo, and D Hoekman (1995). *Exploring QSAR: Fundamentals and applications in chemistry and biology*. American Chemical Society.

Haynes, William M. (2014). *CRC Handbook of Chemistry and Physics*. CRC Press. URL: <https://doi.org/10.1201/b17118>.

He, Jianzhong, Victor F. Holmes, Patrick K. H. Lee, and Lisa Alvarez-Cohen (2007). "Influence of Vitamin B12 and Cocultures on the Growth of Dehalococcoides Isolates in Defined Medium". In: *Applied and Environmental Microbiology* 73.9, pp. 2847–2853. doi: 10.1128/AEM.02574-06.

- He, Y. T., J. T. Wilson, C. Su, and R. T. Wilkin (2015). "Review of Abiotic Degradation of Chlorinated Solvents by Reactive Iron Minerals in Aquifers". In: *Groundwater Monitoring & Remediation* 35.3, pp. 57–75. doi: <https://doi.org/10.1111/gwmr.12111>.
- Hedeselskabet (2002). *Omfattende undersøgelser - Naverland 26AB, Albertslund*. Tech. rep. Københavns Amt.
- Hemendorff, Anne Schouby (2013). "Natural attenuation of a chlorinated solvent plume in a chalk aquifer: Processes and modeling. Case study: Naverland 26AB, Albertslund". MA thesis. Technical University of Denmark.
- Henry, Bruce M. (2010). "Biostimulation for Anaerobic Bioremediation of Chlorinated Solvents". In: *In Situ Remediation of Chlorinated Solvent Plumes*. Ed. by H.F. Stroo and C.H. Ward. New York, NY: Springer New York, pp. 357–423. ISBN: 978-1-4419-1401-9. doi: 10.1007/978-1-4419-1401-9\_12.
- Herrero, Jofre, Diana Puigserver, Ivonne Nijenhuis, Kevin Kuntze, and José M. Carmona (2019). "Combined use of ISCR and biostimulation techniques in incomplete processes of reductive dehalogenation of chlorinated solvents". In: *Science of The Total Environment* 648, pp. 819–829. ISSN: 0048-9697. doi: <https://doi.org/10.1016/j.scitotenv.2018.08.184>. URL: <https://www.sciencedirect.com/science/article/pii/S0048969718331723>.
- Himmelheber, David W., Kurt D. Pennell, and Joseph B. Hughes (2007). "Natural Attenuation Processes during In Situ Capping". In: *Environmental Science & Technology* 41.15. PMID: 17822095, pp. 5306–5313. doi: 10.1021/es0700909.
- Horvath, Ari L., Forrest W. Getzen, and Z. Maczynska (Mar. 1999). "IUPAC-NIST Solubility Data Series 67. Halogenated Ethanes and Ethenes with Water". In: *Journal of Physical and Chemical Reference Data* 28.2, pp. 395–627. ISSN: 0047-2689. doi: 10.1063/1.556039. eprint: [https://pubs.aip.org/aip/jpr/article-pdf/28/2/395/8183483/395\\\_1\\\_online.pdf](https://pubs.aip.org/aip/jpr/article-pdf/28/2/395/8183483/395\_1\_online.pdf).
- Hovedstaden, Region (2007). *Naverland 26AB, Albertslund. Monitering af punktkilde 2007. Rapport udarbejdet*. Tech. rep. Orbicon.
- Huang, Binbin, Chao Lei, Chaohai Wei, and Guangming Zeng (2014). "Chlorinated volatile organic compounds (Cl-VOCs) in environment — sources, potential human health impacts, and current remediation technologies". In: *Environment International* 71, pp. 118–138. ISSN: 0160-4120. doi: <https://doi.org/10.1016/j.envint.2014.06.013>. URL: <https://www.sciencedirect.com/science/article/pii/S0160412014001974>.
- Huang, Hui and Lin Ye (2020). "Chapter 9 - Biological technologies for cHRPs and risk control". In: *High-Risk Pollutants in Wastewater*. Ed. by Hongqiang Ren and Xuxiang Zhang. Elsevier, pp. 209–236. ISBN: 978-0-12-816448-8. doi: <https://doi.org/10.1016/B978-0-12-816448-8.00009-5>.
- Hug, Laura A., Farai Maphosa, David Leys, Frank E. Löffler, Hauke Smidt, Elizabeth A. Edwards, and Lorenz Adrian (2013). "Overview of organohalide-respiring bacteria and a proposal for a classification system for reductive dehalogenases". In: *Philosophical Transactions of the Royal Society B: Biological Sciences* 368.1616, p. 20120322. doi: 10.1098/rstb.2012.0322.
- Hvid, Jens Martin, Frans Van Buchem, Frank Aandreasen, Emma Sheldon, and Ida Lykke Fabricius (2021). "Stratigraphy and petrophysical characteristics of Lower Paleocene cool-water carbonates, Faxe quarry, Denmark". In: *Bulletin of the Geological Society of Denmark*. URL: <https://doi.org/10.37570/bgsd-2021-69-07>.

Hyun, Sung Pil and Kim F. Hayes (2015). "Abiotic reductive dechlorination of cis-DCE by ferrous monosulfide mackinawite". In: *Environmental Science and Pollution Research* 22.21, pp. 16463–16474. ISSN: 1614-7499. doi: 10.1007/s11356-015-5033-2.

Islam, Syful, Asef Redwan, Kayleigh Millerick, Jan Filip, Lingfei Fan, and Weile Yan (2021). "Effect of Copresence of Zerivalent Iron and Sulfate Reducing Bacteria on Reductive Dechlorination of Trichloroethylene". In: *Environmental Science & Technology* 55.8. PMID: 33787255, pp. 4851–4861. doi: 10.1021/acs.est.0c07702.

Jacobsen, R (1991). *Hydraulik og stoftransport i en oprørkset kalkbjerget – lossepladsprojektet*. Tech. rep. H9, Miljøministeriet, Miljøstyrelsen.

Jakobsen, Peter, Magnus Rohde, and Emma Sheldon (2017). "Structures and stratigraphy of Danian limestone, eastern Sjælland, Denmark". In: *The Geological Survey of Denmark and Greenland Bulletin*. URL: <https://geusbulletin.org/index.php/geusb/article/download/4391/10119/29033>.

Jeong, Hoon Y., Karthik Anantharaman, Young-Soo Han, and Kim F. Hayes (2011). "Abiotic Reductive Dechlorination of cis-Dichloroethylene by Fe Species Formed during Iron- or Sulfate-Reduction". In: *Environmental Science & Technology* 45.12. PMID: 21595430, pp. 5186–5194. doi: 10.1021/es104387w.

Jiang, Lisi, Yi Yang, Huijuan Jin, Hongyan Wang, Cynthia M. Swift, Yongchao Xie, Torsten Schubert, Frank E. Löffler, and Jun Yan (2022). "Geobacter sp. Strain IAE Dihaloeliminates 1,1,2-Trichloroethane and 1,2-Dichloroethane". In: *Environmental Science & Technology* 56.6. PMID: 35239320, pp. 3430–3440. doi: 10.1021/acs.est.1c05952.

Jorgensen, L. F., L. Troldborg, M. Ondracek, I. K. Seidenfaden, J. Kidmose, C. Vangsgaard, and K. Hinsby (Sept. 2024). "Groundwater Resilience, security, and safety in the four largest cities in Denmark". In: *Acque Soterranei - Italian Journal of Groundwater* 13.3. doi: 10.7343/as-2024-803.

K.M. Paknikar V. Nagpal, A.V. Pethkar and J.M. Rajwade (2005). "Degradation of lindane from aqueous solutions using iron sulfide nanoparticles stabilized by biopolymers". In: *Science and Technology of Advanced Materials* 6.3-4, pp. 370–374. doi: 10.1016/j.stam.2005.02.016.

Katrin, Mackenzie, Bleyl Steffen, Kopinke Frank-Dieter, Doose Heidi, and Bruns Johannes (2016). "Carbo-Iron as improvement of the nanoiron technology: From laboratory design to the field test". In: *Science of The Total Environment* 563-564, pp. 641–648. ISSN: 0048-9697. doi: <https://doi.org/10.1016/j.scitotenv.2015.07.107>. URL: <https://www.sciencedirect.com/science/article/pii/S0048969715304496>.

Kennedy, Lonnie G., Jess W. Everett, Erica Becvar, and Donald DeFeo (2006). "Field-scale demonstration of induced biogeochemical reductive dechlorination at Dover Air Force Base, Dover, Delaware". In: *Journal of Contaminant Hydrology* 88.1, pp. 119–136. ISSN: 0169-7722. doi: <https://doi.org/10.1016/j.jconhyd.2006.06.007>. URL: <https://www.sciencedirect.com/science/article/pii/S0169772206001136>.

Kocur, Chris M. D., Line Lomheim, Hardiljeet K. Boparai, Ahmed I. A. Chowdhury, Kela P. Weber, Leanne M. Austrins, Elizabeth A. Edwards, Brent E. Sleep, and Denis M. O'Carroll (2015). "Contributions of Abiotic and Biotic Dechlorination Following Carboxymethyl Cellulose Stabilized Nanoscale Zero Valent Iron Injection". In: *Environmental Science & Technology* 49.14. PMID: 26090687, pp. 8648–8656. doi: 10.1021/acs.est.5b00719.

Kondo, Katsuhito, Akihiro Okamoto, Kazuhito Hashimoto, and Ryuhei Nakamura (2015). "Sulfur-Mediated Electron Shuttling Sustains Microbial Long-Distance Extracellular Electron Transfer with

- the Aid of Metallic Iron Sulfides". In: *Langmuir* 31.26. PMID: 26070345, pp. 7427–7434. doi: 10.1021/acs.langmuir.5b01033.
- Krajmalnik-Brown, Rosa, Tina Hölscher, Ivy N. Thomson, F. Michael Saunders, Kirsti M. Ritalahti, and Frank E. Löffler (2004). "Genetic Identification of a Putative Vinyl Chloride Reductase in Dehalococcoides sp. Strain BAV1". In: *Applied and Environmental Microbiology* 70.10, pp. 6347–6351. doi: 10.1128/AEM.70.10.6347–6351.2004.
- Kueper, Bernard H., Hans F. Stroo, Catherine M. Vogel, and C. Herb Ward (2014). "Source Zone Remediation: The State of the Practice". In: *Chlorinated Solvent Source Zone Remediation*. New York, NY: Springer New York, pp. 1–27. ISBN: 978-1-4614-6922-3. URL: [https://doi.org/10.1007/978-1-4614-6922-3\\_1](https://doi.org/10.1007/978-1-4614-6922-3_1).
- Lash, Lawrence H. (2019). "Environmental and Genetic Factors Influencing Kidney Toxicity". In: *Seminars in Nephrology* 39.2. Kidney Safety Science, pp. 132–140. ISSN: 0270-9295. doi: <https://doi.org/10.1016/j.semephrol.2018.12.003>. URL: <https://www.sciencedirect.com/science/article/pii/S0270929518301827>.
- Lee, Woojin and Bill Batchelor (2002). "Abiotic reductive dechlorination of chlorinated ethylenes by iron-bearing soil minerals. 2. Green rust". In: *Environmental Science and Technology* 36.24, pp. 5348–5354. doi: 10.1021/es0258374.
- Lee, Woojin and Bill Batchelor (2004). "Abiotic reductive dechlorination of chlorinated ethylenes by iron-bearing phyllosilicates". In: *Chemosphere* 56.10, pp. 999–1009. ISSN: 0045-6535. doi: <https://doi.org/10.1016/j.chemosphere.2004.05.015>. URL: <https://www.sciencedirect.com/science/article/pii/S004565350400400X>.
- Lemke, Lawrence D., Linda M. Abriola, and Pierre Goovaerts (2004). "Dense nonaqueous phase liquid (DNAPL) source zone characterization: Influence of hydraulic property correlation on predictions of DNAPL infiltration and entrapment". In: *Water Resources Research* 40.1. doi: <https://doi.org/10.1029/2003WR001980>.
- Li, Yaru, He-Ping Zhao, and Lihong Zhu (2021). "Iron Sulfide Enhanced the Dechlorination of Trichloroethene by Dehalococcoides mccartyi Strain 195". In: *Frontiers in Microbiology* 12. doi: 10.3389/fmicb.2021.665281.
- Liang, Xiaoming, R. Paul Philp, and Elizabeth C. Butler (2009). "Kinetic and isotope analyses of tetrachloroethylene and trichloroethylene degradation by model Fe(II)-bearing minerals". In: *Chemosphere* 75.1, pp. 63–69. ISSN: 0045-6535. doi: <https://doi.org/10.1016/j.chemosphere.2008.11.042>. URL: <https://www.sciencedirect.com/science/article/pii/S004565350801446X>.
- Ling, Liu, Yaqiang Wei, Haobo Niu, Hang Zhao, Yuling Chen, Dan Qu, Miao Gao, and Jian Chen (2024). "Long-term effectiveness and sustainability of EHC remediation in carbon tetrachloride-contaminated groundwater: Mechanistic understanding and practical applications". In: *Journal of Cleaner Production* 435, p. 140510.
- Little, R., E. Muller, and R. Mackay (1996). "Modelling of contaminant migration in a chalk aquifer". In: *Journal of Hydrology* 175.1, pp. 473–509. ISSN: 0022-1694. doi: [https://doi.org/10.1016/S0022-1694\(96\)80021-7](https://doi.org/10.1016/S0022-1694(96)80021-7).
- Liu, Xiaokun, Lian Zhang, Rui Shen, Qihong Lu, Qinglu Zeng, Xiaojun Zhang, Zhili He, Simona Rossetti, and Shanquan Wang (2023). "Reciprocal Interactions of Abiotic and Biotic Dechlorination

of Chloroethenes in Soil". In: *Environmental Science & Technology* 57.37. PMID: 37665676, pp. 14036–14045. doi: 10.1021/acs.est.3c04262.

Löffler, Frank E., Jun Yan, Kirsti M. Ritalahti, Lorenz Adrian, Elizabeth A. Edwards, Konstantinos T. Konstantinidis, Jochen A. Müller, Heather Fullerton, Stephen H. Zinder, and Alfred M. Spormann (2013). "Dehalococcoides mccartyi gen. nov., sp. nov., obligately organohalide-respiring anaerobic bacteria relevant to halogen cycling and bioremediation, belong to a novel bacterial class, Dehalococcoidia classis nov., order Dehalococcoidales ord. nov. and family Dehalococcoidaceae fam. nov., within the phylum Chloroflexi". In: *International Journal of Systematic and Evolutionary Microbiology* 63.Pt<sub>2</sub>, pp. 625–635. ISSN: 1466-5034. doi: <https://doi.org/10.1099/ijsm.0.034926-0>.

Lu, Cong, Poul L. Bjerg, Fengjun Zhang, and Mette M. Broholm (2011). "Sorption of chlorinated solvents and degradation products on natural clayey tills". In: *Chemosphere* 83.11, pp. 1467–1474. ISSN: 0045-6535. doi: <https://doi.org/10.1016/j.chemosphere.2011.03.007>. URL: <https://www.sciencedirect.com/science/article/pii/S0045653511002761>.

Major, David W., Michaye L. McMaster, Evan E. Cox, Elizabeth A. Edwards, Sandra M. Dworatzek, Edwin R. Hendrickson, Mark G. Starr, Jo Ann Payne, and Lois W. Buonamici (2002). "Field Demonstration of Successful Bioaugmentation To Achieve Dechlorination of Tetrachloroethene To Ethene". In: *Environmental Science & Technology* 36.23. PMID: 12523427, pp. 5106–5116. doi: 10.1021/es0255711.

Mao, Xinwei, Alexandra Polasko, and Lisa Alvarez-Cohen (2017). "Effects of Sulfate Reduction on Trichloroethene Dechlorination by Dehalococcoides-Containing Microbial Communities". In: *Applied and Environmental Microbiology* 83.8, e03384–16. doi: 10.1128/AEM.03384-16.

Maymó-Gatell, Xavier, Timothy Anguish, and Stephen H. Zinder (1999). "Reductive Dechlorination of Chlorinated Ethenes and 1,2-Dichloroethane by *Dehalococcoides ethenogenes*". In: *Applied and Environmental Microbiology* 65.7, pp. 3108–3113. doi: 10.1128/AEM.65.7.3108-3113.1999.

Miljøstyrelsen, Miljø- og energiministriet (1998). *Vejledning nr. 6 og 7. Oprydning på forurenede lokaliteter*. Tech. rep. Hovedbind og Appendikser. Miljøstyrelsen.

Mohamed, Badr Ali and Mohamed Samer (2023). "Chapter 8 - Biobutanol production from agricultural wastes". In: *Valorization of Wastes for Sustainable Development*. Ed. by Rangabhashiyam Selvasembian, Nur Izyan Wan Azelee, Saravanan Ramiah Shanmugam, Ponnusami Venkatachalam, and Ajay Kumar Mishra. Elsevier, pp. 181–200. ISBN: 978-0-323-95417-4. doi: <https://doi.org/10.1016/B978-0-323-95417-4.00008-1>.

Molenda, Olivia, Andrew T. Quaile, and Elizabeth A. Edwards (2016). "Dehalogenimonas sp. Strain WBC-2 Genome and Identification of Its *< i>trans</i>-Dichloroethene Reductive Dehalogenase, TdrA*". In: *Applied and Environmental Microbiology* 82.1, pp. 40–50. doi: 10.1128/AEM.02017-15.

Moreno, Hector A., David L. Cocke, Jewel A. Gomes, Paul Morkovsky, Jose Parga, Eric Peterson, and C. Garcia (2007). "Electrochemical Generation of Green Rust using Electrocoagulation". In: *ECS Transactions* 3.18, p. 67. doi: 10.1149/1.2753225.

Mortan, Siti Hatijah, Lucía Martín-González, Teresa Vicent, Gloria Caminal, Ivonne Nijenhuis, Lorenz Adrian, and Ernest Marco-Urrea (2017). "Detoxification of 1,1,2-trichloroethane to ethene in a bioreactor co-culture of Dehalogenimonas and Dehalococcoides mccartyi strains". In: *Journal of Hazardous Materials* 331, pp. 218–225. ISSN: 0304-3894. doi: <https://doi.org/10.1016/j.jhazmat.2017.02.043>. URL: <https://www.sciencedirect.com/science/article/pii/S0304389417301310>.

- Mouvet, Christophe, Delphine Barberis, and Alain C.M. Bourg (1993). "Adsorption isotherms of tri- and tetrachloroethylene by various natural solids". In: *Journal of Hydrology* 149.1. Conventry Groundwater Investigation: Sources and Movement of Chlorinated Hydrocarbon Solvents, pp. 163–182. issn: 0022-1694. doi: [https://doi.org/10.1016/0022-1694\(93\)90105-I](https://doi.org/10.1016/0022-1694(93)90105-I).
- Müller, Jochen A., Bettina M. Rosner, Gregory von Abendroth, Galit Meshulam-Simon, Perry L. McCarty, and Alfred M. Spormann (2004). "Molecular Identification of the Catabolic Vinyl Chloride Reductase from *< i>Dehalococcoides</i> sp. Strain VS and Its Environmental Distribution". In: *Applied and Environmental Microbiology* 70.8, pp. 4880–4888. doi: 10.1128/AEM.70.8.4880-4888.2004.*
- Muyzer, Gerard and Alfons J. M. Stams (June 1, 2008). "The ecology and biotechnology of sulphate-reducing bacteria". In: *Nature Reviews Microbiology* 6.6, pp. 441–454. issn: 1740-1534. doi: 10.1038/nrmicro1892. url: <https://doi.org/10.1038/nrmicro1892>.
- Nakamura, Ryuhei, Toshihiro Takashima, Souichiro Kato, Ken Takai, Masahiro Yamamoto, and Kazuhito Hashimoto (2010). "Electrical Current Generation across a Black Smoker Chimney". In: *Angewandte Chemie International Edition* 49.42, pp. 7692–7694. doi: <https://doi.org/10.1002/anie.201003311>.
- Němeček, Jan, Kristýna Marková, Roman Špánek, Vojtěch Antoš, Petr Kozubek, Ondřej Lhotský, and Miroslav Černík (2020). "Hydrochemical Conditions for Aerobic/Anaerobic Biodegradation of Chlorinated Ethenes—A Multi-Site Assessment". In: *Water* 12.2. issn: 2073-4441. doi: 10.3390/w12020322. url: <https://www.mdpi.com/2073-4441/12/2/322>.
- Nilsson, Bertel and Peter Gravesen (2018). "Karst Geology and Regional Hydrogeology in Denmark". In: *Karst Groundwater Contamination and Public Health*. doi: 10.1007/978-3-319-51070-5\_34.
- Ottosen, Cecilie Bang (2020). "Documentation and quantification of in situ natural and enhanced degradation of chlorinated ethenes". PhD thesis. Technical University of Denmark.
- Ottosen, Cecilie Fisker and Mette Martina Broholm (2024). *Vidensopsamling Naverland Sammenfatning af eksisterende viden samt udpegning af videnshuller*.
- P. T. McCauley M. Robinson, F. B. Daniel and G. R. Olson (1995). "The Effects of Subacute and Subchronic Oral Exposure to Cis-1,2-Dichloroethylene in Sprague-Dawley Rats". In: *Drug and Chemical Toxicology* 18.2-3. PMID: 7497910, pp. 171–184. doi: 10.3109/01480549509014319.
- Popek, Emma (2018). "Chapter 2 - Environmental Chemical Pollutants". In: *Sampling and Analysis of Environmental Chemical Pollutants (Second Edition)*. Second Edition. Elsevier, pp. 13–69. ISBN: 978-0-12-803202-2. doi: <https://doi.org/10.1016/B978-0-12-803202-2.00002-1>.
- Pósfai, Mihály and Rafal E Dunin-Borkowski (2006). "Sulfides in biosystems". In: *Reviews in Mineralogy and Geochemistry* 61.1, pp. 679–714.
- PubChem (2025). *PubChem Annotation Record for cis-1,2-Dichloroethylene, Source: Hazardous Substances Data Bank (HSDB)*. <https://pubchem.ncbi.nlm.nih.gov>. National Center for Biotechnology Information, National Library of Medicine (US), Retrieved February 4, 2025.
- Puri, Shammy (2003). "Transboundary Aquifer Resources". In: *Water International* 28, pp. 276–279. url: <https://api.semanticscholar.org/CorpusID:153241299>.
- Rathbun, R. E. (1998). "Transport, behavior, and fate of volatile organic compounds in streams". In: *U.S. Geological survey*. doi: 10.3133/pp1589.

- Reilly, Thomas E., L. Niel Plummer, Patrick J. Phillips, and Eurybiades Busenberg (1994). "The use of simulation and multiple environmental tracers to quantify groundwater flow in a shallow aquifer". In: *Water Resources Research* 30, pp. 421–433. URL: <https://api.semanticscholar.org/CorpusID:129050485>.
- Rosenbom, Annette (2005). "Preferential flow and transport in variably saturated fractured media". PhD thesis. Technical University of Denmark.
- Sahoo, Dipak and James A. Smith (1997). "Enhanced Trichloroethene Desorption from Long-Term Contaminated Soil Using Triton X-100 and pH Increases". In: *Environmental Science & Technology* 31.7, pp. 1910–1915. doi: 10.1021/es960655t.
- Sakuratani, Yuki, Kenji Kasai, Yoshiyuki Noguchi, and Jun Yamada (2007). "Comparison of Predictivities of Log P Calculation Models Based on Experimental Data for 134 Simple Organic Compounds". In: *QSAR & Combinatorial Science* 26.1, pp. 109–116. doi: <https://doi.org/10.1002/qsar.200630019>.
- Salzer, Joel S (2013). "Sorption capacity and governing parameters for transport of chlorinated solvents in chalk aquifers". MA thesis. Technical University of Denmark.
- Sander, Rolf, William E. Acree, Alex De Visscher, Stephen E. Schwartz, and Timothy J. Wallington (2022). "Henry's law constants (IUPAC Recommendations 2021)". In: *Pure and Applied Chemistry* 94.1, pp. 71–85. doi: doi:10.1515/pac-2020-0302.
- Schmidt, K. R. and A. Tiehm (Sept. 2008). "Natural attenuation of chloroethenes: identification of sequential reductive/oxidative biodegradation by microcosm studies". In: *Water Science and Technology* 58.5, pp. 1137–1145. ISSN: 0273-1223. doi: 10.2166/wst.2008.729. eprint: <https://iwaponline.com/wst/article-pdf/58/5/1137/436253/1137.pdf>. URL: <https://doi.org/10.2166/wst.2008.729>.
- Scholl, Martha A. and Ronald W. Harvey (1992). "Laboratory investigations on the role of sediment surface and groundwater chemistry in transport of bacteria through a contaminated sandy aquifer". In: *Environmental Science & Technology* 26.7, pp. 1410–1417. doi: 10.1021/es00031a020.
- Schulze-Makuch, Dirk (2005). "Longitudinal dispersivity data and implications for scaling behavior". In: *Groundwater* 43.3, pp. 443–456. doi: <https://doi.org/10.1111/j.1745-6584.2005.0051.x>.
- Sheu, Y.T., S.C. Chen, C.C. Chien, C.C. Chen, and C.M. Kao (2015). "Application of a long-lasting colloidal substrate with pH and hydrogen sulfide control capabilities to remediate TCE-contaminated groundwater". In: *Journal of Hazardous Materials* 284, pp. 222–232. ISSN: 0304-3894. doi: <https://doi.org/10.1016/j.jhazmat.2014.11.023>. URL: <https://www.sciencedirect.com/science/article/pii/S0304389414009303>.
- Siegel, M.D. and C.R. Bryan (2003). "9.06 - Environmental Geochemistry of Radioactive Contamination". In: *Treatise on Geochemistry*. Ed. by Heinrich D. Holland and Karl K. Turekian. Oxford: Pergamon, pp. 205–262. ISBN: 978-0-08-043751-4. doi: <https://doi.org/10.1016/B0-08-043751-6/09049-6>.
- Sø, Helle Ugilt (2023). *Naverland 26A-B, Albertslund Forureningskilder, potentialeforhold og forureningsudbredelse - 2023*. Tech. rep. HOFOR Plan Vand.
- Sonnenborg, Torben O. (2006). "Vandressource- og stoftransportmodellering i kalk: status og muligheder - KALK PÅ TVÆRS ATP Jord og Grundvand". In: *Danmarks og Grønlands Geologiske Under-*

- søgelser (GEUS). URL: <https://backend.miljoeogresssourcer.dk/media/lix/3130/Sonnenborg.pdf>.
- Sørensen, Mie Barrett (2013). "Remediation potential for chlorinated ethene contamination by enhanced reductive dechlorination in a chalk aquifer". MA thesis. Technical University of Denmark.
- Spormann, Alfred M. (2006). *Factors Affecting Cis-Dichloroethene and Vinyl Chloride Biological Transformation Under Anaerobic Conditions*. Tech. rep. Stanford University.
- Stams, Alfons J. M. (Mar. 1, 1994). "Metabolic interactions between anaerobic bacteria in methanogenic environments". In: *Antonie van Leeuwenhoek* 66.1, pp. 271–294. ISSN: 1572-9699. doi: 10.1007/BF00871644. URL: <https://doi.org/10.1007/BF00871644>.
- Stroo, Hans, Marvin Unger, Herb Ward, Michael Kavanaugh, Catherine Vogel, Andrea Leeson, Jeffrey Marqusee, and Bradley Smith (2003). "Peer Reviewed: Remediating Chlorinated Solvent Source Zones". In: *Environmental Science & Technology* 37.11. PMID: 12831011, 224A–230A. doi: 10.1021/es032488k.
- Sun, Chen and Jun Dong (2025). "Effects of engineering injection and supplement mode of in-situ biogeochemical transformation enhancement EVO-FeSO<sub>4</sub> on the remediation of tetrachloroethylene contaminated aquifer". In: *Journal of Environmental Sciences* 154, pp. 200–211. ISSN: 1001-0742. doi: <https://doi.org/10.1016/j.jes.2024.08.017>. URL: <https://www.sciencedirect.com/science/article/pii/S1001074224004224>.
- Sun, Yuankui, Kaiwei Zheng, Xueying Du, Hejie Qin, and Xiaohong Guan (2024). "Insights into the contrasting effects of sulfidation on dechlorination of chlorinated aliphatic hydrocarbons by zero-valent iron". In: *Water Research* 255, p. 121494. ISSN: 0043-1354. doi: <https://doi.org/10.1016/j.watres.2024.121494>. URL: <https://www.sciencedirect.com/science/article/pii/S0043135424003968>.
- Thiruvenkatachari, R., S. Vigneswaran, and R. Naidu (2008). "Permeable reactive barrier for groundwater remediation". In: *Journal of Industrial and Engineering Chemistry* 14.2, pp. 145–156. ISSN: 1226-086X. doi: <https://doi.org/10.1016/j.jiec.2007.10.001>. URL: <https://www.sciencedirect.com/science/article/pii/S1226086X0700024X>.
- Thorling, Lærke, Christian Nyrop Albers, Birgitte Hansen, Jacob Kidmose, Anders R. Johnsen, Jolanta Kazmierczak, Mette Hilleke Mortensen, and Lars Troldborg (2024). *Grundvandsovervågning Status og udvikling 1989 – 2023*. Tech. rep. The Geological Survey of Denmark and Greenland. URL: [https://data.geus.dk/pure-pdf/Grundvandsoverv%C3%A5gning.%20Status%20og%20udvikling%201989-2023\\_web.pdf](https://data.geus.dk/pure-pdf/Grundvandsoverv%C3%A5gning.%20Status%20og%20udvikling%201989-2023_web.pdf).
- Tobiszewski, Marek and Jacek Namieśnik (July 1, 2012). "Abiotic degradation of chlorinated ethanes and ethenes in water". In: *Environmental Science and Pollution Research* 19.6, pp. 1994–2006. ISSN: 1614-7499. doi: 10.1007/s11356-012-0764-9.
- Toxic Substances, Agency for and Disease Registry (1996). *Toxicological Profile for 1,2-Dichloroethene*. Tech. rep. Prepared in accordance with guidelines developed by ATSDR and EPA. Atlanta, GA: U.S. Department of Health and Human Services, Public Health Service. URL: [https://hero.epa.gov/hero/index.cfm/reference/details/reference\\_id/723873](https://hero.epa.gov/hero/index.cfm/reference/details/reference_id/723873).
- U.S. Environmental Protection Agency (2011). *Archived Technical Fact Sheet on 1,2-Dichloroethylene*. Technical Report EPA/690/R-11/020F. U.S. Environmental Protection Agency. URL: <https://archive>.

[epa.gov/water/archive/web/pdf/archived-technical-fact-sheet-on-1-2-dichloroethylene.pdf](https://www.epa.gov/waterarchive/web/pdf/archived-technical-fact-sheet-on-1-2-dichloroethylene.pdf).

Vidic, Radisav D (2001). "Permeable reactive barriers: Case study review". In: *Technology Evaluation Report TE01-01*.

Vogel, Maria, Ivonne Nijenhuis, Jonathan Lloyd, Christopher Boothman, Marlén Pöritz, and Katrin Mackenzie (2018). "Combined chemical and microbiological degradation of tetrachloroethene during the application of Carbo-Iron at a contaminated field site". In: *Science of The Total Environment* 628-629, pp. 1027–1036. issn: 0048-9697. doi: <https://doi.org/10.1016/j.scitotenv.2018.01.310>. URL: <https://www.sciencedirect.com/science/article/pii/S0048969718303528>.

Vogel, T M and P L McCarty (1985). "Biotransformation of tetrachloroethylene to trichloroethylene, dichloroethylene, vinyl chloride, and carbon dioxide under methanogenic conditions". In: *Applied and Environmental Microbiology* 49.5, pp. 1080–1083. doi: [10.1128/aem.49.5.1080-1083.1985](https://doi.org/10.1128/aem.49.5.1080-1083.1985).

Wang, S.Y., Y.C. Kuo, Y.Z. Huang, C.W. Huang, and C.M. Kao (2015). "Bioremediation of 1,2-dichloroethane contaminated groundwater: Microcosm and microbial diversity studies". In: *Environmental Pollution* 203, pp. 97–106. issn: 0269-7491. doi: <https://doi.org/10.1016/j.envpol.2015.03.042>. URL: <https://www.sciencedirect.com/science/article/pii/S0269749115001724>.

Wang, Xiaohui, Jia Xin, Mengjiao Yuan, and Fang Zhao (2020). "Electron competition and electron selectivity in abiotic, biotic, and coupled systems for dechlorinating chlorinated aliphatic hydrocarbons in groundwater: A review". In: *Water Research* 183, p. 116060. issn: 0043-1354. doi: <https://doi.org/10.1016/j.watres.2020.116060>. URL: <https://www.sciencedirect.com/science/article/pii/S0043135420305972>.

Weerasooriya, R. and B. Dharmasena (2001). "Pyrite-assisted degradation of trichloroethene (TCE)". In: *Chemosphere* 42.4, pp. 389–396. issn: 0045-6535. doi: [https://doi.org/10.1016/S0045-6535\(00\)00160-0](https://doi.org/10.1016/S0045-6535(00)00160-0).

Whiting, Kent, Patrick J. Evans, Carmen Lebrón, Bruce Henry, John T. Wilson, and Erica Becvar (2014). "Factors Controlling In Situ Biogeochemical Transformation of Trichloroethene: Field Survey". In: *Groundwater Monitoring & Remediation* 34.3, pp. 79–94. doi: <https://doi.org/10.1111/gwmr.12068>.

Witthüser, K., B. Reichert, and H. Hotzl (2003). "Contaminant Transport in Fractured Chalk: Laboratory and Field Experiments". In: *Groundwater* 41.6, pp. 806–815. doi: <https://doi.org/10.1111/j.1745-6584.2003.tb02421.x>.

Wu, Naijin, Yi Li, Yizhou Liu, Yangfan Feng, Wenbo Fei, Tianwen Zheng, Liming Rong, Nan Luo, Yun Song, Wenxia Wei, and Peizhong Li (2025). "Reductive dechlorination of 1,1,2-trichloroethane in groundwater by zero valent iron coupled with biostimulation under sulfate stress: Differences and potential mechanisms". In: *Environmental Research*, p. 121574. issn: 0013-9351. doi: <https://doi.org/10.1016/j.envres.2025.121574>. URL: <https://www.sciencedirect.com/science/article/pii/S0013935125008254>.

Wu, Naijin, Wen Zhang, Wenxia Wei, Sucai Yang, Haijian Wang, Zhongping Sun, Yun Song, Peizhong Li, and Yong Yang (2020). "Field study of chlorinated aliphatic hydrocarbon degradation in contaminated groundwater via micron zero-valent iron coupled with biostimulation". In: *Chemical Engineering Journal* 384, p. 123349. issn: 1385-8947. doi: <https://doi.org/10.1016/j.cej.2019.123349>. URL: <https://www.sciencedirect.com/science/article/pii/S1385894719327627>.

- Wu, Rifeng, Rui Shen, Zhiwei Liang, Shengzhi Zheng, Yong Yang, Qihong Lu, Lorenz Adrian, and Shanquan Wang (2023). "Improve Niche Colonization and Microbial Interactions for Organohalide-Respiring-Bacteria-Mediated Remediation of Chloroethene-Contaminated Sites". In: *Environmental Science & Technology* 57.45. PMID: 37902991, pp. 17338–17352. doi: 10.1021/acs.est.3c05932.
- Yamaguchi, Akira, Masahiro Yamamoto, Ken Takai, Takumi Ishii, Kazuhito Hashimoto, and Ryuhei Nakamura (2014). "Electrochemical CO<sub>2</sub> Reduction by Ni-containing Iron Sulfides: How Is CO<sub>2</sub> Electrochemically Reduced at Bisulfide-Bearing Deep-sea Hydrothermal Precipitates?" In: *Electrochimica Acta* 141, pp. 311–318. ISSN: 0013-4686. doi: <https://doi.org/10.1016/j.electacta.2014.07.078>. URL: <https://www.sciencedirect.com/science/article/pii/S0013468614014832>.
- Yamamoto, Masahiro, Ryuhei Nakamura, Kazumasa Oguri, Shinsuke Kawagucci, Katsuhiko Suzuki, Kazuhito Hashimoto, and Ken Takai (2013). "Generation of Electricity and Illumination by an Environmental Fuel Cell in Deep-Sea Hydrothermal Vents". In: *Angewandte Chemie International Edition* 52.41, pp. 10758–10761. doi: <https://doi.org/10.1002/anie.201302704>.
- Yang, Yi, Steven A Higgins, Jun Yan, Burcu Şimşir, Karuna Chourey, Ramsunder Iyer, Robert L Hettrich, Brett Baldwin, Dora M Ogles, and Frank E Löffler (Aug. 2017). "Grape pomace compost harbors organohalide-respiring *Dehalogenimonas* species with novel reductive dehalogenase genes". In: *The ISME Journal* 11.12, pp. 2767–2780. ISSN: 1751-7362. doi: 10.1038/ismej.2017.127.
- Yang, Zhilong, Xiao-li Wang, Hui Li, Jie Yang, Li-Yang Zhou, and Yong-di Liu (2017). "Re-activation of aged-ZVI by iron-reducing bacterium *Shewanella putrefaciens* for enhanced reductive dechlorination of trichloroethylene". In: *Journal of Chemical Technology & Biotechnology* 92.10, pp. 2642–2649. doi: <https://doi.org/10.1002/jctb.5284>.
- Yoshikawa, Miho, Ming Zhang, Yoshishige Kawabe, and Taiki Katayama (May 2021). "Effects of ferrous iron supplementation on reductive dechlorination of tetrachloroethene and on methanogenic microbial community". In: *FEMS Microbiology Ecology* 97.5, fiab069. ISSN: 0168-6496. doi: 10.1093/femsec/fiab069.
- Zhang, Yaru, Zhaoyong Bian, Feng Wang, Yiyin Peng, Wenyu Xiao, and Qiang Zhang (2025). "In-situ synthesis of FeS nanoparticles enhances Sulfamethoxazole degradation via accelerated electron transfer in anaerobic bacterial communities". In: *Water Research* 273, p. 123025. ISSN: 0043-1354. doi: <https://doi.org/10.1016/j.watres.2024.123025>. URL: <https://www.sciencedirect.com/science/article/pii/S0043135424019250>.



## APPENDICES



# A

## APPENDIX A

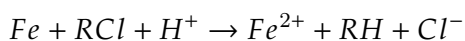
### A.1 Other remediation techniques

#### A.1.1 Green rust (GR)

Green Rust (GR), also called fougereite, is a layered double hydroxides (a family of minerals) and has "the general chemical formula of  $[Fe(II)_{(1-x)}Fe(III)_xOH_2]^{x+}[(x/n)A^{n-}mH_2O]^{x-}$  where  $A^{n-}$  is an anion intercalated between two brucite-like layers, and  $x$  is the fraction of Fe(III) out of total Fe" [Han et al., 2012]. The types of GRs are carbonate ( $CO_3$ ),  $Cl^-$ , and sulphate ( $SO_4$ ) GR [Han et al., 2012]. GRs are highly reactive (and therefore unstable) and are capable of reducing organic compounds, including DCE [Moreno et al., 2007]. Sulphate GR has been shown to rapidly and effectively dechlorinate cDCE and VC as well as lead to benign byproducts [Han et al., 2012; Lee et al., 2002]. This study also found similar results to FeS, there is a dependence of pH on the dechlorination rate constant, increasing the pH from 6.8 to 10.1 increases the dechlorination of TCE and freeze-drying would oxidise the sulfate GR [Lee et al., 2002]. Like Hyun et al., 2015's study, the identity and purity of synthesised iron-bearing mineral was confirmed using X-ray diffraction. However, sulfate GR has a greater surface area-normalised pseudo-first order initial rate constant than  $FeS_2$  by a factor of 3.4 - 8.2. The surface phase of GR is more reactive when there is excess dissolved Fe(II), increasing the rate of dechlorination of cDCE and VC [Han et al., 2012].

#### A.1.2 Zero Valent Iron (ZVI)

ZVI degrades chlorinated solvents by oxidation of Fe(0) to Fe(+2), donating its electron to the CE (or other contaminant) as shown below;



The form of ZVI that requires trenching to be put into the subsurface is granular ZVI; however, through direct injection and soil mixing, micro ZVI (mZVI) can be added, while nano ZVI (nZVI) can be added through injection wells (and direct injection). At the same time, mZVI and nZVI have lower longevity as they have smaller particle diameters and higher reac-

tive surface areas. ZVI dechlorinates CEs via the beta elimination pathway ([Figure 3.3](#)). Furthermore, ZVI exhibits limited environmental stability due to rapid corrosion in  $\text{Fe}_0/\text{H}_2\text{O}$  systems, which diminishes its reactivity over time as surface passivation occurs, e.g. through the precipitation of iron hydroxides and carbonates [Guan et al., 2015](#).

### A.1.3 Combined ZVI-Biotic Systems

[Herrero et al., 2019](#) compared i) MNA, ii) biostimulation with lactic acid, iii) In-Situ Chemical Reduction (ISCR) with ZVI and iv) a combined strategy with lactic acid and ZVI and found that the combined strategy was the fastest and sustained complete dechlorination of PCE for pools in the transition zone. This was supported by [Sheu et al., 2015](#); [X. Wang et al., 2020](#); [Ling et al., 2024](#) as well. It accelerates the initiation of biotic dehalogenation using the intrinsic reductive capabilities of ZVI [[N. Wu, Yi Li, et al., 2025](#)]. ZVI corrosion reaction and chemical reduction of naturally occurring electron acceptors result in the redox potential of the aquifer being lowered [[N. Wu, Yi Li, et al., 2025](#)]. Providing the dechlorinating microorganisms with electron donors, hence a suitable setting for organohalide respiration which facilitates reductive dehalogenation and depends on OHRB [[Kocur et al., 2015](#); [S. Wang et al., 2015](#); [Mortan et al., 2017](#); [Dong et al., 2019](#); [Němeček et al., 2020](#); [N. Wu, W. Zhang, et al., 2020](#); [Jiang et al., 2022](#)]. Furthermore, the oxidised layer on the surface of  $\text{Fe}_0$  may be corroded by dissimilatory iron-reducing bacteria, revealing active areas [[Z. Yang et al., 2017](#)].

[Islam et al., 2021](#) used a customised contamination system to perform bench-scale tests on TCE dechlorination under the combined action of ZVI and SRB. They discovered that the main mechanism for TCE reduction in the coupled SRB-ZVI system was abiotic dechlorination. Even in the absence of direct interaction between nZVI and FeS, synthetic FeS particles can improve ZVI's dechlorination performance as sulfidation improves electron-mediated dechlorination [[N. Wu, Yi Li, et al., 2025](#); [Guo et al., 2023](#)]. And SRB may affect ZVI's reactivity in a variety of mechanisms depending on the remediation setting [[N. Wu, Yi Li, et al., 2025](#)]. However, even though S-mZVI (sulfidated micro ZVI) reacts more strongly to chlorinated ethanes than mZVI, it doesn't improve dechlorination of other chlorinated aliphatic hydrocarbons unlike S-nZVI (sulfidated nano ZVI) which shows a differential trend [[Y. Sun et al., 2024](#)]. Coupling nZVI and biostimulation shows an improved dechlorination efficiency from 66.7% to 80.2% when the  $\text{SO}_4^{2-}$  reached 400 mg/L, and by the 20th day, ethylene and ethane formed from VC (from 1,1,2-TCA) [[N. Wu, Yi Li, et al., 2025](#)]. Similarly, GEOFORM® Extended Release consists of mZVI and FeS and can be applied through direct push injection, hydraulic or pneumatic fracturing or soil mixing to create a permeable reactive barrier (PBR) [[EVONIK, n.d.\(a\)](#)].

Another combination is composite material Carbo-Iron which combines colloidal activated carbon ( $d_{50} < 1\mu\text{m}$ ) and nZVI whose intention is to accumulate PCE for ERD. It was tested 4 - 6 mbs in the first aquifer of the site [[Katrín et al., 2016](#)]. However, as VC wasn't found and when CSIA was conducted, isotope fractionation was found as is known from

sorption-dominated processes, microbial dechlorination by OHRB is less likely and therefore [M. Vogel et al., 2018](#) suggests microbial oxidation of cDCE.

## A.2 Grain size

The following experiment was conducted to determine the appropriate grain size range for limestone and to identify the range at which fine limestone particles are not extracted when collecting water samples using a syringe and needle. As shown in [Figure A.1](#), the cloudiness in the bottle containing grain sizes <1 mm remained significantly high, indicating that this range is unsuitable and will not be considered for further use.

[Figure A.2](#) demonstrates that allowing the batch to settle for several hours after mixing is advisable if the vials sent for analysis are not filtered. This settling period helps prevent the extraction of fine particles.

Based on the results, the optimal grain size range is 1-5 mm. Within this range, the 3-5 mm fraction produces the clearest water samples, while the 1-2 mm fraction, which is similar in size to coarse sand, allows for greater exposure of the water to the limestone due to its larger surface area. Additionally, using 900 mL of water and 300 g of limestone leaves approximately 100 mL of headspace, which is ideal for the experimental setup.

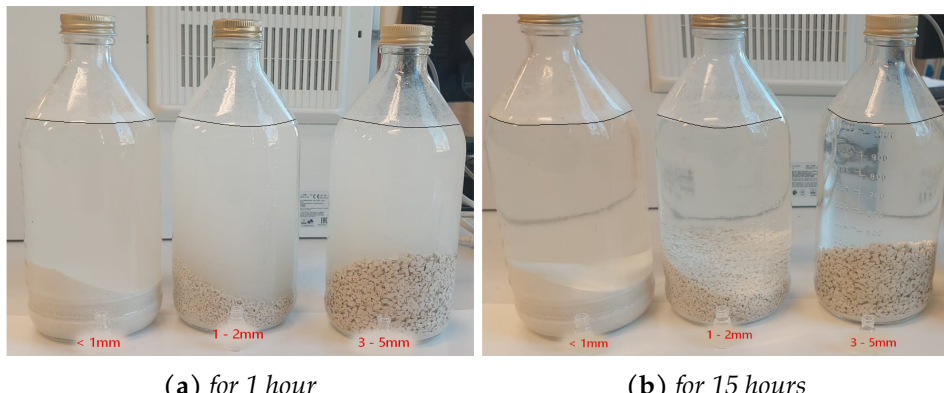


**Figure A.1:** Batch test bottles after the limestone settles

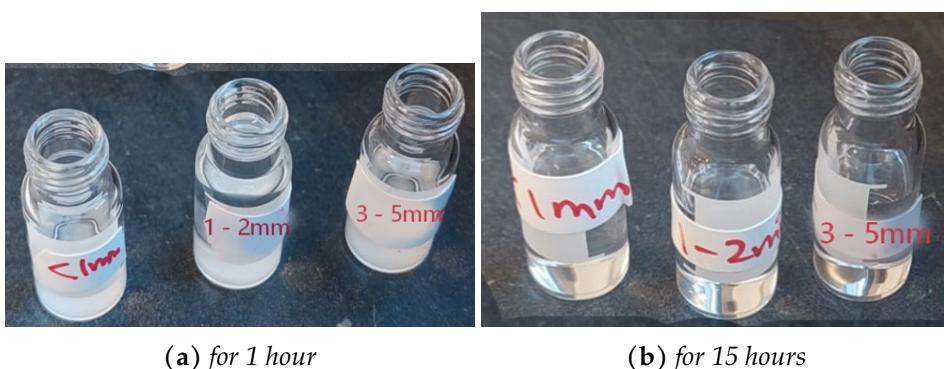


**Figure A.2:** Vials of water extracted after the limestone settles

## A.3 Reagent calculations

### A.3.1 Hydrogen consumption

#### Scenario B and C

**Table A.1:** The calculated maximum hydrogen consumption in moles for a batch consisting 1000 mL ground-water.

Reaction	Concentration [mg/L]	Concentration [mol]	H consumption [mol]
$2H_2 + O_2 \rightarrow 2H_2O$	<0.01	3.125E-07	0.000000625
$6H_2 + 2NO_3^- \rightarrow N_2 + 6H_2O$	<0.3	4.84E-06	1.45E-05
$H_2 + Mn^{4+} \rightarrow Mn^{2+} + H^+$	est 0.1 (no record)	1.82E-06	1.82E-06
$1H_2 + 2Fe^{3+} \rightarrow 2Fe^{2+} + 2H^+$	0.053	9.49E-07	4.74E-07
$1H_2 + 2Fe^{3+} \rightarrow 2Fe^{2+} + 2H^+$	999.947	0.018	0.00895
$9H_2 + 2SO_4^{2-} \rightarrow 2HS^- + 8H_2O$	110	0.00115	0.00515
$9H_2 + 2SO_4^{2-} \rightarrow 2HS^- + 8H_2O$	890	0.009265043	0.0416
$C_2Cl_2H_2 + 2H_2C_2H_4 + 2H^+ + 2Cl^- \rightarrow$	0.15	1.55E-06	3.09E-06
Total			0.0558

DGU-NR: 200. 5096 Sample journal number: 835-2016-80391103 from Eurofins Denmark A/S except for Mn4+

349.2 g H<sub>2</sub> is produced by 1 Kg ELS concentrate and the total organic carbon (TOC) of ELS concentrate is approximately 58%.

$$\text{Mass of hydrogen required [g]} = \text{H}_2 \text{ consumption [mol]} \cdot \text{H}_2 \text{ molar mass [g/mol]} = 0.056 \cdot 2.015 = 0.113 \text{ g}$$

$$\text{ELS concentrate mass required [g]} = (\text{Mass of H}_2 \text{ required [g]} / 58\%) / \text{mass of H}_2 \text{ produced per ELS concentrate kg [g/g]} = 0.194 / 0.349 = 0.556 \text{ g}$$

$$\text{The concentration of ELS Microemulsion is 15g/L, volume of ELS Microemulsion required [mL]} = \text{ELS concentrate mass [g]} / \text{concentration of ELS Microemulsion} = 0.556 / 15 = 37.075 \text{ mL}$$

**Scenario D****Table A.2:** The calculated maximum hydrogen consumption in moles for a batch consisting 1000 mL ground-water.

Reaction	Concentration [mg/L]	Concentration [mol]	H consumption [mol]
$2H_2 + O_2 \rightarrow 2H_2O$	<0.01	3.125E-07	0.000000625
$6H_2 + 2NO_3^- \rightarrow N_2 + 6H_2O$	<0.3	4.84E-06	1.45E-05
$H_2 + Mn^{4+} \rightarrow Mn^{2+} + H^+$	est 0.1 (no record)	1.82E-06	1.82E-06
$1H_2 + 2Fe^{3+} \rightarrow 2Fe^{2+} + 2H^+$	0.053	9.49E-07	4.74E-07
$9H_2 + 2SO_4^{2-} \rightarrow HS^- + 8H_2O$	110	0.00115	0.00515
$C_2Cl_2H_2 + 2H_2C_2H_4 + 2H^+ + 2Cl^- \rightarrow$	0.15	1.55E-06	3.09E-06
Total			0.00517

DGU-NR: 200. 5096 Sample journal number: 835-2016-80391103 from Eurofins Denmark A/S except for Mn4+

$$\text{Mass of hydrogen required [g]} = \text{H}_2 \text{ consumption [mol]} \cdot \text{H}_2 \text{ molar mass [g/mol]} = 0.005 \cdot 2.015 = 0.018 \text{ g}$$

$$\text{ELS concentrate mass required [g]} = (\text{Mass of H}_2 \text{ required [g]} / 58\%) / \text{mass of H}_2 \text{ produced per ELS concentrate kg [g/g]} = 0.018 / 0.349 = 0.052 \text{ g}$$

The concentration of ELS Microemulsion is 3g/L, volume of ELS Microemulsion required [mL] = ELS concentrate mass [g] / concentration of ELS Microemulsion = 0.052/3 = 17.368 mL

## A.4 Experimental setup

As shown in [Figure A.3](#), groundwater was added to the batch bottles using a 60-mL dispenser while the headspace was continuously flushed with nitrogen (black tube). Prior to addition, the first 120 mL of groundwater was discarded.



**Figure A.3:** Addition of groundwater to the batches

### A.4.1 GeoForm to water ratio

As the volume of amendments is lower, the better; the minimal amount of water required to dissolve the powder GeoForm was tested, [Figure A.4](#) shows the result of dissolving 12.16g of GeoForm powder in 10, 20 and 50 mL of tap (aerobic) water. In 10 ml, it was thick like cake batter, while 20 ml was still not fully dissolved; therefore, batches B and C, GeoForm (12.16g), were dissolved in 50 ml of nitrogen-purged water as it had the appropriate consistency.

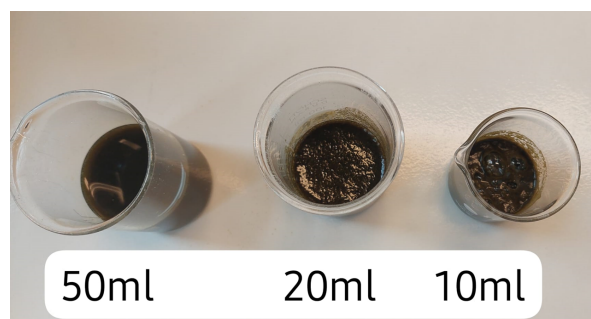


**Figure A.4:** Results of dissolving GeoForm powder in varying water quantities

Figure A.5 shows GeoForm and ELS Microemulsion prepared, which were mixed together with a magnetic stirrer and then injected into the microcosms.

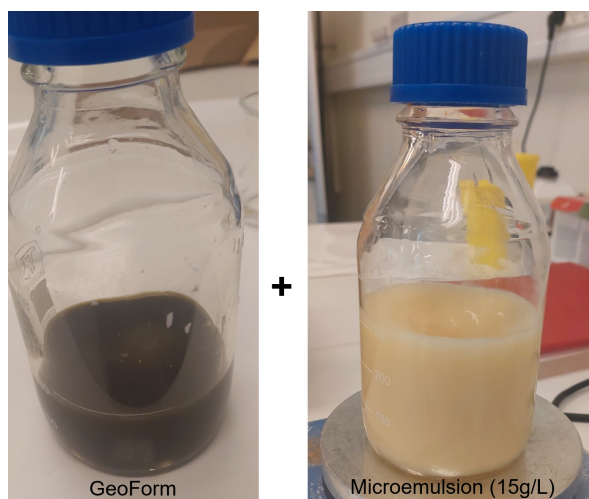


**Figure A.5:** GeoForm and ELS Microemulsion prepared for batches B and C

#### A.4.2 KB-1

It is important to note that due to unexpected delays by the time the KB-1 was added to the batches, it was technically expired by 3 weeks. This is probably why the KB-1 changed in appearance as shown in Figure A.6; however, when shaken, it looked the same as before as seen in Figure 5.7.



**Figure A.6:** KB-1 comparison

#### A.4.3 Oxygen

The oxygen concentration was given in percentage Concentration of oxygen dissolved in water [mg/L] =  $C_a[\%] \cdot 101325 \cdot K_h[mol/m^3 Pa] [mol/L]^*$  molecular weight of oxygen [mg/mol]

### A.5 Sampling frequency and instruments

Water samples	Instrument	Volume required (mL)	Sampling days	Total volume											
Chlorinated ethylenes	GC-MS	12	13	156											
Fatty acids	HPLC	2.5	9	22.5											
NVOC	TOC analyser	10	9	90											
Anions (Sulfate)	IC	2	7	14											
Anions (Nitrate)	Discrete analysis														
Cations (Mn, Fe)	ICP-OES	11.5	7	80.5											
pH	Indicator paper	0.5	6	3											
Headspace															
Methane, ethane, acetylene, ethene and oxygen	GC		1	13	13										
Total for sampling (ml)					366										
Total water needed (ml)					732										
Exact days		0	1	3	7	10	13	17	21	25	29	34	38	40	
Chlorinated ethylenes		1	2	3	4	5	6	7	8	9	10	11	12	13	13
Headspace		1		2	3	4	5	6	7	8	9	10	11	12	
Fatty acids		1	2	3		4		5	6		7	8	9		
NVOC		1	2	3		4		5	6		7	8	9		
Anions (Sulfate, Nitrate)		1	2		3		4		5		6		7		
Cations (Mn, Fe)		1	2		3		4		5		6		7		
pH		1			2		3		4		5		6		

**Figure A.7:** Sampling frequency and volume

### A.5.1 Chlorinated ethylenes and ethanes

Water samples are collected in containers with no headspace where after a certain volume is transferred to a GCMS vial containing internal standard (chloroform). Heated and agitated incubation of the samples is done automatically by the autosampler of the GC-MS prior to injection. Calibration and control solutions are prepared in the same type of containers as the samples are collected. Two levels of calibrations are typically used; low (0.02 – 40 µg/l) and high (20 – 2000 µg/l). Analysis time on the GC-MS is 30 min per sample including GC cool down time. Sample vials are incubated in a rotary shaker at 250 rpm 85 °C for 5 min and 250 µl headspace is injected in splitless mode for the low range and 2:1 split mode for the high range at 80 °C. Chromatographic separation is achieved on a 30 m x 0.32 mm I.D x 20.00 µm film thickness HP-PLOT/Q capillary column (Agilent Technologies). The initial column temperature is set to 40 °C for 4 min then ramped at 35 °C min<sup>-1</sup> to 290 °C. The final temperature is held for 7 min and the total run time is 18.1 min with Helium (1.6 ml min<sup>-1</sup>) as carrier gas. Detection is achieved using an Agilent 5975C electron impact (70 eV) triple-axis mass-selective detector. The mass-selective detector temperatures are 230 °C for the EI source and 150 °C for the quadropole with the transfer line held at 250 °C. The spectra are monitored in selected ion monitoring (SIM) mode.

### A.5.2 Gas analysis

The runtime for each sample was 2.50 min at a temperature of 130°C. Unfortunately methane and carbon dioxide could not be measured as there was too long time between the sample being extracted into the vials and measured so the samples came out as below the detection limit even though when a sample for batch C3 and D2 directly from the headspace on day 55 showed 4.4% CO<sub>2</sub> and 0.7% CO<sub>2</sub> respectively.

### A.5.3 VFA

Samples are injected automatically by the Thermo AI/AS 1310 Series Autosampler, 1 µl are injected. Chromatographic separation is achieved on Agilent J&W GC capillary Column (Length 30 meters, Diam. 0,530 mm, Film thickness 1,50 µm, Temp limits from 40°C to 250°C). The initial column temperature is set to 40°C for 6 min, then it rises by 20°C/min to 200°C. The final temperature is held for 6 min and the total run-time is 20 min, with Helium as carrier gas. Detection is achieved using a Thermo Scientific TRACE™ 1300 Gas Chromatograph, equipped with a Flame Ionization Detector (FID).

### A.5.4 Anions

Anions are separated on an anion-exchange column equipped with a guard column (IonPac AS22, 4 x 250mm, Ionpac AS22 Guard column, 4 x 50 mm, Thermo Scientific). Separation is achieved at isocratic conditions with 4.5 mM bicarbonate/ 1.4 mM carbonate as eluant. The flow is kept constant at 1,2 ml/min, the column compartment at 20 degrees and the total

analysis time is 13 min per sample (Appendix A). A 200  $\mu\text{l}$  sample loop is used, enabling an injection volume up to 100  $\mu\text{l}$ . The Dionex AERS 500 is an electrolytically regenerated suppressor enabling it to operate continuously with a water source as a regenarent. The suppressor (Dionex AERS 500 for Carbonate, 4 mm, ThermoScientific) is operated at 41 mA when using the chromatographic conditions above with the compartment held at 20 °C. Detection is achieved by a conductivity detector (ICS-5000 Conductivity detector, ThermoScientific) held at 20 °C.

## A.6 Results

Relevant equations:

$$M_T = C_w \cdot V_w + K_d \cdot C_w \cdot M_s + K_h \cdot C_w \cdot V_a$$

$$M_{T,new} = M_{T,before} - (C_w \cdot V_{w,out}) - (C_w \cdot K_h \cdot V_{a,out})$$

The dry density was  $265\text{g}/\text{cm}^3$  therefore the volume of limestone is  $0.001132\text{L}$



**Figure A.8:** Batch B1 and B3 on day 57, showing darkening of B3 similar to B1 on day 43

As shown in [Figure A.9](#), the internal standard area (ISTD Area) in yellow is double the rest of the data and therefore the cDCE concentration of the first 16 samples should be doubled from approximately  $60\mu\text{g}/\text{L}$  to  $120\mu\text{g}/\text{L}$ .



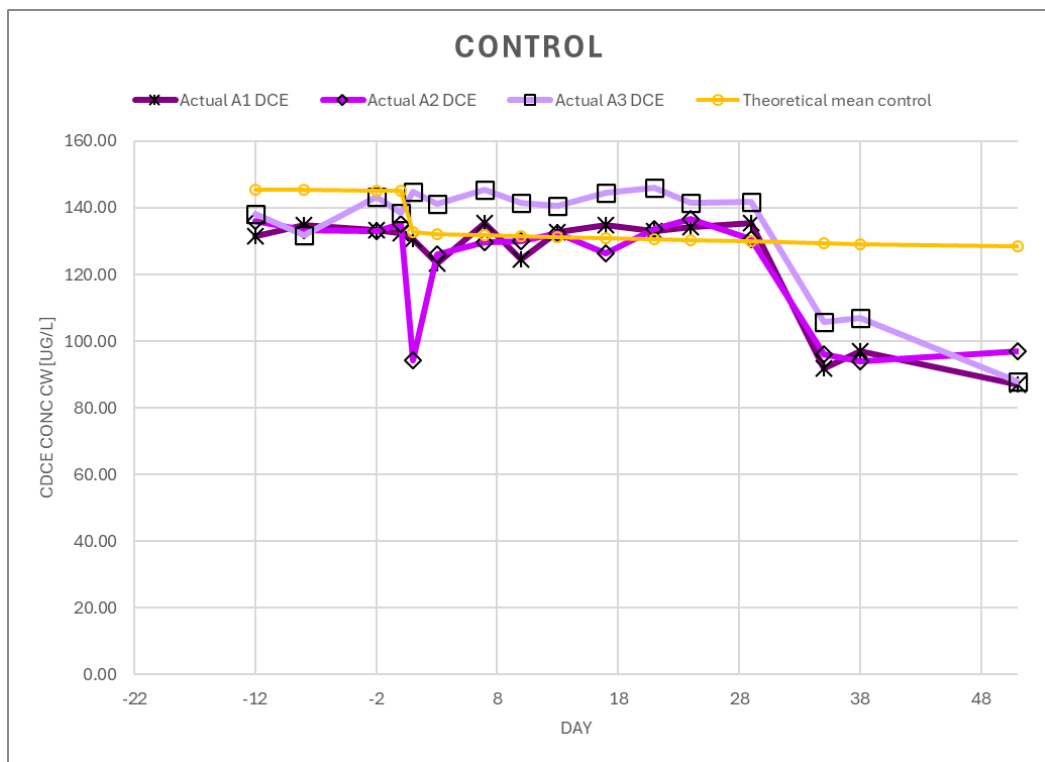


**Figure A.10:** cDCE levels in the control batches over time

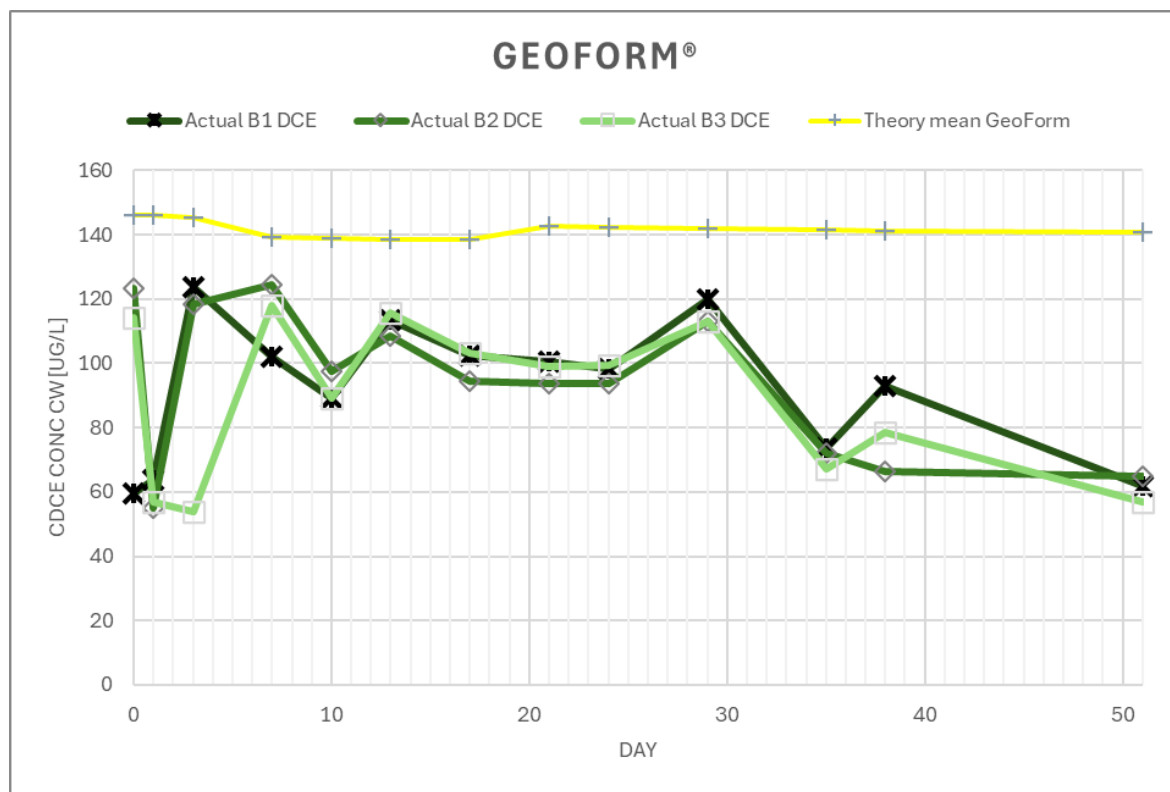


**Figure A.11:** cDCE levels in GeoForm batches over time, on day 0, ELS Microemulsion and GeoForm was added

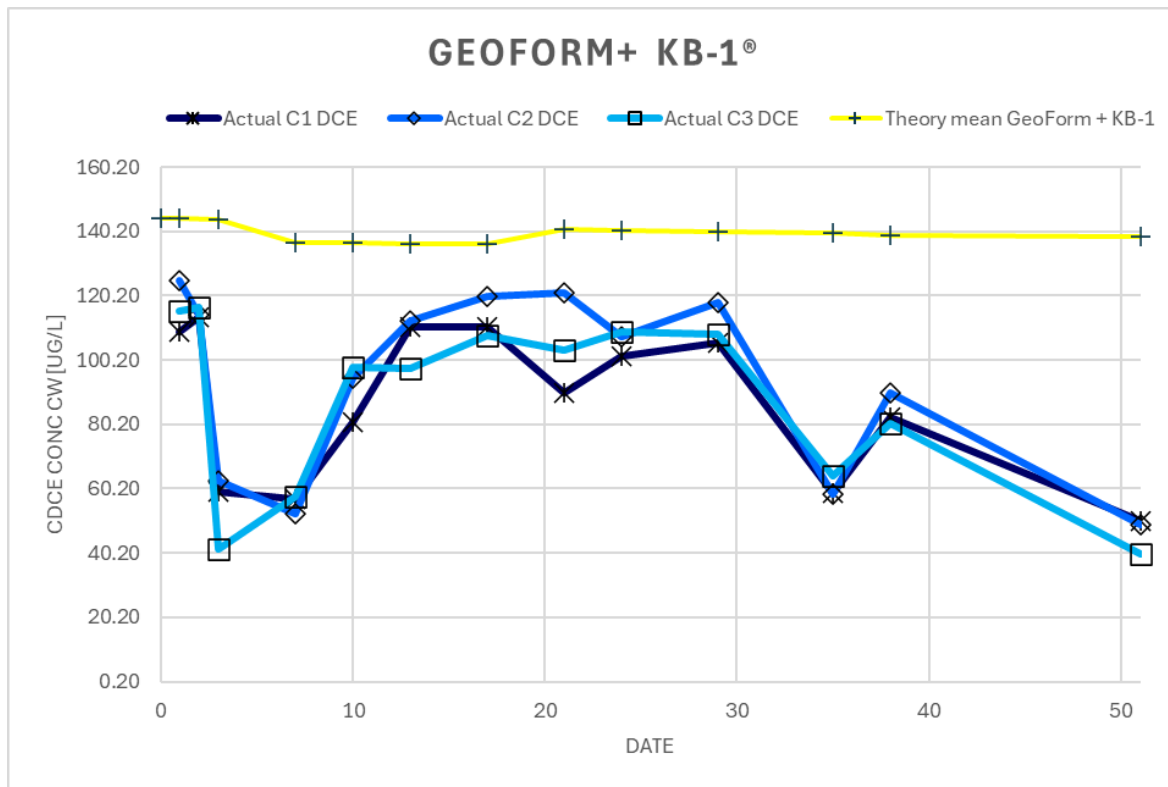


**Figure A.12:** cDCE levels in GeoForm + KB-1 batches over time, on day 0, ELS Microemulsion, KB-1 and GeoForm was added

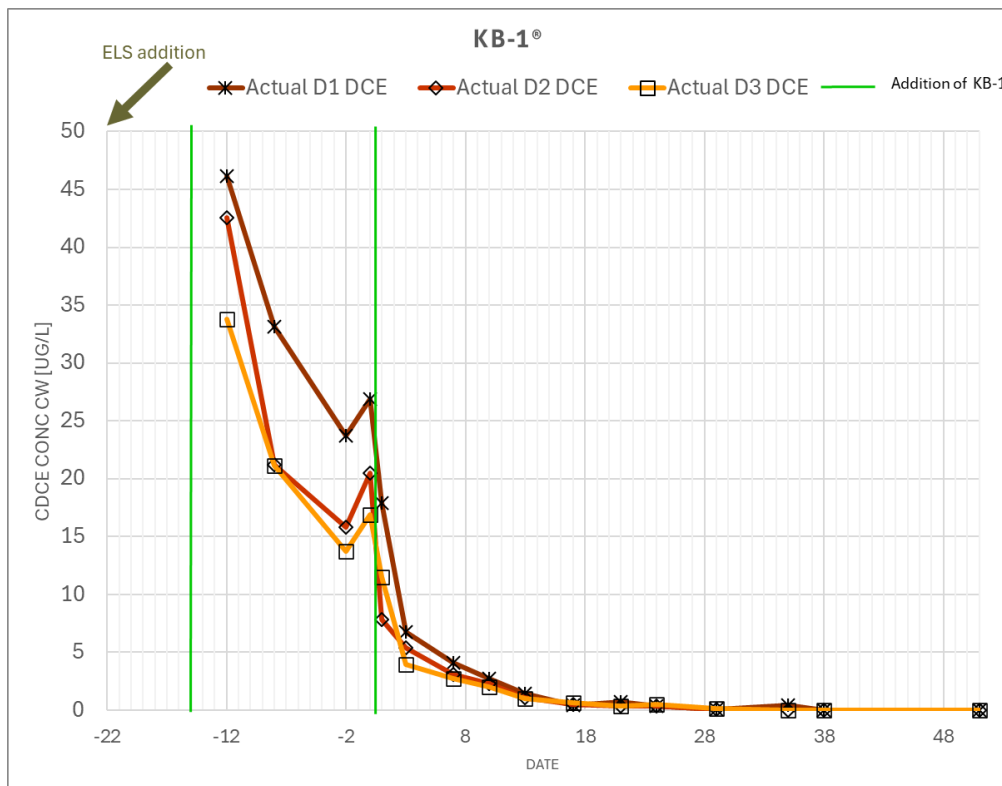


**Figure A.13:** cDCE levels in KB-1 batches over time

### A.6.1 Molar fraction of CE

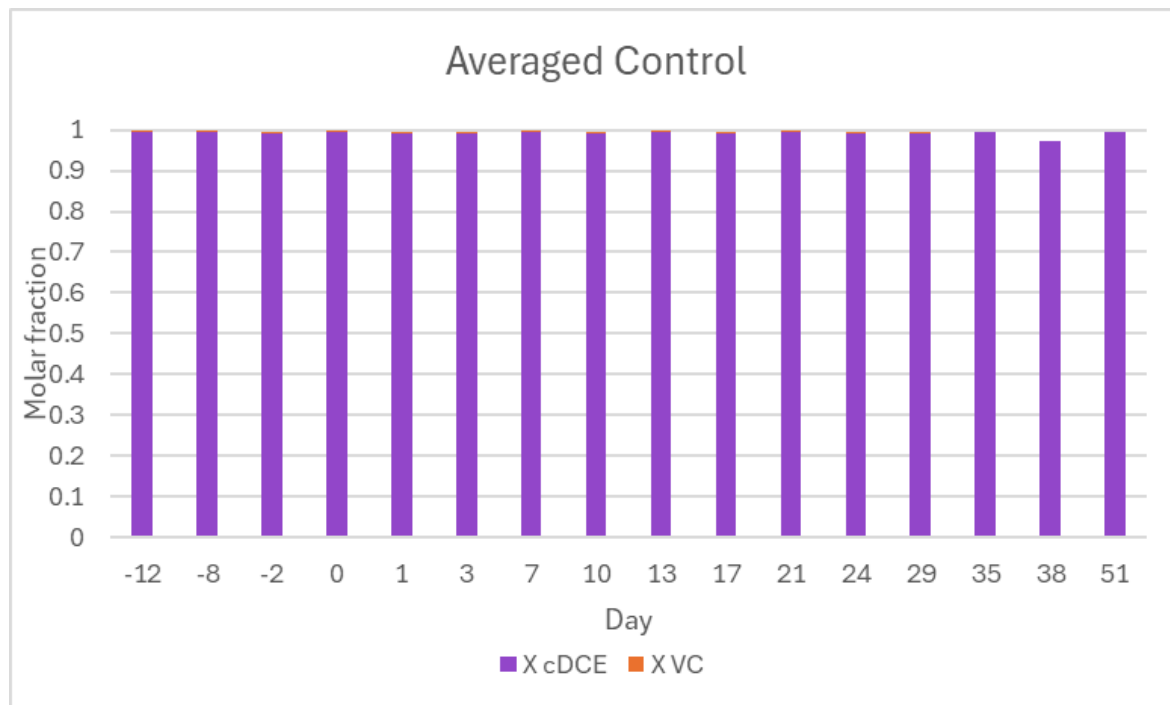


Figure A.14: Molar fraction of control over time

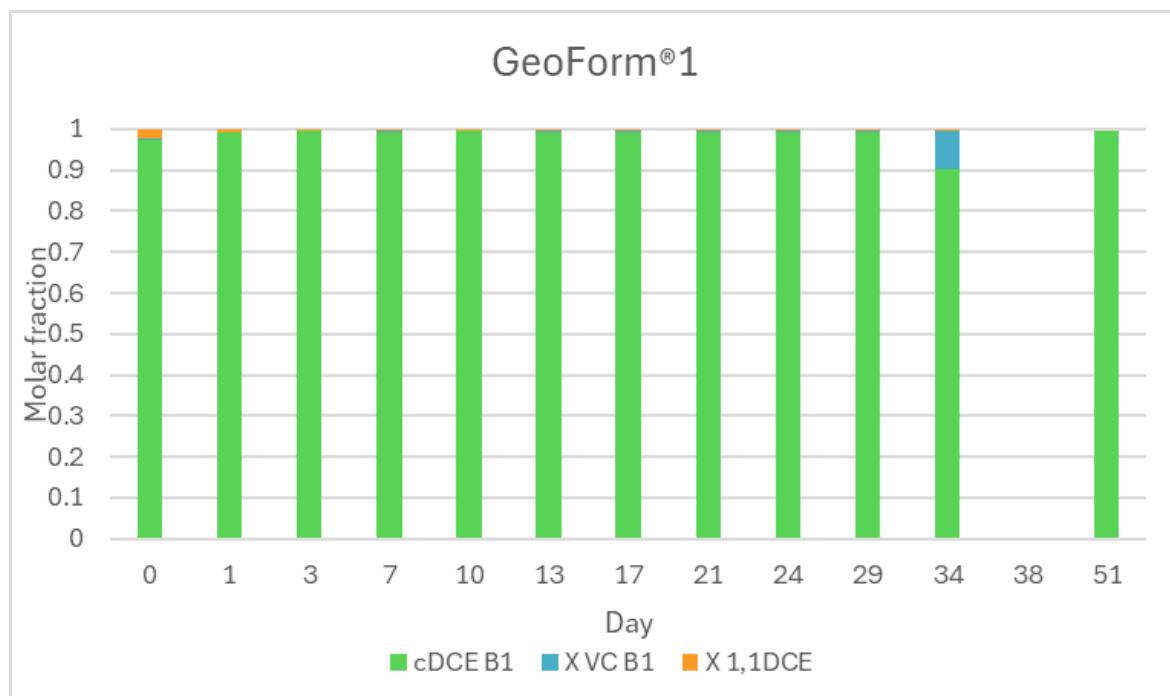
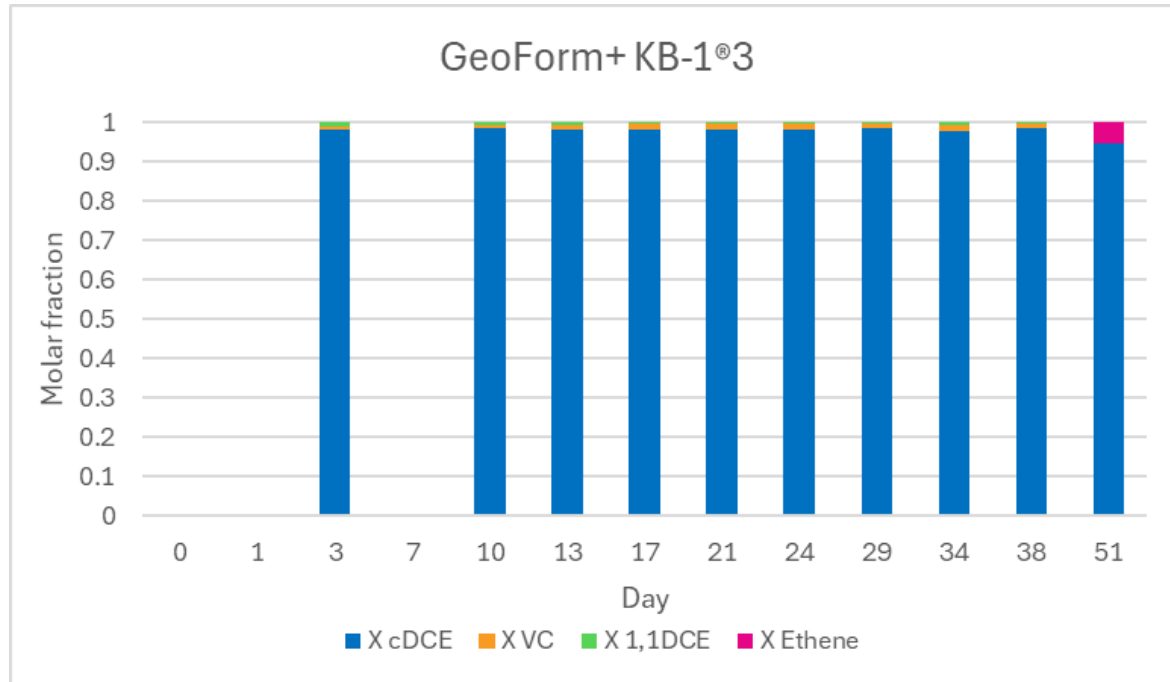
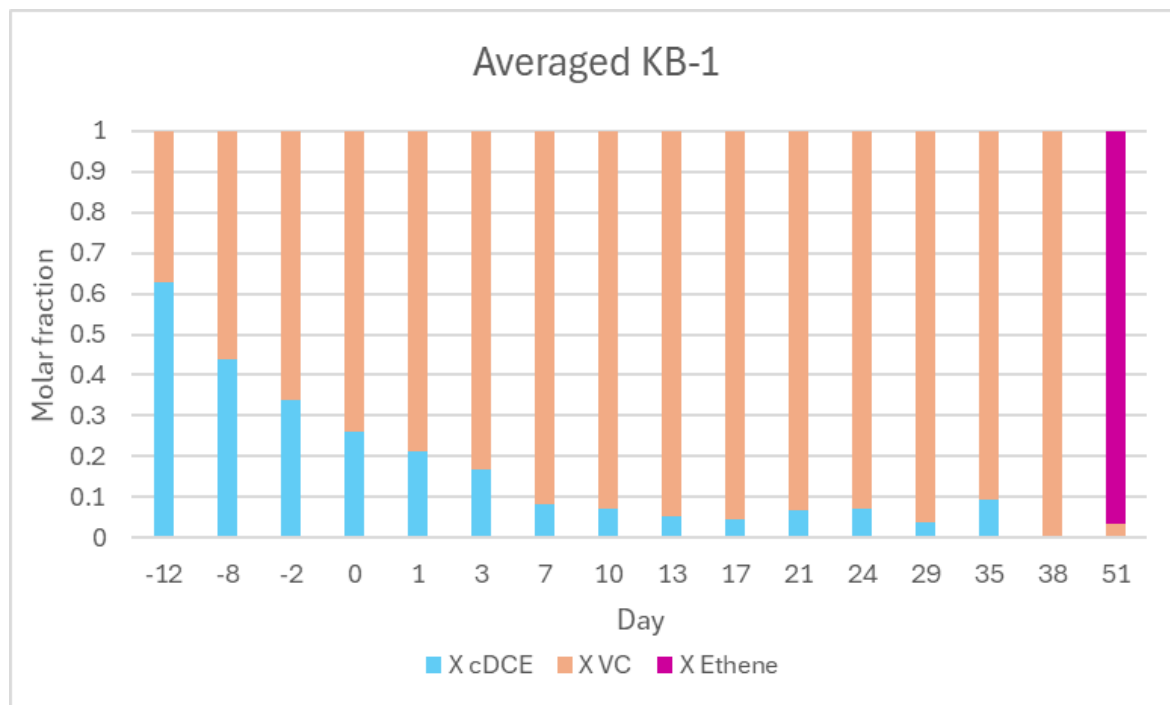


Figure A.15: Molar fraction of GeoForm over time



**Figure A.16:** Molar fraction of GeoForm+KB-1 over time



**Figure A.17:** Molar fraction of KB-1 over time, without ethane or ethene except for day 73 (day 51 if. Ethene probably formed)

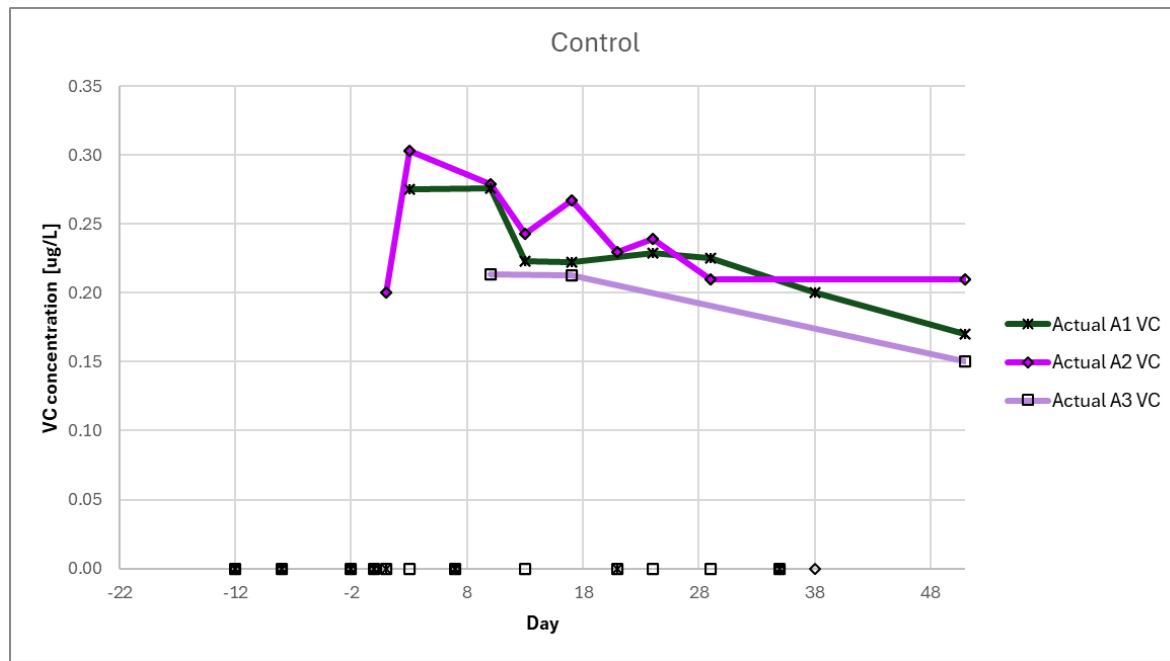


**Figure A.18:** VC levels in the control batches

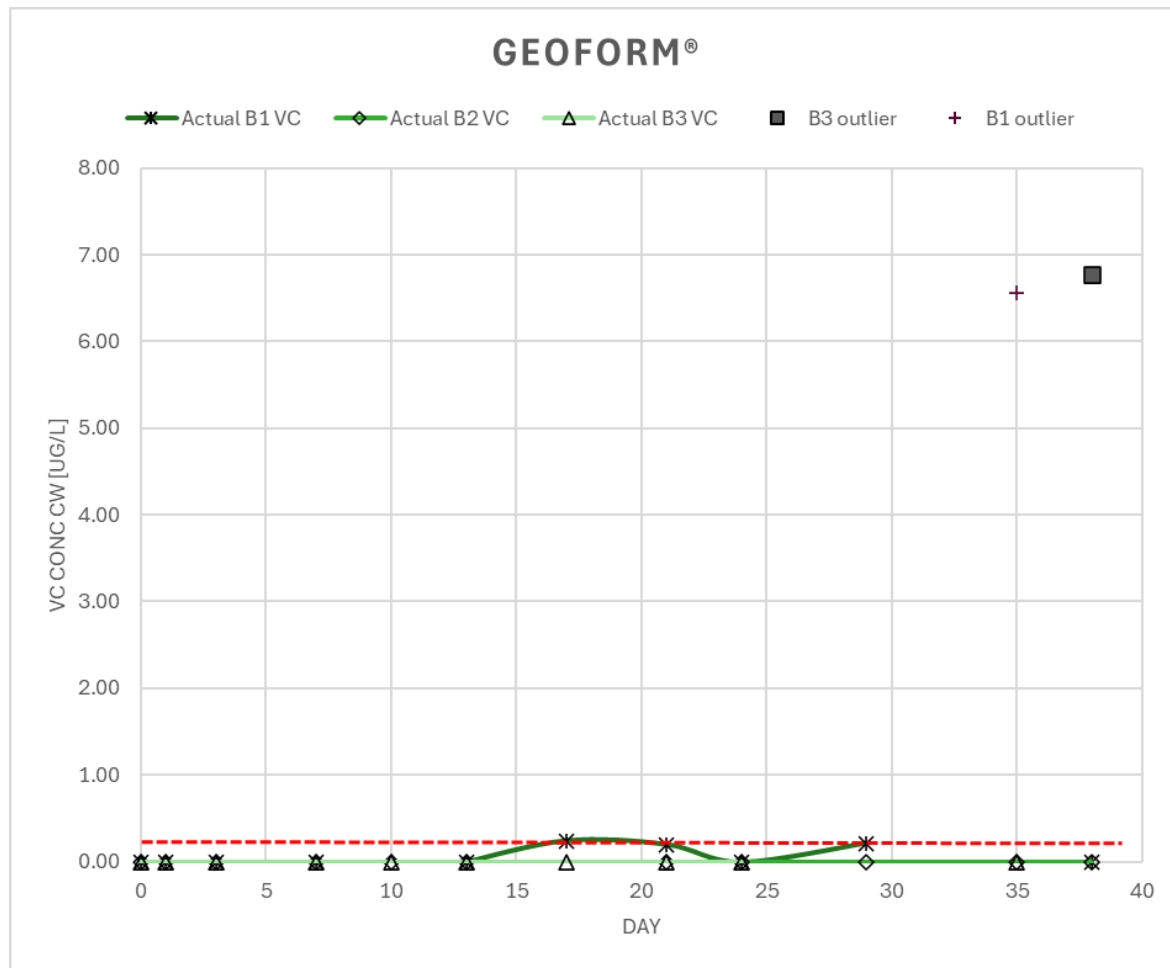


**Figure A.19:** VC levels in the GeoForm batches. The outliers seen in B1 and B3 were ignored and not considered because it was not seen on day 51 and there was no ethene formation for it to be degradation and in this microcosm would have to be abiotic, if any. The interferences in the VC measurements is also a reason the error bars are not in all points of the GeoForm-containing batches.

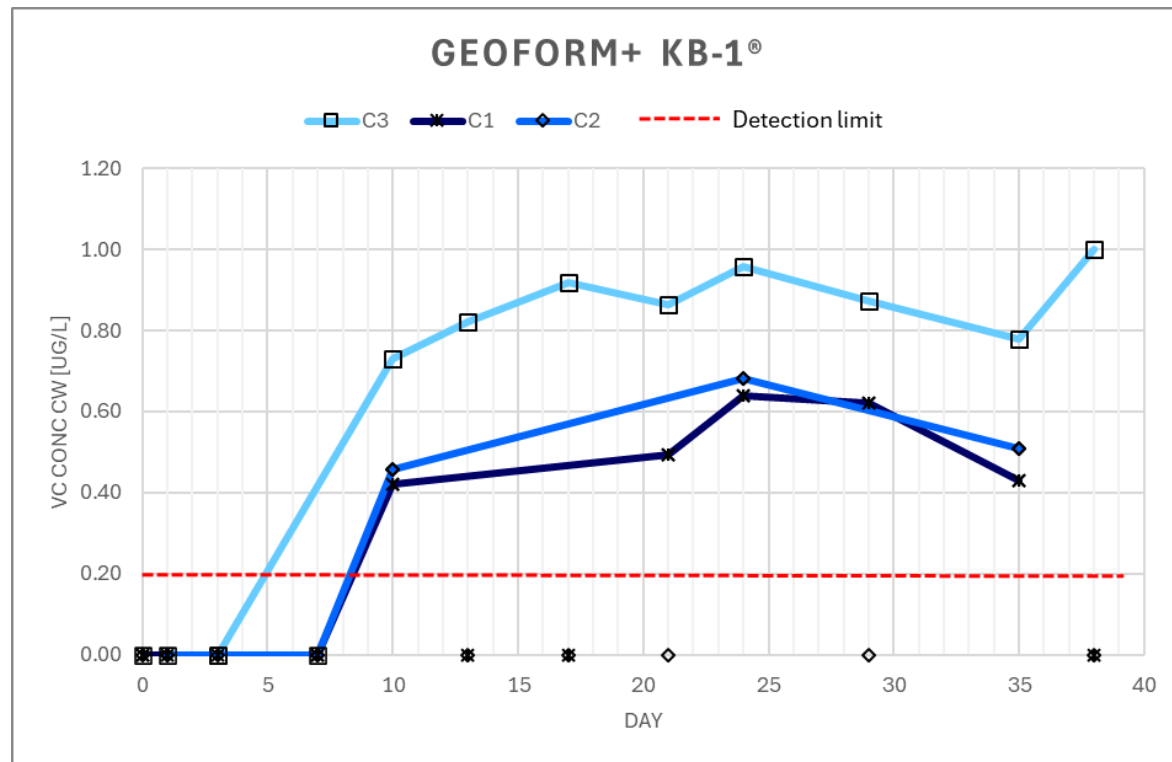


**Figure A.20:** VC levels in the GeoForm+KB-1 batches

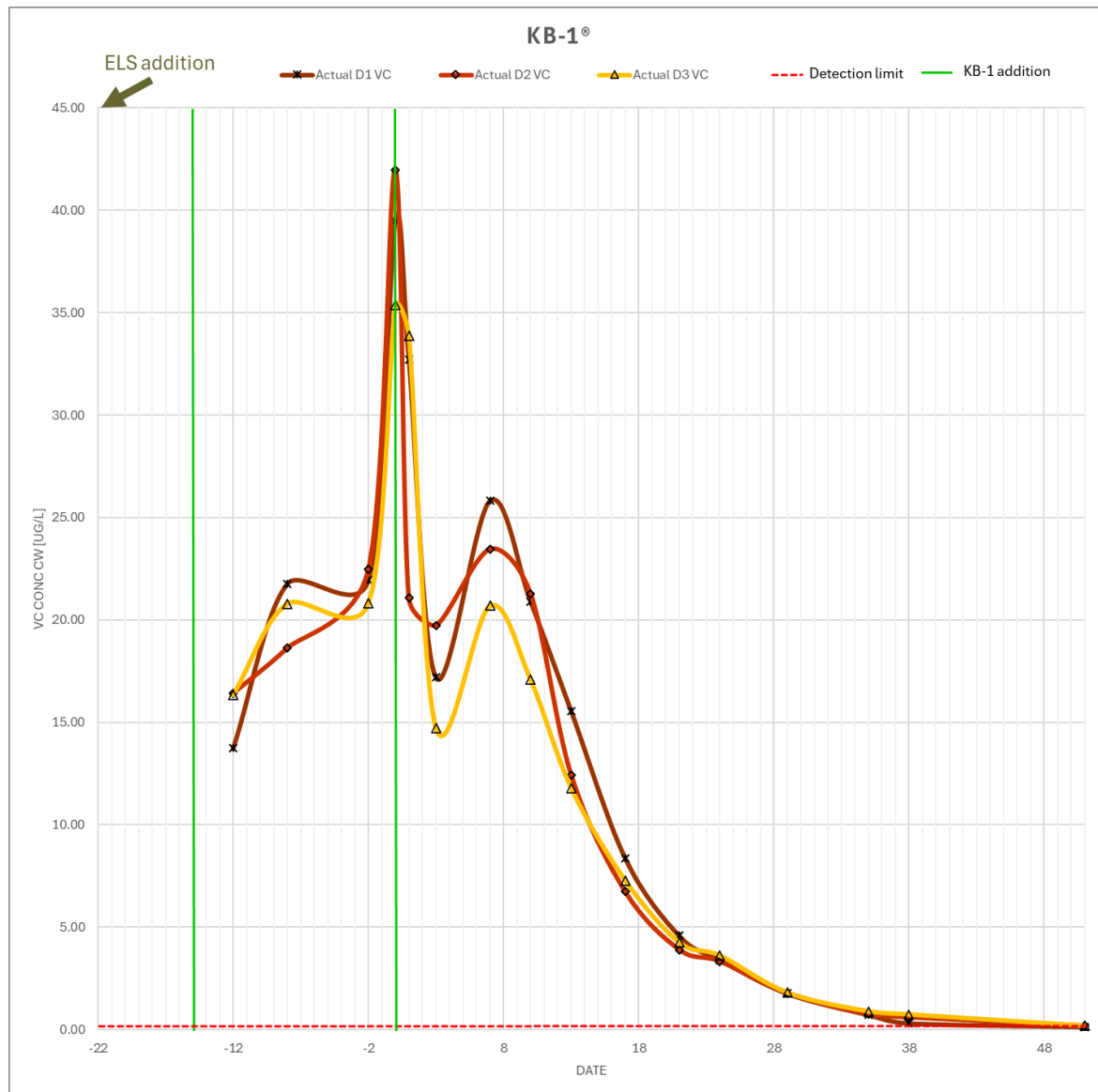


**Figure A.21:** VC levels in the KB-1 batches

### A.6.2 Manganese

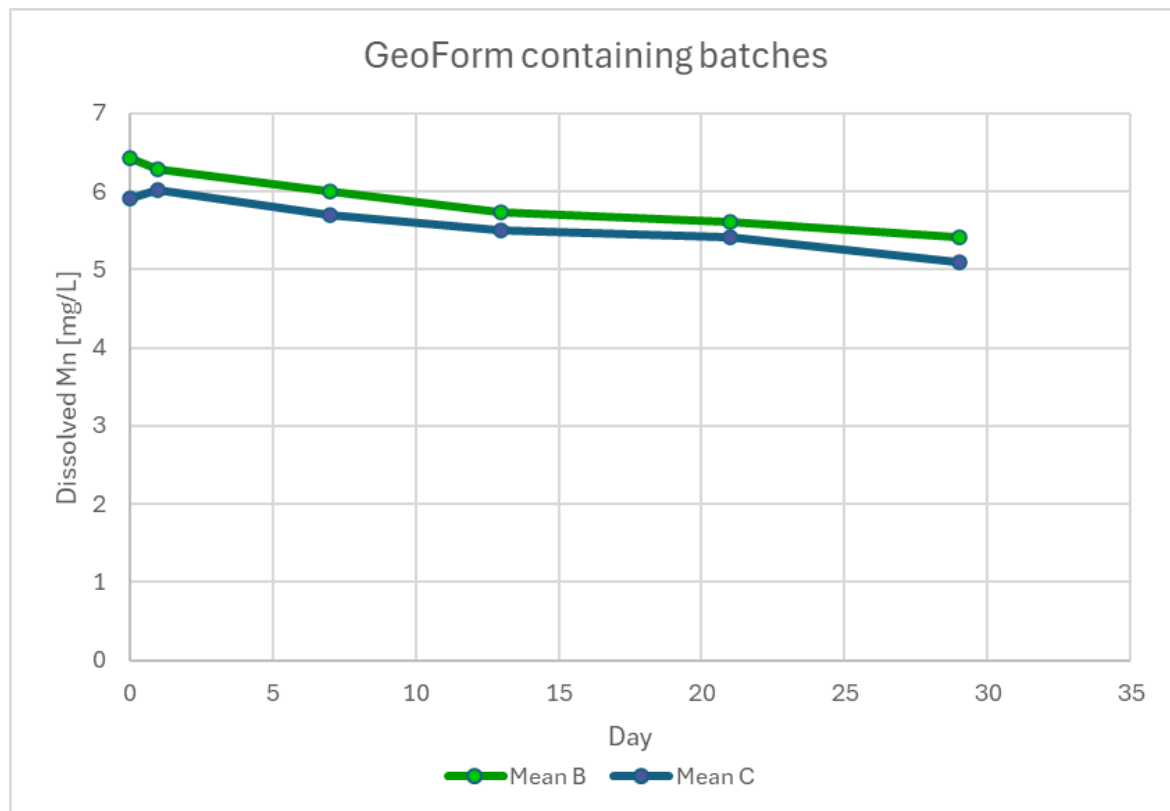


**Figure A.22:** Average Mn concentration over time in the GeoForm containing batches (batch B and C)

### A.6.3 Nitrate

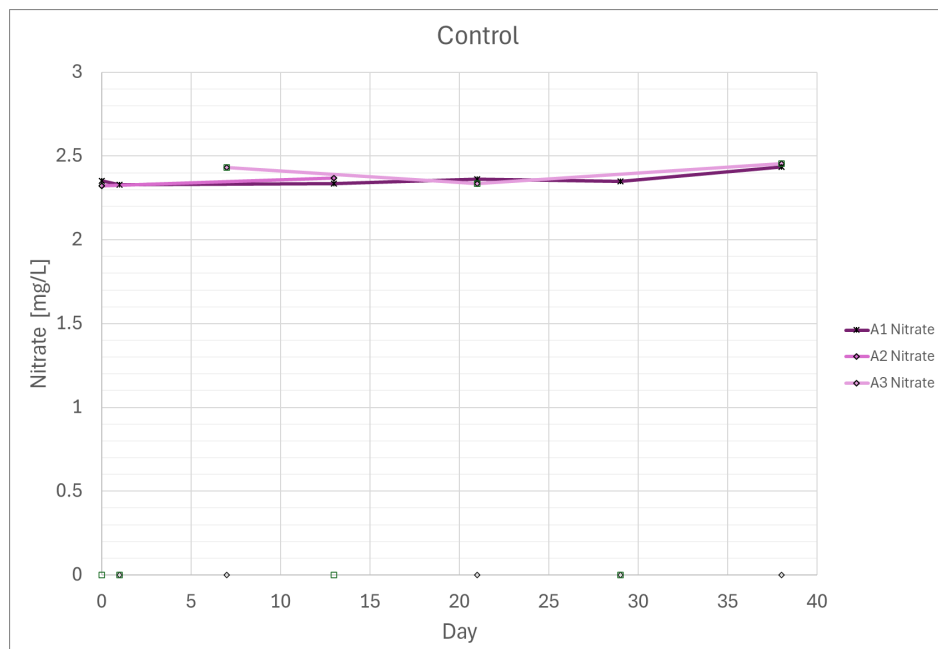


**Figure A.23:** Nitrate levels over time in the control batches

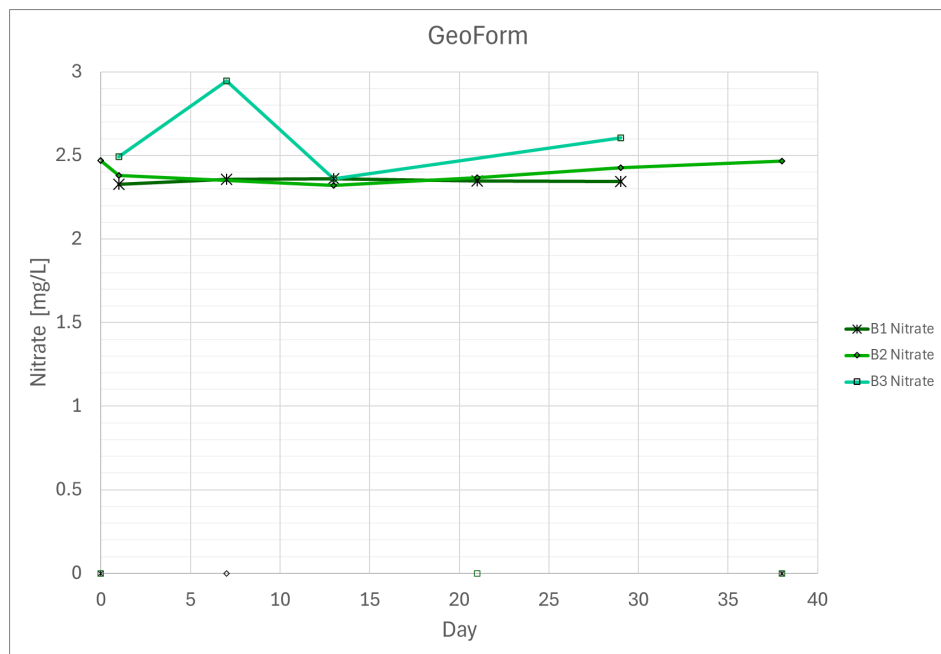


**Figure A.24:** Nitrate levels over time in GeoForm batches

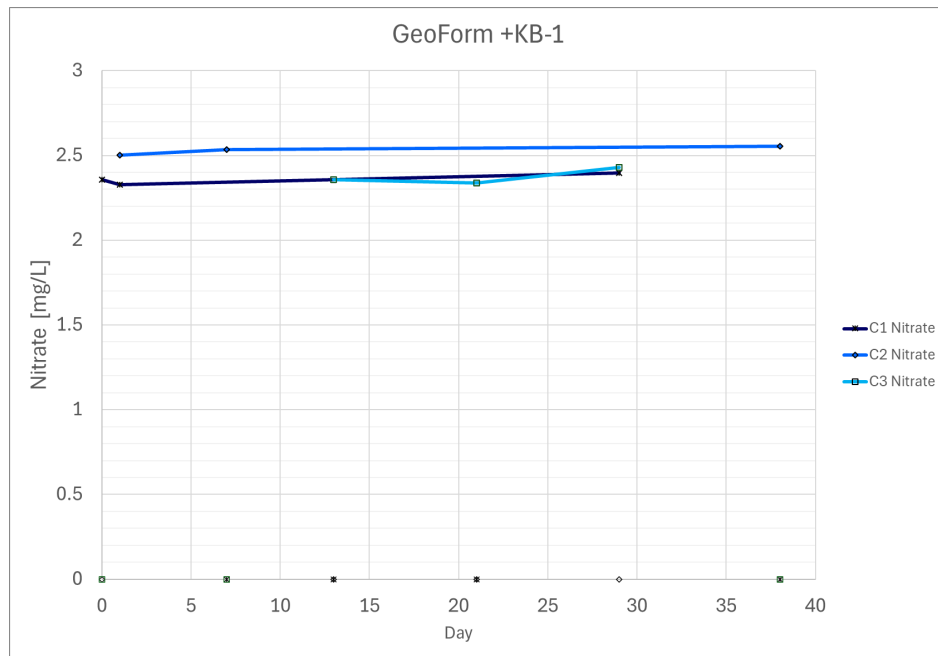


**Figure A.25:** Nitrate levels over time in the GeoForm + KB-1 batches

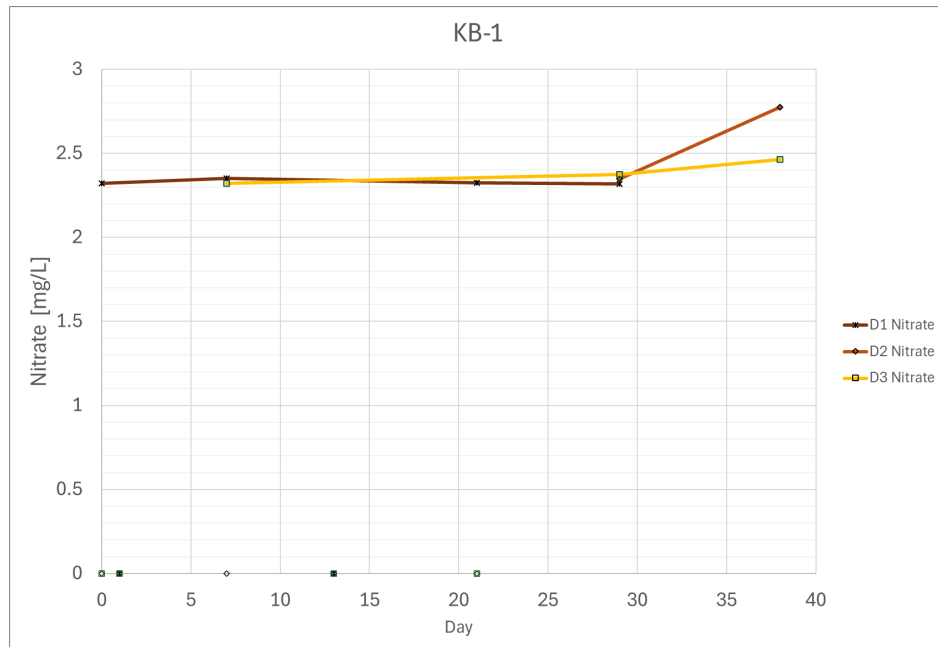


**Figure A.26:** Nitrate levels over time in the KB-1 batches

#### A.6.4 NVOC

**Table A.3** shows the exact NVOC levels in all 12 batches throughout the experiment. The values in blue are within the calibration curve, while the empty cells are due to some of the labels coming off the test tubes and, therefore, are impossible to identify. In **Figure A.6.4**, the points above the red line are the points beyond the calibration curve and are shown because samples were measured.

**Table A.3:** NVOC levels [mg/L] in all 12 batches throughout the experiment

Day	A1	A2	A3	B1	B2	B3	C1	C2	C3	D1	D2	D3	
0	1810	1828	49.3	81.3	1986	2036	1869	1900	1912	68.9	125.1	81.6	
1	48.5			1997	17.4	55.4		1799	55.6	34.3	1900	87.7	41.4
3		63.0		2006	1887	1944		2060	1998	73.5	91.5	1887	90.2
7	66.9	1965	60.8	1877		36.9	1838		18.0	1838	108.1	1891	
17	65.7	65.2	64.1	1978	67.5		82.2	2014	1960	1993		1856	
21	1976	1818.3					35.7			1953			
29	1906	52.5	82.1				1836	7.39	87.7	1879	93.7	68.5	
34	1819	1966	99.6	1872	51.8	1903		64.6			66.0	1995	
38	61.2	1940		63.3	1797		64.2	1998	121.6	1823	1971	1950	

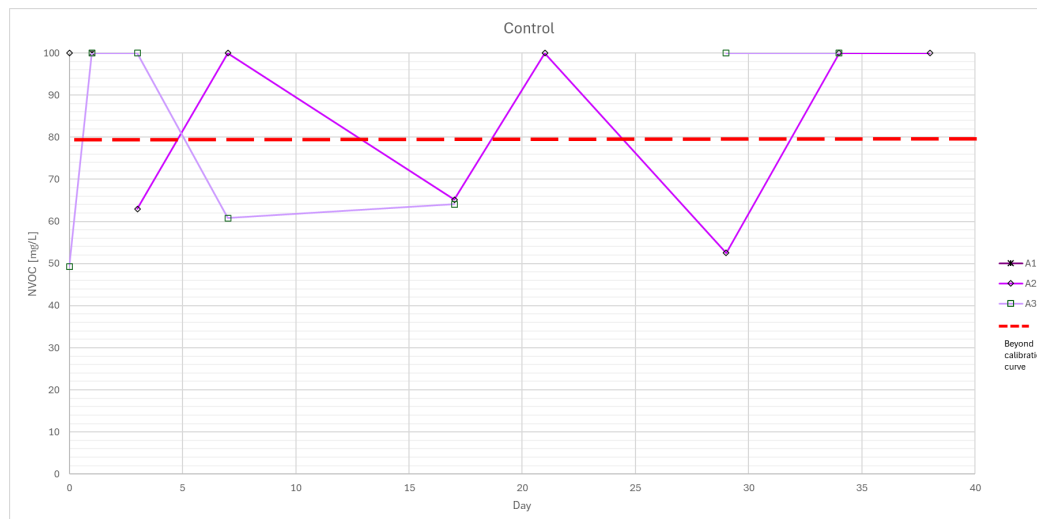


**Figure A.27:** NVOC levels in batch A, only points below the red line should be considered

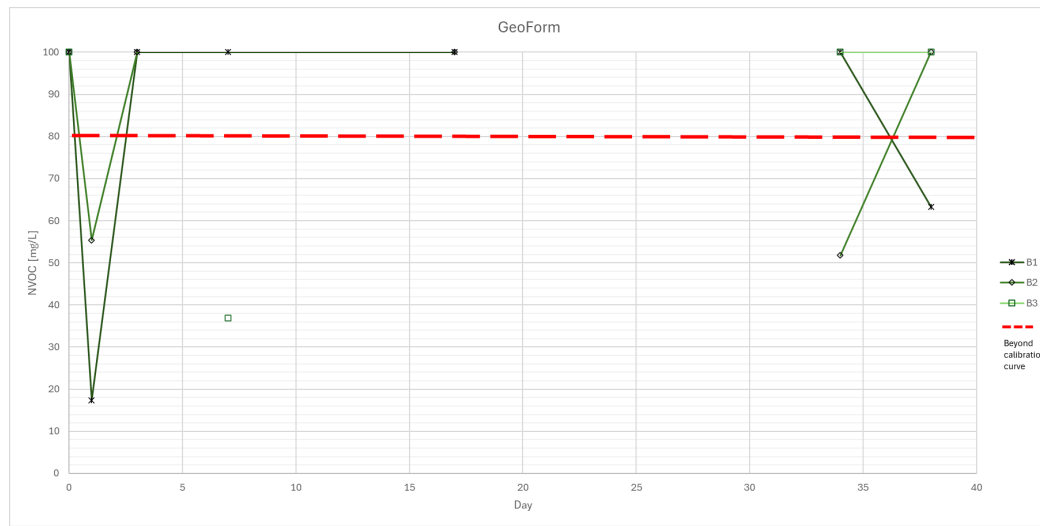


**Figure A.28:** NVOC levels in batch B, only points below the red line should be considered

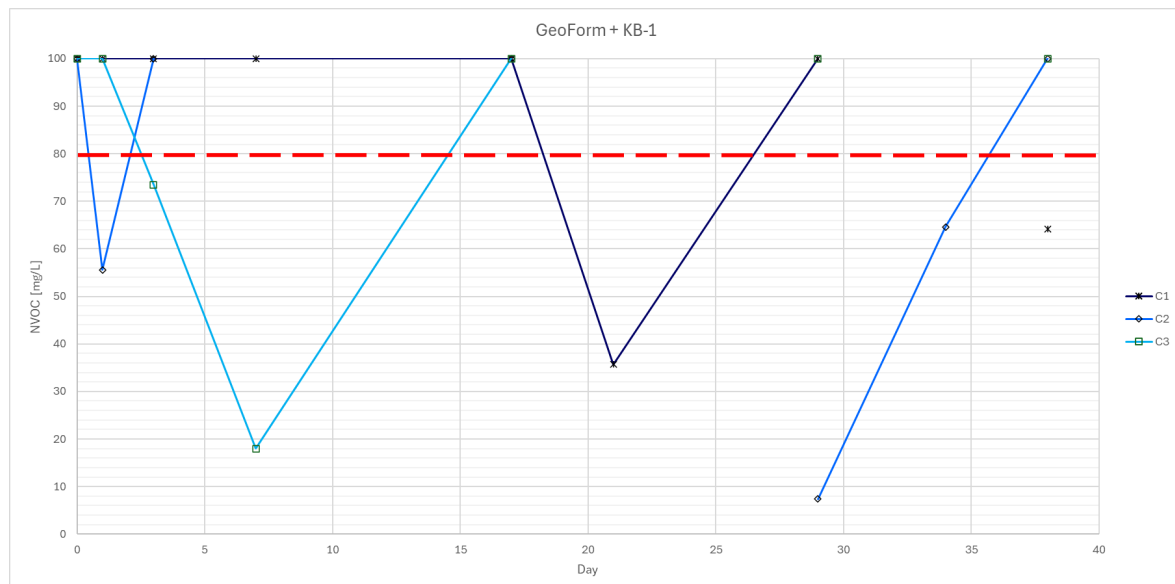


**Figure A.29:** NVOC levels in batch C, only points below the red line should be considered

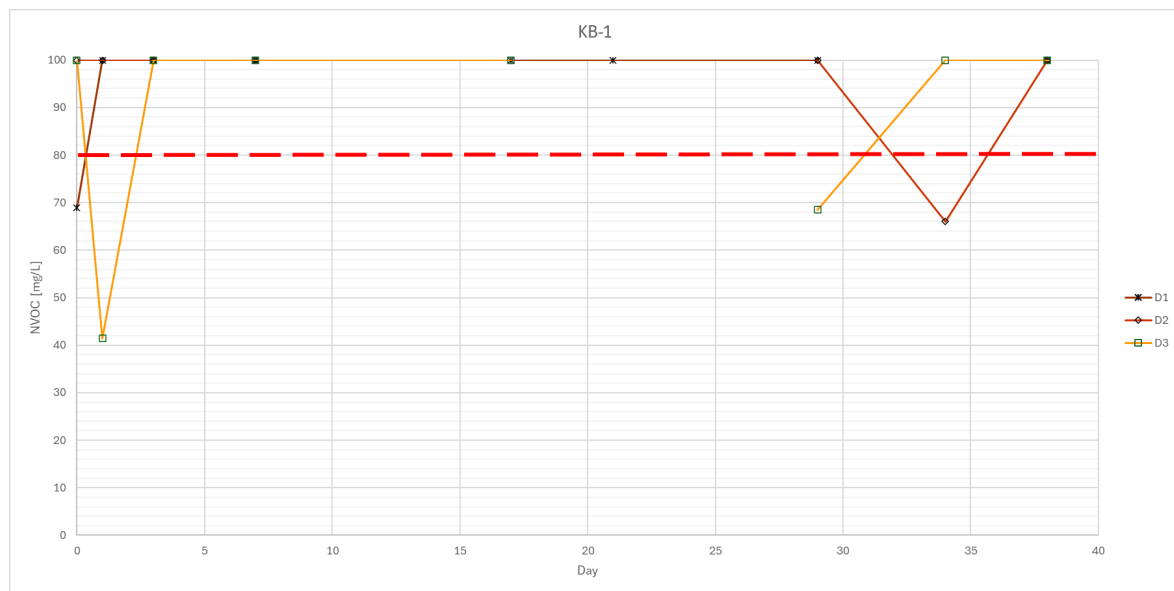


**Figure A.30:** NVOC levels in batch D, only points below the red line should be considered

| B

## APPENDIX B

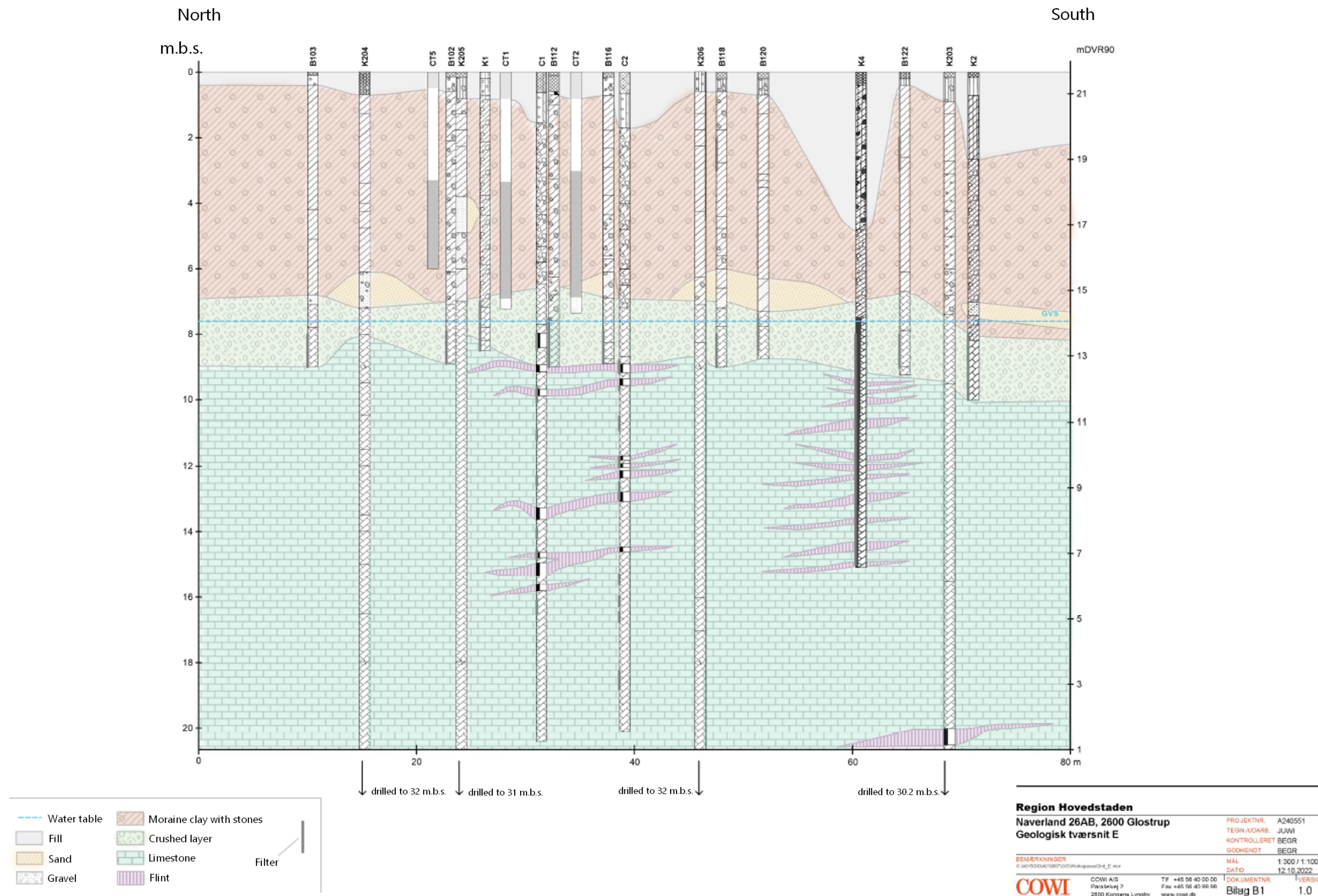


Figure B.1: Geology of the Naverland site COWI, 2023

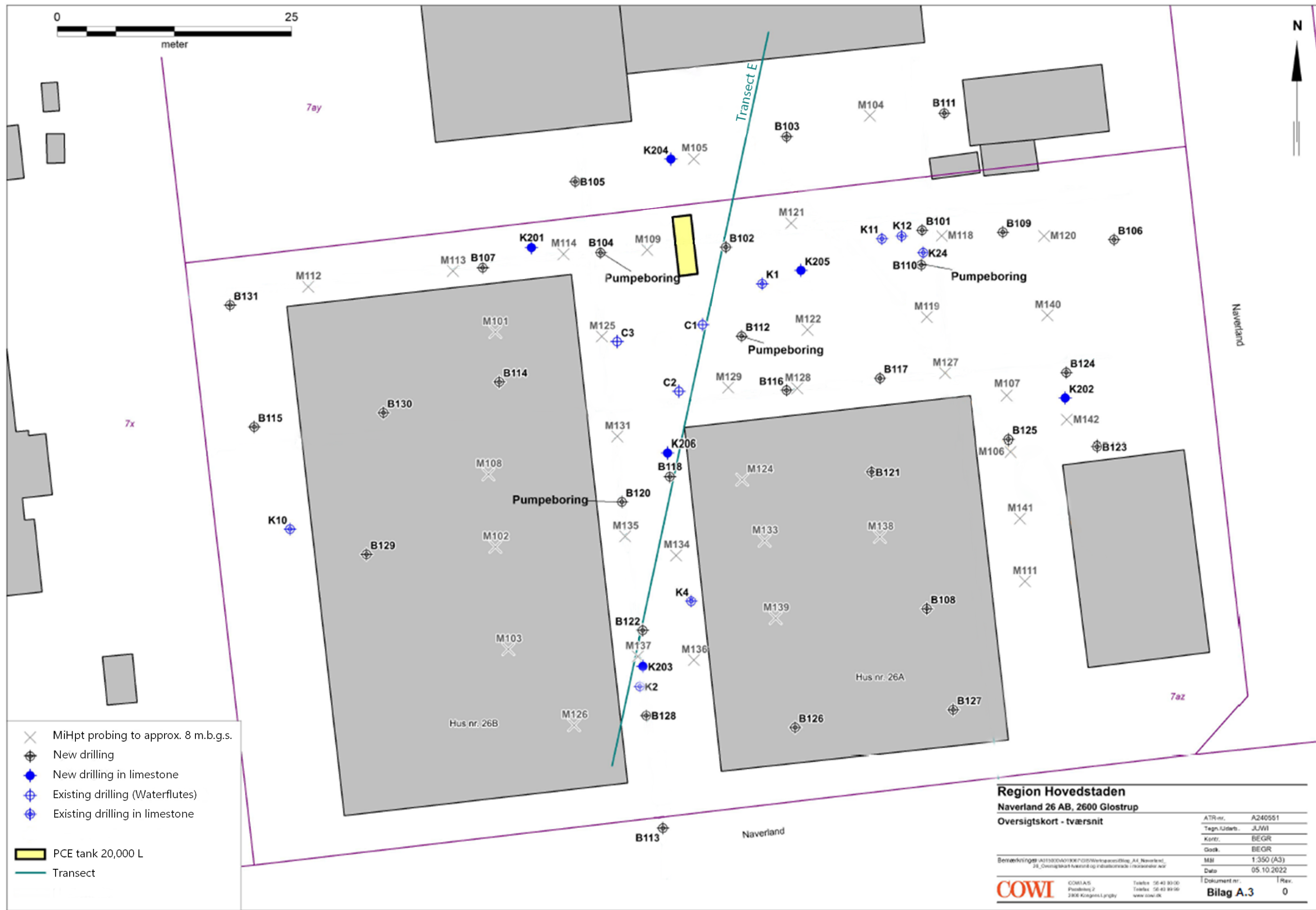


Figure B.2: The transect of the geology cross-section shown in Figure 4.1 from COWI, 2023

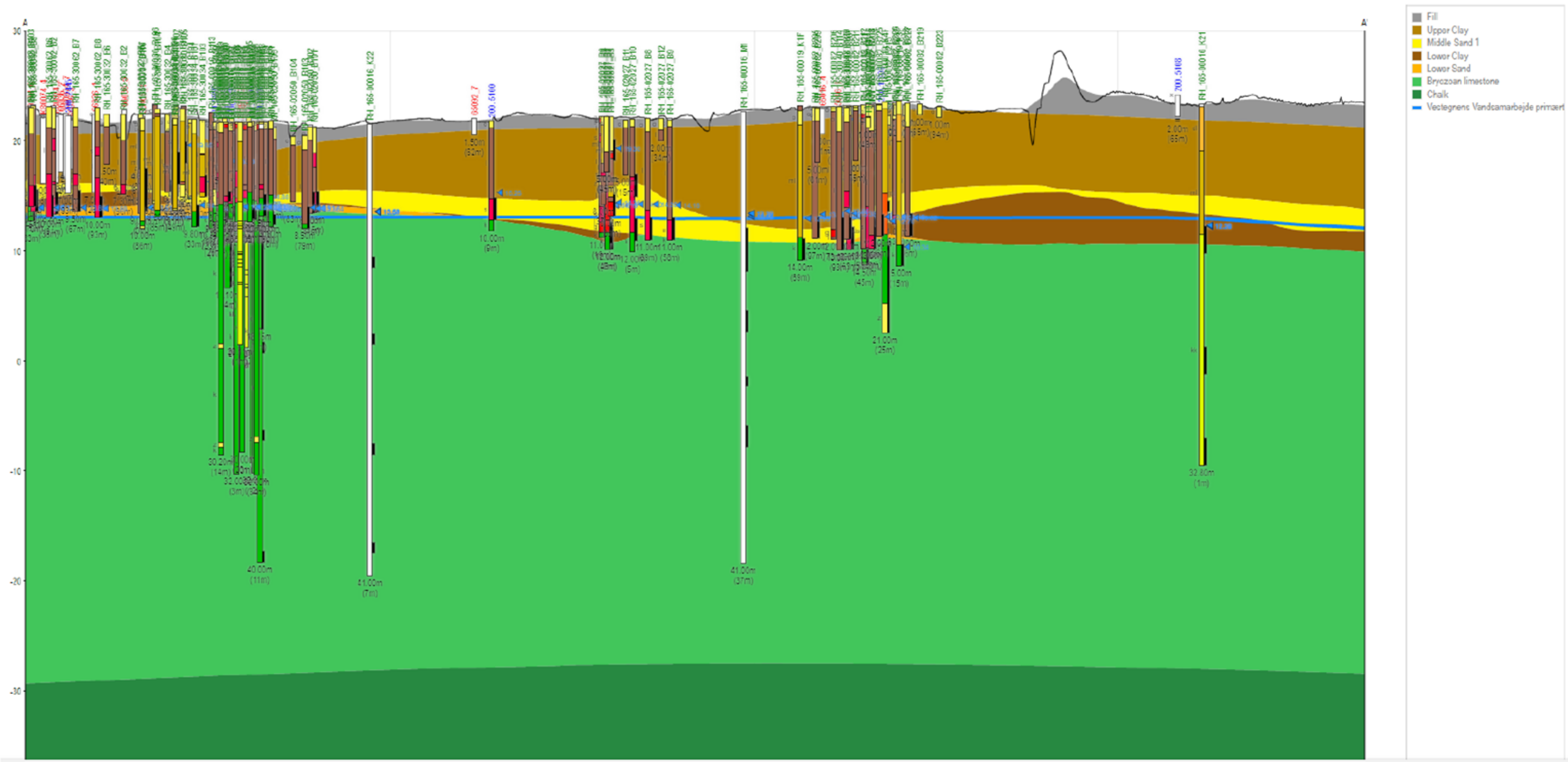


Figure B.3: Smaller scale geology of the site COWI, n.d.